Bioengineering and Cell-derived Strategies for Salivary Gland Regeneration

DONG, Jiao

2023

Document Version:
Publisher's PDF, also known as Version of record

Bioengineering and Cell-derived Strategies for Salivary Gland Regeneration

JIAO DONG
DEPARTMENT OF EXPERIMENTAL MEDICAL SCIENCE | LUND UNIVERSITY

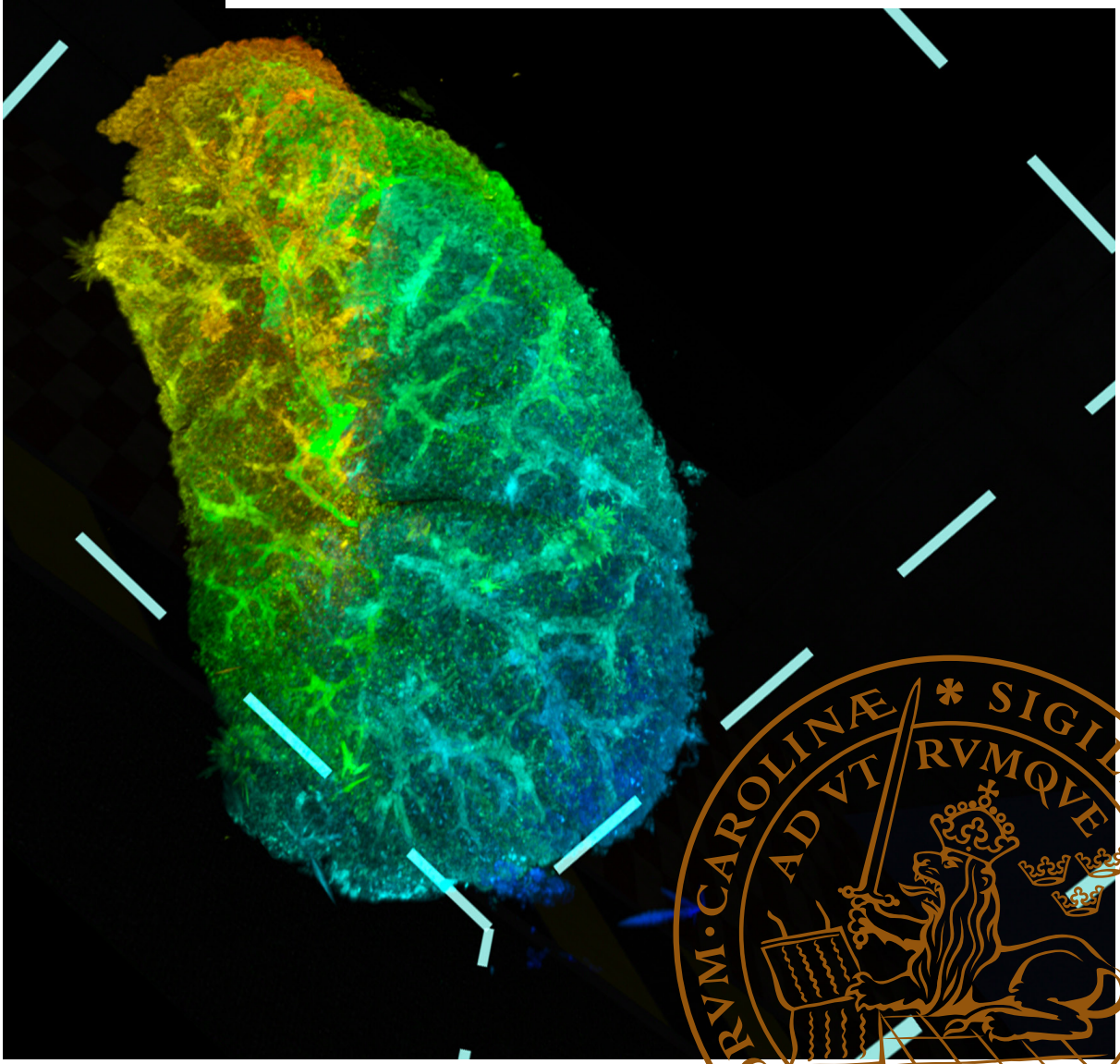

Bioengineering and Cell-derived Strategies for Salivary Gland Regeneration

Bioengineering and Cell-derived Strategies for Salivary Gland Regeneration

Jiao DONG

DOCTORAL DISSERTATION

Joint Degree Doctoral Dissertation for Doctor of Philosophy (PhD)

by due permission of the Faculty of Medicine, Lund University and Graduate School of Medicine, Nagoya University.

To be publicly defended on 08 February 2023 at 9 am (Lund time) in the Universal Conference Room at the Third Building, Graduate School of Medicine, Nagoya University

Faculty opponent
Prof. Kirsten H. Limesand

Organization: LUND UNIVERSITY

Document name: DOCTORAL DISSERTATION **Date of issue: 08 February 2023**

Author(s): Jiao DONG **Sponsoring organization:**

Title and subtitle: Bioengineering and Cell-derived Strategies for Salivary Gland Regeneration

Abstract:

Xerostomia (dry mouth symptoms) is a group of incurable debilitating conditions of salivary glands caused by aging, irradiation/chemical exposure or aberrant inflammation in the salivary glands. For this PhD thesis, I aimed to evaluate whether cell-derived strategies (e.g. extracellular vesicles, EVs) could be a potential new therapy to ameliorate salivary gland injury and restore function after radiotherapy or in autoimmune diseases. In addition, we also explored the possibility to promote a precision cut salivary gland slices (PCSS) ex vivo model for evaluating salivary gland disease mechanisms or potential therapy application. In addition, we aimed to develop new imaging techniques for both 2D and 3D analysis of larger samples which allows for quantification of disease and regenerative features. Firstly, we developed an in vivo murine model of 25 Gy irradiation-induced salivary gland damage to evaluate the potential of human dental pulp stem cell (hDPSCs)-derived EVs. EVs were injected 3x weekly via tail vein, beginning immediately after irradiation. Salivary gland function was evaluated 18 days after irradiation using salivary gland flow rate (SFR), gene expression (by qRT-PCR) and histopathology for analysis. Next, we tested different methods to generate PCSS using a vibratome and evaluated the slices in terms of their viability (by WST-1), gene expression (by qRT-PCR), secreted α-amylase activity and histological/light sheet fluorescence microscopy (LSFM) three-dimensional imaging. Following irradiation, SFR decreased while senescence-associated β-galactosidase-positive cells (via immuno-fluorescence) and senescence-related genes and secretory-phenotypes (e.g. *p21* and *MMP3* in qRT-PCR) increased. SFR was unchanged following EVs treatment but senescence-associated genes and secretory-phenotypes decreased. We also demonstrated that in an animal model of Sjögren's syndrome, which exhibited dry mouth symptoms, hDPSCs-EVs could inhibit the acquisition of the senescent phenotype in salivary gland epithelial cells (SGECs) and alleviate the loss of glandular function. EVs were also found to perform these effects through an underlying immunomodulatory mechanism. For PCSS, we developed protocols to produce viable slices of controlled thicknesses which retained the ability to secrete functional α-amylase for at least two days in ex vivo culture. Phenotypic salivary gland cell epithelial markers (e.g. *Keratin 5* and *Aquaporin 5*) increased over time in PCSS (by qRT-PCR), indicating the retention of cells that are necessary for salivary gland function. We developed workflows to perform LSFM 3D visulization in whole salivary glands as well as the PCSS model. In conclusion, hDPSCs-EVs reduced the senescence of salivary gland epithelial cells in both murine irradiaiton and Sjögren's syndrome models and may become a promising future for xerostomia patients. For the murine PCSS, we successfully established an executable operating procedure at the methodological level to reliably generate viable and functional murine PCSS, and developed new state-of-the-art analytical methods (such as LFSM 3D imaging and qRT-PCR) to increase the diversity of objective tools to evaluate PCSS. Therefore, this work laid the foundation for the future application of other therapies (such as irradiation therapy or EVs therapy) to the PCSS model. The future application could include drug screening or mechanism of injury study. At the same time we developed a sustainable histology process to reduce xylene utilization in histological processing for salivary gland tissue processing. Therefore, this work has developed a set of in vitro and in vivo experiments with state-of-the-art methods to better understand disease mechanisms and to evaluate new therapies for salivary glands.

Key words: extracellualr vesicles, human dental pulp stem cells, precision-cut tissue slices, salivary gland, sustainable histology and histology scoring

Classification system and/or index terms (if any)

Supplementary bibliographical information **Language: English**

ISSN and key title: 1652-8220 **ISBN**:978-91-8021-354-7

Recipient's notes **Number of pages**: 141

Price: Security classification

Signature: Jiao DONG Date 2023-01-02

Bioengineering and Cell-derived Strategies for Salivary Gland Regeneration

Jiao DONG

LUND
UNIVERSITY

DOCTORAL DISSERTATION

Joint Degree Doctoral dissertation for Doctor of Philosophy (PhD)

by due permission of the Faculty of Medicine, Lund University and Graduate School of Medicine, Nagoya University.

To be publicly defended on 08 February 2023 at 9 am (Lund time) in the Universal Conference Room at the Third Building, Graduate School of Medicine, Nagoya University

Faculty opponent
Prof. Kirsten H. Limesand

Supervisor: Senior Lecturer and Associate professor Darcy E. Wagner, PhD

Co-supervisor: Assistant professor Kiyoshi Sakai, PhD

Co-supervisor: Professor Hideharu Hibi, PhD

Co-supervisor: John Stegmayr, PhD

Faculty of Medicine

Department of Experimental Medical Science

ISBN 978-91-8021-354-7

ISSN 1652-8220

Printed in Sweden by Media-Tryck, Lund University

Lund 2023

To my families, Dr. Darcy, and Sakai sensei

Table of Contents

List of Papers **12**

Abstract **13**

Populärvetenskaplig sammanfattning **15**

摘要总结 **18**

概要 **20**

Abbreviations **22**

Introduction **25**

Saliva 25
The composition of saliva 25
Physiology and chemistry of saliva secretion 27
Function of saliva 29

Decreased production of saliva (dry mouth) 31
Causes 31
Symptoms and diagnosis 31

Salivary gland organs 33
Salivary gland embryology 33
Major and minor salivary glands 34

Salivary gland histology 37
Terminal secretory units 38
Treelike salivary gland ducts 39
Myoepithelial cells 39
Connective stroma tissue 40

Salivary gland disorders and pathology 41
Complications after irradiation therapy 41
Sjögren's Syndrome 43
Salivary gland tumors 45

Animal disease model 47

Senescence 50

Treatment and prevention of dry mouth 52
Artificial saliva 52

Salivary gland transfer surgery 53
Protective drugs used in radiotherapy..... 54
Intensity modulated radiotherapy..... 54
Gene therapy 55
Molecular therapy..... 56
Stem cell-based transplantation 57
Human dental pulp stem cells 58
Stem cells in salivary gland 59
Cell free therapy-Extracellular vesicles 60
Tissue engineering regenerative medicine (TERM) 62
Three-dimensional organoids or spheroids..... 62
Allogeneic tissue specific ECM in tissue engineering..... 63
Precision-cut salivary gland slices..... 64
Advanced in vitro imaging techniques..... 65
Light sheet fluorescence microscopy (LSFM) imaging..... 65
New developments in pathology and image-based analysis 66
Aims of the thesis 69
Materials and Methods..... 70
Animal (murine) usage..... 70
Paper I..... 70
Paper II 70
Paper III 70
In vitro cell culture of hDPSCs and EVs characteristics..... 71
Irradiation and NOD model and mouse treatment..... 72
Irradiation model..... 72
Precision-cut salivary gland slices (PCSS) organotypic culture 73
Irradiate on PCSS 74
NOD model..... 74
Measurement of stimulated saliva flow 74
Primary epithelial cell isolation by MACS 74
Sphere-formation assay and cellular senescence detection 75
Metabolic Assay (WST-1)..... 75
α-amylase-activity assay 75
Assay of superoxide anion scavenging activity..... 76
Histological analysis and xylene-free tissue processing 77
For Paper I 77
For Paper II and IV..... 78
For Paper III..... 79

Real-time RT-PCR ... 79
For Paper I and III ... 79
For Paper II ... 79
Light-sheet fluorescence microscopy ... 82
Statistical analysis ... 83
Summary of Results and Discussion ... 84
Paper I ... 84
EVs could be generated from hDPSCs ... 84
In vivo irradiation model shows decreased salivary output and no remarkable improvement on SFR shown after sEV administration ... 86
Irradiation induces cellular senescence in submandibular glands and hDPSC-sEV reduces the number of senescent cells ... 88
EVs play a role by reversing the oxidative microenvironment ... 90
Paper II ... 91
Metabolic activity exists in murine PCSS model at 0 hour of ex vivo culturing. ... 91
Murine PCSS exhibit metabolic activity up to 96 hours ... 92
Culture supernatant of PCSS has physiological α-amylase secretory function during the first 48 hours of culture. ... 93
McCoy's 5A medium maintains diverse epithelial and mesenchymal phenotypes. ... 93
McCoy's 5A culture media retains the general structural integrity and neuro-innervation distribution in mouse PCSS ... 94
Three-dimensional imaging is feasible for PCSS and native salivary gland using light sheet microscopy. ... 95
Paper III ... 96
NOD mice are a suitable animal model for Sjögren's Syndrome ... 96
EVs play an important role in reducing senescence in NOD mice submandibular gland epithelium at 22 weeks ... 97
Salivary glands cells of NOD mice lose the ability to form spheres, but EVs restore this ability and reduce senescence ... 99
Paper IV ... 99
Establishment of xylene-free tissue processing ... 99
Relation of Paper IV to this thesis ... 101
Conclusion and Future Perspectives ... 103
For Paper I and Paper III ... 103
Conclusion ... 103
Future perspectives ... 104
For Paper II ... 110
Conclusion ... 110

Future perspectives 111
For Paper IV 116
Conclusion 116
Future perspective 116
Overall Conclusion of the Thesis 118
Acknowledgements 119
References 122

List of Papers

Paper I

J Dong, K Sakai, Y Koma, J Watanabe, K. H. Liu, H Maruyama, K Sakaguchi, H Hibi. Dental pulp stem cell-derived small extracellular vesicle in irradiation-induced senescence. Biochemical and Biophysical Research Communications. 2021 Oct 20; 575:28-35

Paper II

J Dong, K Sakai, Y Koma, C Ceberg, N Gvazava, H Hibi, J Stegmayr, DE. Wagner. Precision-cut salivary gland slices are functional ex vivo model system to study physiopathology of salivary gland ex vivo. American Journal of Physiology (manuscript)

Paper III

Y Koma, K Sakai, **J Dong**, J Watanabe, S Yamaguchi, H Maruyama, H Hibi. Alleviation of cell aging in Sjögren Syndrome model mice. Journal of Dental Research (submitted 2022 Sep 20)

Paper IV

IAN Silva, N Gvazava, DA Bölükbas, M Stenlo, **J Dong**, S Hyllen, L Pierre, S Lindstedt, DE. Wagner. A semi-quantitative scoring system for green histopathological evaluation of large animal models of a lung injury. Bio Protocol. 2022 Aug 20; 12(16): e4493

Abstract

Xerostomia (dry mouth symptoms) is a group of incurable debilitating conditions of salivary glands caused by aging, radiation/chemical exposure, or aberrant inflammation in the salivary glands. During this PhD thesis, we aimed to evaluate whether cell-derived strategies (e.g., extracellular vesicles, EVs) could be a potential new therapy to ameliorate salivary gland injury and restore function after radiotherapy or in autoimmune diseases. In addition, we aimed to develop new imaging techniques for both 2D and 3D analysis of larger samples which allows for quantification of disease and regenerative features. Firstly, we constructed an in vivo murine model of 25 Gy irradiation-induced salivary gland damage to evaluate the potential of human dental pulp stem cell (hDPSCs)-derived EVs. EVs were injected 3x weekly via tail vein, beginning immediately after irradiation. Salivary gland function was evaluated 18 days after irradiation using salivary gland flow rate (SFR), gene expression (by qRT-PCR) and histopathology. Next, we tested different methods to generate PCSS using a vibratome and evaluated the slices in terms of viability (by WST-1), gene expression (by qRT-PCR), secreted α-amylase activity (by α-amylase assay kit) and histological/light sheet fluorescence microscopy (LSFM) three-dimensional imaging. Following irradiation, SFR decreased while senescence-associated β-galactosidase-positive cells (via immunofluorescences) and senescence-related genes and secretory-phenotypes (e.g., *p21* and *MMP3* in qRT-PCR) increased. SFR was unchanged following EVs treatment, but senescence-associated genes and secretory-phenotypes decreased. We also demonstrated that in an animal model of Sjögren's syndrome, which exhibit dry mouth symptoms, that hDPSCs-EVs could inhibit the acquisition of the senescent phenotype in salivary gland epithelial cells (SGECs) and alleviate the loss of glandular function. EVs were also found to perform these effects through an underlying immunomodulatory mechanism. For PCSS, we developed protocols to produce viable slices of controled thicknesses which retained the ability to secrete functional α-amylase for at least two days in ex vivo culture. Phenotypic salivary gland cell epithelial markers (e.g., *Keratin 5* and *Aquaporin 5*) increased over time in PCSS (by qRT-PCR), indicating the retention of cells that are necessary for salivary glands' function. We developed workflows to perform LSFM 3D visualization in whole salivary glands as well as the PCSS model. In conclusion, hDPSCs-EVs reduced senescence of salivary gland epithelial cells in both murine irradiation and Sjögren's syndrome models and may become a promising future for xerostomia patients. For the murine PCSS, we successfully established an

executable operating procedure at the methodological level to reliably generate viable and functional murine PCSS and developed new state-of-the-art analytical methods (such as LFSM 3D imaging and qRT-PCR) to increase the diversity of objective tools to evaluate PCSS. Therefore, this work laid the foundation for the future application of other therapies (such as irradiation therapy or EVs therapy) to the PCSS model. Those future applications could include drug screening or mechanism of injury study. At the same time, we developed a sustainable histology process to reduce xylene utilization in histological processing for salivary gland tissue processing. Therefore, this work has developed a set of in vitro and in vivo experiments with state-of-the-art methods to better understand disease mechanisms and to evaluate new therapies for salivary glands.

Populärvetenskaplig sammanfattning

Xerostomi, är en kliniskdiagnos för muntorrhet. Muntorrheten kan uppkomma till följd av åldersförändringar, strålnings- och kemikalieexponering eller en inflammation i spottkörtlarna. Extracellulära vesiklar (EVs) är små vesiklar (i nanometerstorlek) vilka normalt används vid cellers kommunikation med varandra. EVs har visats ha positiv effekt i djurförsök vid skada eller sjukdom i tex lunga, hjärta, njure mm. Detta avhandlingsarbete fokuserar på att undersöka om EVs, från celler som även testas inom stamcellsterapier, skulle kunna användas som behandlingsmetod vid skada på spottkörtlarna eller vid autoimmuna sjukdomar. Hittills har det inte gjorts många undersökningar kring att använda EVs vid skador eller sjukdomar som drabbar just spottkörtlarna. Den stora fördelen med att använda EVs framför stamceller är att du inte behöver injicera hela celler i djuret. Att injicera hela celler utgör en risk då cellerna kan bli bortstötta eller riskerar att ge upphov till tumörer. För att testa teorin kring att använda EVs konstruerade vi först en musmodell med en strålningsinducerad skada i spottkörtlarna för att sedan evaluera potentialen i EVs från humana stamceller från pulpan i tänder (human dental pulp stem cell, hDPSC). hDPSC är en möjlig effektiv källa för EVs då de kan utvinnas ganska lätt ur kirurgiskt avfall från de flesta tandläkarkliniker (dvs tänder). Vårt lab har sedan tidigare tagit fram metoder för isolering och karakterisering av EVs från hDPSC. EVs injicerades 3 gånger i veckan via svansvenen på strålade möss, med första injektionen direkt efter strålningen. Spottkörtlarnas funktion undersöktes 18 dagar efter strålningen genom att vi mätte flödeshastigheten av saliv i spottkörtlarna (salivary gland flow rate, SFR), genuttryck (med en kvantitativmetod för genuttryck som kallas qRT-PCR) och vävnadsanalys i mikroskop (dvs histologi). Resultaten visar, som förväntat, att efter strålning minskar SFR, medan celler associerade med åldrande (β-galaktosidaspositiva celler) samt gener och ämnen associerade med åldrande celler (*p21* och *MMP3*) ökade. Åldrande celler är celler som inte längre delar sig, men inte heller dör. Dessa celler utsöndrar ämnen som kan vara skadliga för kringliggande vävnad, denna fenotyp benämns ”senescence associated secretory phenotype” (SASP). SFR förblev oförändrat låg även efter EV-behandling medan genuttryck och fenotyp associerat med SASP minskade. Vi visade också i en djurmodell av Sjögrens syndrom, där patienterna uppvisar symptom av muntorrhet, att hDPSC-EVs kunde förhindra att epitelcellerna i spottkörtlarna utvecklade fenotypen av åldrande celler samt bidrog till att bibehålla en större del av körtelfunktionen. Vi visade även att EVs kan ge dessa effekter genom att påverka immunsystemet. Vi drar därmed slutsatsen att hDPSC-EVs minskar åldrandet av

epitelcellerna i spottkörtlarna både i strålningsskadade musmodeller och i modeller av Sjögrens syndrom och därmed utgör en tänkbar kandidat för behandling av patienter som lider av xerostomi.

Då användning av djurförsök kräver många djur var ett andra mål i detta avhandlingsarbete att ta fram vävnadssnitt, precisionsskurna skivor av spottkörtlar s.k. precision cut salivary gland slice (PCSS), som en användbar *ex vivo* modell för sjukdomsmekanismer i spottkörtlar. PCSS skulle kunna minska antalet djur drastiskt eftersom det gå att få många vävnadssnitt från ett djur, en spottkörtel kan ge upp till 20 vävnadssnitt. Dessa tekniker kan även användas på mänsklig vävnad (som tex kirurgiskt avfall). Vi började med att prova olika metoder för att producera PCSS med en vibratom och utvärderade vävnadssnittens kvalité med avseende på viabilitet (med WST-1), genuttryck (med qRT-PCR), aktivitet hos utsöndrat α-amylas (α-amylas kit) samt histologiskt med light sheet fluorescence microscopy (LSFM, ett laserbaserat mikroskop som framförallt genererar 3D videor av vävnaden som sedan analyseras. Vi tog fram en metod för att få viabla vävnadssnitt i olika, förutbestämda, tjocklekar som producerade funktionellt α-amylas under en period av två dygn. För att undersöka hur lika dessa PCSS är hela spottkörtlar, utvecklade vi även metoder för att möjliggöra LSFM 3D visualisering av både hela spottkörtlar och vår PCSS-modell. Det vi såg var att med vår metod bibehölls vävnadsstrukturen i PCSS, inklusive spottkörtlarnas olika lober. Vi såg även att markörer för epitelceller i spottkörtlar (*Keratin 5* och *Aquaporin 5*) ökade över tid i våra PCSS (undersöktes med qRT-PCR) vilket visar på att dessa celltyper, som är de celler som främst står för spottkörtelns funktion, finns kvar och lever i vår modell. Det finns några få tidigare artiklar som visar att PCSS kan tas fram, det vi har gjort är att vi har jämfört olika cellmedium för att hitta det som kan hålla PCSS vid liv samt utvecklat nya state-of-the-art analysmetoder (som LFSM 3D avbildning och qRT-PCR). Därmed har detta arbete lagt grunden för framtida användningsområden inom andra terapier i PCSS modellen (som strålbehandling eller EV-behandling) samt läkemedels-screening eller studier av skade- och sjukdomsmekanismer.

En sak vi noterade under våra *in vivo*- och *in vitro*-studier var att mycket av bedömningen, både av vävnadsskador och av läkning, görs med hjälp av histologi. Histologiska undersökningar är väldigt komplexa och subjektiva och det kan behövas många vävnadsprov för en säker diagnos. Då vi även försöker minska på de giftiga kemikalier som används i dagligt laboratoriearbete, har vi, som ett komplement, utvecklat och testat xylen-fri hantering av vävnader vid histologi och infärgning. Först behövde vi säkerställa att den xylenfria behandlingen av vävnadsproven ger pålitliga resultat. Först jämförde vi vävnad från spottkörtlar som genomgått xyleninnehållande eller xylenfri vävnadsbehandling, sedan även andra organ. Vi kom fram till att genom att byta xylen mot isopropanol och förlänga inkubationstiden samt paraffininbäddningstiden, kunde vi få bort xylen ur vävnadshanteringen utan försämrat resultat. Efter detta ville vi ta fram ett nytt och optimerat histologiskt poängsystem för en systematiserad klassificeringsmetod för

vävnad. Vi gjorde först detta i lungvävnad, då vi hade många prover från just lunga, men ska framöver även använda denna klassificeringsmetod på sjukdomar i spottkörtelvävnad. Många av fenotyperna från lungvävnad kan även användas i spottkörtelvävnad (som närvaro av inflammatoriska celler eller tecken på vävnads fibros) men spottkörtelvävnad är väldigt varierad och fler histologiska prov behövs för framtida klassificering. Dock är detta viktigt för utvärdering av olika sjukdomsmodeller och framtida terapier.

Detta avhandlingsarbete har utvecklat en ny verktygslåda för *in vitro* och *in vivo* experiment samt state-of-the-art metodologi för en bättre förståelse av de sjukdomar och sjukdomsmekanismer som kan drabba spottkörtlar samt utvärdering av nya terapier.

摘要总结

口干症（唾液分泌不足）是一种因唾液腺老化或放线辐射/或免疫攻击唾液腺造成的使唾液腺无法治愈的功能衰弱症状群。在我的博士期间，我的目的是评估无细胞衍生策略，例如干细胞来源的细胞外囊泡，是否具有改善放疗后或自体免疫类疾病中唾液腺损伤的功能的治疗价值。此外，我们也探索并推进了精密切割唾液腺切片 (PCSS) 离体模型的制备方法。这一器官样培养模型更能模拟天然唾液腺的细胞多样性和组织结构复杂性。我们评估这一模型对于摸索唾液腺疾病的致病机制或开发潜在的治疗方法方面的可能性。最终我们结合可持续发展的原则，目标是开发无二甲苯添加的组织学处理和染色方法来应对未来医疗环境下诊断样本量大且病情繁杂的情况。另一方面，病理学家利用组织学染色来评判组织损伤的方法，十分容易受主观干扰的影响。面对这些挑战，我们认为发展并完善组织学评分，使其系统化，将有助于形成根据组织学来评估和分类唾液腺疾病的策略，从而成为应对未来挑战的一种解决方案。首先我们构建了一个 25 Gy 辐射诱导唾液腺损伤的小鼠体内模型，以评估人牙髓干细胞衍生外泌体的潜力。在放射线照射后立即开始每周通过尾静脉注射 3 次固定剂量的外泌体，在放射线照射后 18 天后，进行唾液腺流速 (SFR)、基因表达 (实时荧光聚合酶链式反应，qRT-PCR) 和组织病理学染色以评估唾液腺功能情况。然后，我们使用高频震动机，测试了生成 PCSS 器官样切片模型的不同方法，并评估了该切片随着时间的推移，在各项指标如生存能力 (借助 WST-1 检测)、功能基因表达（借助 qRT-PCR 检测）、分泌的 α-淀粉酶活力（借助 α-淀粉酶活力测试检测）和组织学或光片荧光显微镜（light sheet immunofluorescence imaging, LSFM) 三维成像等方面的情况。结果表明，对于放射线照射小鼠模型，放射线照射唾液腺后 SFR 降低，而衰老相关 β-半乳糖苷酶阳性细胞（通过免疫荧光染色检测）和衰老相关基因和分泌因子（如 qRT-PCR 检测 *p21* 和 *MMP3* 基因表达）增加。而在外泌体静脉给与后，小鼠 SFR 没有变化，但衰老相关基因及分泌因子在照射后唾液腺器官中表达降低。人牙髓来源干细胞外泌体 （hDPSCs-EVs）在舍格伦综合征口干症的动物模型中同样显示，hDPSCs-EVs 能够缓解在唾液腺上皮细胞中发生的细胞老化，并且缓解腺体功能的丧失，同时发现，这种作用是hDPSCs-EVs通过免疫调节机制实现的。对于PCSS器官样切片模型，体外培养两天内组织切片能够保证存活并保持对功能性 α-淀粉酶的分泌。qRT-PCR 的结果显示在 PCSS 器官样切片模型中唾液腺上皮细胞表型标记物，

例如角蛋白 5（keratin 5）和水通道蛋白 5（aquaporin 5）随着时间的推移而增加表达。此外，我们还开发了在整个唾液腺和 PCSS 器官样切片模型中进行光片荧光显微镜三维成像的工作流程。我们的结论是，人牙髓干细胞来源外泌体能够减少小鼠唾液腺放射线辐射模型中的细胞老化，也能在患有舍格伦综合征口干症候群的动物模型上，缓解唾液腺上皮细胞 （SGECs）的细胞衰老过程。因此，在不远的将来，人牙髓干细胞来源的外泌体可能为口干症患者的治疗带来福音。对于小鼠 PCSS 器官样切片模型，我们在方法论层面建立了一套可行性高的操作流程，能够保证连续产生厚度一致的组织切片，并在培养短期内保持组织切片中细胞活力和功能。我们同时还为这一模型开发和验证了若干较为先进的分析方法，比如LSFM荧光三维成像和qRT-PCR。我们的目标是通过开发适用于 PCSS 模型的分析方法，来增加 PCSS 器官样切片模型评估方法的多样性和准确性，从而为以后将其他治疗方法如放射线治疗或外泌体治疗，应用到 PCSS 器官样模型上进行疗法开发或药物筛选或机制研究奠定了基础。最后，我们将组织学处理中减少二甲苯利用的可持续组织学理念引入到唾液腺的组织学研究中。 我们的目标是开发能够分类不同类别的唾液腺疾病和能够对唾液腺组织的病变损伤进行评分和分级的组织学评分和分级系统。例子包括针对免疫细胞灶进行组织学集聚评分或针对放射线照射后真核细胞核的形态变化进行组织学评分。这样，我们的研究有助于在不远的将来，将人工智能技术与组织学评分相结合并应用到医学诊断 （通过组织学切片）中，从而提高唾液腺组织学评分系统在评估病情、分类病情和诊断疾病中的准确率和客观性。以上所有努力都是我们致力于为唾液腺疾病的机制研究、疾病模拟、医学诊断和疗法开发，提供一整套的方法论和实践论方面的解决方案，从而为唾液腺疾病的诊断、治疗和研究打下坚实的基础。

概要

口腔乾燥症は、自己免疫疾患、加齢や放射線・化学物質への曝露によって引き起こされる炎症に起因した唾液腺の難治性疾患である。博士課程では、幹細胞由来細胞外小胞が、放射線治療後や自己免疫疾患における唾液腺損傷の改善や機能回復のための新しい治療法となり得るかどうかを評価することを目的とした。また、唾液腺疾患メカニズムの評価や治療への応用の可能性を探るため、Precision Cut Salivary gland Slice (PCSS) ex vivo モデルの構築を目指した検討もした。はじめにヒト歯髄幹細胞（hDPSCs）由来の EV の可能性を評価するために、25 Gy 放射線誘発唾液腺障害の in vivo マウスモデルを構築した。照射直後から週 3 回、尾静脈から EV を注入し、照射 18 日後に唾液腺流量（SFR）、遺伝子発現（qRT-PCR）、病理組織学的に唾液腺機能を評価した。次に、ビブラトームを用いて PCSS を作製するための様々な方法を検証した。スライスの生存率（WST-1 による）、遺伝子発現（qRT-PCR による）、分泌 α-アミラーゼ活性（α-アミラーゼアッセイキットによる）、組織学／光シート蛍光顕微鏡（LSFM）三次元画像について評価した。その結果、照射後、SFR が低下することがわかった。同時に、老化に関連する SA-β-ガラクトシダーゼ陽性細胞（免疫蛍光法）、老化関連遺伝子や分泌表現型（qRT-PCR における *p21* や *MMP3* など）が増加しました。SFR は EV 処理後も変化しなかったが、老化関連遺伝子と分泌表現型は減少した。また、ドライマウス症状を示すシェーグレン症候群患者の動物モデルにおいて、hDPSCs-EV が唾液腺上皮細胞の老化表現型の獲得を抑制し、腺機能の低下を緩和することを明らかにした。また、EV は免疫調節機構を基礎としてこれらの効果を発揮することも明らかにした。PCSS については、機能性 α-アミラーゼを分泌する厚みの異なるスライスを 3 日間かけて生着させるプロトコールを開発した。唾液腺細胞上皮マーカー（例：ケラチン 5 およびアクアポリン 5）は、PCSS において経時的に増加した（qRT-PCR による）。唾液腺全体と PCSS モデルで LSFM 3D 可視化を行うためのワークフローを開発し、結論として、hDPSCs-EVs はマウス照射モデルとシェーグレン症候群モデルの両方で唾液腺上皮細胞の老化を抑制し、口腔乾燥症患者に対する将来の有望な治療法であることが示唆されました。マウス PCSS については、方法論レベルで実行可能な操作手順を確立し、生存可能で機能的なマウス PCSS の確実な作製に成功

しました。また、PCSS を評価する客観的ツールの多様性を高めるため、LFSM 3D imaging や qRT-PCR といった最先端の分析手法を新たに確立しました。したがって、この研究は、将来的に PCSS モデルへの他の治療法（照射療法や EVs 療法など）の適用、すなわち薬剤スクリーニングや病態メカニズム研究への基礎を築いたと考えられます。同時に、唾液腺組織処理の組織学的処理におけるキシレン使用量を削減するための持続可能な組織学的処理法を開発しました。このように、本研究では、疾病メカニズムの解明するための新規ツールを最先端の方法を用いた一連の in vitro および in vivo 実験で開発しました。

Abbreviations

2D	two-dimensional
3D	three-dimensional
ACC	adenoid cystic carcinoma
AQP5	aquaporin 5
ASCs	adipose-derived mesenchymal stem cells
cAMP	cyclic adenosine monophosphate
DCM	dichloromethane
DDR	DNA damage response
ED	excretory ducts
EGF	epidermal growth factors
ER	endoplasmatic reticulum
ESCs	embryonic stem cells
EVs	extracellular vesicles
FGF	fibroblast growth factors
FN	fibronectin
GAGs	glycosaminoglycans
GDNF	glial cell-line derived neurotrophic growth factor
HNC	head and neck cancers
IGF-1	insulin-like growth factor-1
IL6	interleukin six
iPSCs	induced pluripotent stem cells
LG	lacrimal glands
M3R	muscarinic acetylcholine receptor III
MC	mucoepidermoid carcinoma

MSCs	mesenchymal stem cell
MSGT	malignant salivary gland tumors
NGF	nerve growth factor
NRTN	neurotrophic factor neurturin
NTA	nanoparticle tracking analysis
OI	optical imaging
PAI	photoacoustic imaging
PBMCs	peripheral blood mononuclear cells
PET	positron emission tomography
PG	parotid gland
pSS	primary Sjögren's syndrome
RI	refractive indices
RT	radiation therapy
SASP	senescence-associated secretory phenotypes
Sca-1	stem cell antigen-1
SEM	scanning electron microscopy
SG	salivary gland
SGECs	salivary gland epithelial cells
Shh	sonic hedgehog
SLG	sublingual gland
SMG	submandibular gland
SOX	SRY-related HMG-box
SPECT	single photon emission computed tomography
sSS	secondary Sjögren's syndrome
SWS	stimulated whole saliva
TEM	transmission electron microscopy
TGF-α	transforming growth factor-α
TGF-β	transforming growth factor-β
TNF	tumor necrosis factor

TRPM2	transient receptor potential type M2
UWS	unstimulated whole saliva
VAS	visual analog scales
VIP	vasoactive intestinal peptide
WSI	whole slide images
ZO-1	Occludens 1

Introduction

Saliva

The composition of saliva

The mouth of mammals is lubricated with a complex solution coating inside the oral cavity called saliva[1]. Both the major and minor salivary glands secrete saliva, which is a thick, colourless, opalescent fluid mixture, consisting of water derived from blood and 1 % organic and inorganic electrolytes antimicrobial compounds, enzymes, and growth factors and so on. It maintains a physiologically healthy environment for teeth and oral soft tissues (Table 1). Approximately 1.0 - 1.5 litres of saliva with pH around 6.35 - 6.85 and hypotonic to plasma are secreted by salivary glands in healthy persons each day. The major salivary glands (There are parotid gland, submandibular gland, and sublingual gland, respectively) produce 93 % of saliva, with the remaining amount of saliva originating from around 800 - 1,000 tiny glands (7 %) located around the mouth and tongue.

A large number of proteins and peptides can be found in saliva, including lysozyme, immunoglobulin, salivary α-amylase, histones, mucin protein, and peroxidase[3]. Each protein has distinct and important functions, and the composition of saliva varies depending on the physiological state. For example, salivary mucins are extremely abundant and serve to both lubricate the mucous membrane and reduce the chance of infection[4]. Saliva composition also varies depending on the gland that produces it. In parotid saliva, salivary α-amylase is the most abundant secreted protein. The knowledge regarding the salivary proteome has expanded in recent years due to new 'omics' tools and can be used to detect and identify saliva components, such as proteins, to better understand normal physiology and disease. The saliva proteome can thus be viewed as an accurate and repeatable measurements to identify biomarkers and can be used to diagnose diseases early as well as monitor general health[5]. In the past decade, salivary protein analysis has shifted to detect disease-related proteome differences[6]. Several proteins have also been identified as potential systemic biomarkers for endocrine function, stress, psychological state, infectious agents, drug or other xenobiotic use, and cancer. Therefore, the study of salivary proteomics can help identify disease biomarkers and enable the detection and treatment of diseases at an early stage.

Table 1. Components and functions of saliva[7].

Saliva Componentst	Percentage	Detailed Categories			Function
Water	99.5 %	-			Mucosal integrity, lavange or cleansing, help with taste and speech
Solids	0.5 %	Organic substances	Proteins	α-amylase, maltase, lingual lipase, other protease, ribonuclease; glycoproteins or mucins; agglutinin.	Digestion, lubrication, and pellicle formation, antimicrobial
			Growth factors	EGF, TGF-α, TGF-β, FGF, NGF, IGF-1	Protective tissue repair role in wound contraction
			Immunoglobulin	IgG, IgM, IgA.	Antimicrobial
			Antibacterial proteins	Lysozymes, lactoferrin, transfer, secretory leucocyte proteinase inhibitor, peroxidase or salioperoxidase	Hydrolysis to bacterial cell membrane, antimicrobial
			Others	Urea, glucose, vitamins, free amino acids, uric acid, creatinine, other polypeptides:histatins, cystatins.	Buffering, antimicrobial
		Inorganic substances (electrolytes)	Sodium, bicarbonate, calcium, chloride, fluoride, phosphate, potassium, thiocynate.		Buffering, remineralization, antimicrobial, mucosal integrity
		Cellular components	Epitheliala cells, white blood cells, microbes.		-
		Gases	O_2, CO_2, N_2		-

Physiology and chemistry of saliva secretion

The main cell type responsible for salivary production and secretion are acinar cells. Their histological appearance varies depending on the type of proteins they secrete, which are stored in large cytoplasmic granules. Acinar cells' histological appearance depends on the types of proteins they secrete; these proteins are stored in large granules in their cytoplasm. Storage particle content is an indication of the type of saliva produced, which can be divided roughly into mucin-containing and non-mucin-containing saliva. During secretion, three events occur: (i) fluid is filtered from plasma into the acinar lumen by neurocholinergic stimulation, (ii) proteins that contain cytoplasmic granules are exocytosed into the acinar lumen, and (iii) the secretory terminals are mechanically activated by specialized myoepithelial cells. Saliva secretion relies on an abundance of arterioles around ducts and acini, as well as highly autonomic innervation with parasympathetic and sympathetic nerve supply. There can be many stimuli that trigger salivation. The periodontal ligament and the tongue's dorsum activate mechanoreceptors to trigger salivation. Gustatory stimulation of mucous membranes stimulates minor salivary glands, motor or tactile stimulation may affect lip and palate secretions more[8]. Various aromatic compounds are found in or released by food and increase submandibular and sublingual gland secretions, but not parotid gland secretions[9] (see Table 2).

Table 2. Saliva reflex.

Types	Characteristics
Unconditioned reflex	An inborn reflex, induces secretion of saliva when any substance is placed in oral cavity.
Conditioned reflex	A reflex acquired by experience. Sound, sight, smell, taste of food, masticatory stimuli, or thoughts about previously enjoyed foods initiates salivary secretion.

The formation of macromolecular components

Protein storage granules are exocytosed primarily by salivary acinar cells activated by norepinephrine. Norepinephrine binds to β1-adrenergic receptors on acinar cells and increases intracellular cyclic AMP[10] levels. Signals from the parasympathetic nerves also act through the release of vasogut polypeptide, which also acts by increasing intracellular cyclic AMP. The entire cycle is fairly quick, completing within 30 minutes of the initial stimulation. Intracellular cAMP levels are elevated, resulting in degranulation. The release of granule contents in both PG and SMG glands results in the shrinkage of individual acinar cells, which significantly decrease in size following degranulation[11] (Figure 1A).

The secretion of saliva's ionic components and its modification by ducts.

Firstly, from the endoplasmic reticulum Ca^{2+} storage, free Ca^{2+} is released under parasympathetic nerve stimulation. This leads to a quick increase in the

concentration of free cytoplasmic Ca^{2+}, resulting in significant compensatory changes, such as releasing K^+ channels basolateral and opening Cl^- channels apically to release Cl^- into the lumen. This ionic gradient pulls Na^+ into the lumen through the luminal surface. Due to the changes in osmotic pressure, water is transported into the lumen. Isotonic plasma-like fluid is secreted by the acini into the lumen (Figure 1A and B).

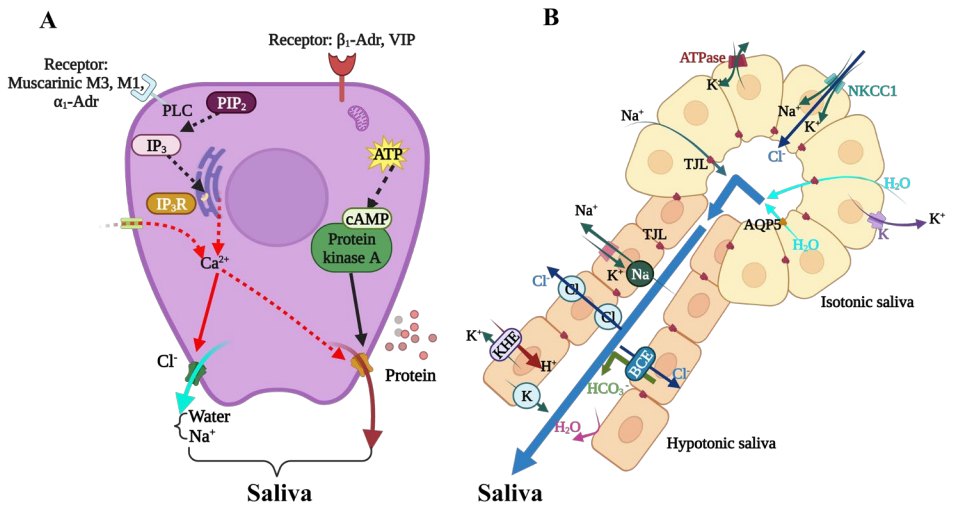

Figure 1. The intracellular coupling of nerve-mediated reflexes to protein and water secretion in acinar cells.

(A) The secretion of fluid is primarily influenced by acetylcholine released by parasympathetic nerves, which activate muscarinic M3 receptors. An increase in cytoplasmic calcium levels, released from endoplasmic reticulum stores, causes chloride release as a result of intracellular coupling. Among the main mechanisms that activate protein secretion are noradrenaline release, β-1 adrenoceptor activation, and vasointestinal peptide release, due to vasointestinal peptide release from parasympathetic nerves, binding to VPAC receptors (vasoactive intestinal peptide). In intracellular signaling, cyclic AMP is increased, causing protein kinase A (PKA) to phosphorylate, which in turn leads to protein release into saliva. (B) Active sodium pumps (ATP) secrete saliva when intracellular sodium concentrations are low. Saliva secretions start when sodium and chloride ions enter the acinar lumen; water follows because of the osmotic gradient of salt, moving between cells or passing through aquaporin 5 (AQP5) channels to enter the acinar lumen. Different ion-transport membranes transport sodium and chloride in acinar cells: a chloride channel opens upon glandular stimulation; sodium flows between cells via leaky tight junctions. Using the basolateral membrane as a co-transporter, chloride enters acinar cells via a concentration gradient of low intracellular sodium. It is isotonic saliva secreted by the acinar cells. In ductal cells, sodium and chloride are removed due to membrane transporter proteins and a low intracellular sodium concentration produced by the sodium pump. There are no leaky junctions between ductal cells (TJT) and no water channels. Saliva becomes hypotonic after the ducts secrete bicarbonate. α1-Adr, α1 adrenoceptor; IP3, inositol triphosphate; IP3R, inositol triphosphate receptor; PIP2, phosphatidyl inositol biphosphate; PLC, phospholipase C. ATPase, sodium, potassium ATPase; BCE, bicarbonate, chloride exchanger; Cl, chloride channel; KHE, potassium, proton exchanger; Na, sodium channel; NKCC1, sodium, potassium, chloride co-transporter. Created with BioRender.com

Function of saliva

The traditional roles that viscoelastic saliva is capable to play are to maintain oral homeostasis, lubrication to maintain mucosal integrity, remineralization of teeth, aiding food digestion, and facilitating taste, as well as helping distribute antimicrobial, antiviral, and antifungal molecules to protect the whole mouth and body from numerous environmental hazards and offering immunity and healing role (Figure 2). For example, saliva can lubricate mucosa so that it does not dry out, which is the most fundamental function it performs[12]. The enzymes contained in saliva protect teeth from bacterial decay because it helps break down food particles trapped in dental crevices[13]. The enzymes also assist in the first steps of digestion of dietary starches and fats. Through saliva, food clumps can be wetted and broken down into smaller pieces for easier swallowing, thus allowing swallowing to start.

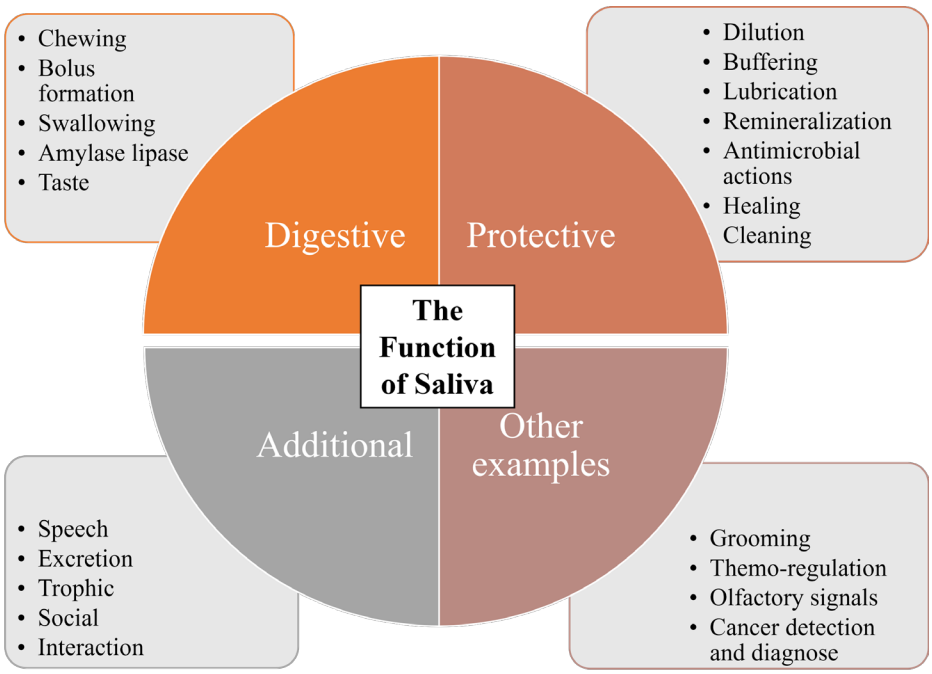

Figure 2. Different categories of saliva's function

Among the many protective properties and benefits of saliva are its capacity to buffer pH changes in the oral cavity, maintain oral mucosa integrity, remineralize teeth, increase immune defense, form boluses for digestion, lubricate the oral mucosa. Its composition can also be used to diagnose diseases by analyzing the proteome. Created by the author. Copyright by the author.

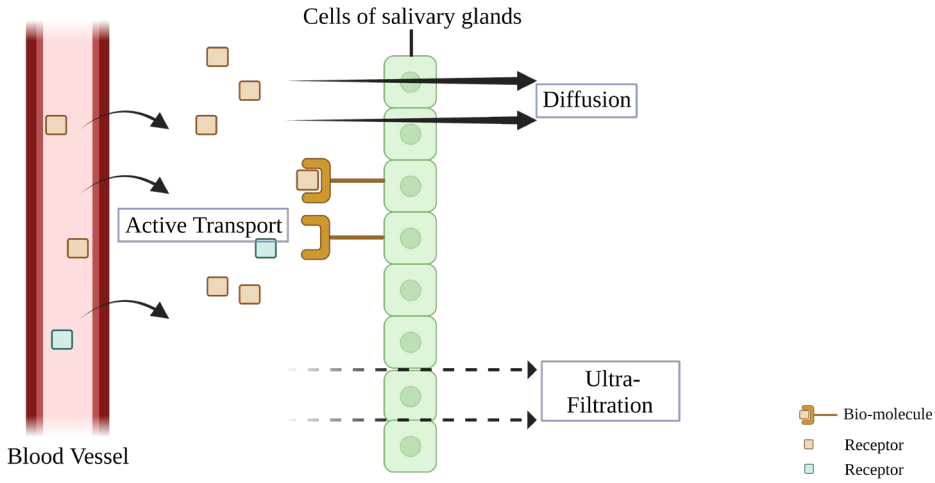

Figure 3. Schematic illuatrations the route of how serum molecules take to enter saliva.
When it comes to diagnostic purposes, saliva can be viewed as functionally equivalent to serum due to the movement of constituents from serum to saliva. Created with BioRender.com.

In addition to its biological functions, the use of saliva as a body fluid for early diagnosis, detection, and disease prediction for progression and prognostics has developed rapidly over the past 20 years[14]. As the liquid component of saliva is derived from blood, there is a high degree of correlation between saliva and blood (Figure 3). Thus, while saliva has many similarities with blood, it has the advantage of being able to be collected using non-invasive approaches (see Table 3 for other merits and drawbacks)[15]. As such, the use of saliva for diagnostic purposes is growing rapidly. With the exploration and expansion of saliva-based assays (salimetrics), our understanding of its proteome, transcriptome, microbiome, and metabolome (which can be combined as the study of salivaomics[16]) has improved; over 1100 proteins and peptides were identified in human saliva in a comprehensive study published in 2008 and built an even more solid foundation for the application of human saliva diagnostics in personalized medicine[17]. For example, MMP8 contained in saliva was identified as a possible marker for periodontal diseases[18]. In the liquid biopsy field, EVs from distal cancer can also be identified in saliva indicating they had travelled to the salivary gland, thus making saliva likely to be a potential diagnostic indicator of circulating DNA in tumors (ct DNA)[19] when compared to its traditional detection in blood using next generation sequencing (NGS) and digital polymerase chain reaction[20]. Therefore, future saliva diagnostics could be used to increase the knowledge regarding the close relationship between oral and systemic health by utilizing biomarkers in saliva; dentistry may be viewed as a primary care provider by incorporating chairside screening for medical conditions.

Table 3. Salivary testing as a diagnostic tool: advantages and disadvantages.

Advantages	Disadvantages
1) Easy, noninvasive, and inexpensive. 2) Safer than serum sampling (there are no needles). 3) Timely screening of the entire population for a specific disease. 4) Medical personnel do not need to be trained. 5) Multiple samples are easy to obtain. 6) Home screening and collection are possible. 7) Cross-contamination risks are minimal. 8) More economical to sample, ship, and store than serum. 9) Requires less manipulation during diagnostic procedures than serum. 10) Commercially available assays for screening.	1) Detection systems are not accurate and portable. 2) Lacking cheap sampling methods. 3) There are no specific biomarkers for diseases. 4) Still causes a lot of pain.

Decreased production of saliva (dry mouth)

Causes

Dry mouth, or xerostomia, is a widespread condition due to a lack of saliva production to keep the mouth moist[21]. On its own, dry mouth isn't a serious medical condition but is a sign that another underlying condition requires treatment. Such conditions may include systemic and local health conditions like dehydration or mouth breathing but also conditions like Alzheimer's disease, uncontrolled diabetes, autoimmune disorders, anxiety, poor nutrition[22], or be due to lifelong habits of tobacco and alcohol consumption[23]. Other major clinical problems may include salivary gland tumors treated with partial or complete glandectomy in conjunction with tumor resection, which results in loss of salivary secretory function. Importantly, dry mouth is a significant long-term and common complication after radiotherapy or chemotherapy for malignant head and neck cancer (HNC) patients[24]. Around 550,000 patients are annually diagnosed globally with HNC, with irradiation therapy (RT) to be the main supplemental treatment[25]. Although uncommon, sleep-related xerostomia is also a category of dry mouth, meaning sleep is interrupted by the need for fluids inside mouth at night and the dryness of the throat. For such patients, the adjustment of night-time monitoring can therefore greatly reduce their night-time discomfort and improve their sleep quality. Fast diagnosis therefore requires a complete assessment of medical and medication (such as stimulants and antihypertensives) history accompanied with patients' age and gender. Treatments for dry mouth are dependent on their cause.

Symptoms and diagnosis

With less saliva, the patient may experience symptoms like burning sensations in their mouth, sticky saliva, and oral fungal infections, difficulty speaking, and

swallowing[26] (Table 4, with detailed treatment introduced later). In addition, there may be issues such as bad breath, sore throat, cracked lips, and difficulty eating or drinking, which all cause various life-impacting pathological events that compromise both dental and general health.

Table 4. Symptoms and palliative treatments[27].

	Symptoms	Current symptomatic therapy
Mouth	Dry mouth Painful mucositis Difficulty eating, speaking, swallowing Increased thirst Bad breath	Review patients' medications Breathe through your nose Drink plenty of water
Teeth	Tooth decay and rampant cavities Trouble wearing dentures	Good oral hygiene Prevent tooth decay Other dentures solutions
Nose	Dry feeling in your nose	Moisturizer
Skin	Dry skin Skin rash	Skin protection cream Immunomodulator: thymulin
Throat, lip and tongue	Dryness and pain Hoarseness	Use a humidifier in you room Change diet styles
Eye	Dry eye	Pilocarpine
Taste	Taste disorders	Avoid caffeine, tobacco, alcohol

In terms of diagnosis, with the development of more reliable and valid questionnaires, more accurate saliva flow measurement devices, and more sophisticated imaging methods, diagnostic techniques for xerostomia have developed in recent years[28]. Tracing a patient's past diseases, past treatment history, and past medication history is the fastest and most effective way to diagnose xerostomia. Xerostomia is a subjective feeling, so the first developed and golden-standardized diagnosis for dry mouth is a subjectively natured questionnaire with a rating scale (visual analog scales (VAS) for the patient to fill out[29-31]). The salivary secretion test is the most clinically applicable way to supplement for diagnosis[32], including measurement of unstimulated whole saliva flow (UWS, less than simulated 0.1 mL/min) and stimulated whole saliva flow rate (SWS, less than 0.5 - 0.7 mL/min). There is a need for such a salivary secretion test because the secretory components (depending on the gland which serves as the source of secretion) and the amount of saliva secreted at various times of the day as well as whether they are stimulated or not vary greatly for humans within the cycle of a day[32]. Standardizing the measurement of saliva secretion through the creation of special devices[33,34] has contributed to help make saliva an accurate diagnostic tool. Contrast-enhanced computed tomography (CT), magnetic resonance imaging (MRI), and ultrasound imaging are examples of imaging methods[35] for diagnosing because in cases of dry mouth, the salivary glands may have atrophy after irradiation, or there may be inflammation or necrosis, showing corresponding changes in MRI signals[36]. A

technetium 99m pertechnetate (TPT)[37] scan of the head and neck is an advanced imaging option. For MR sialography[38] which uses saliva itself to be the contrast medium, small changes in the amount of saliva can be observed and the status of salivary ducts could be observed without using ionizing irradiation as in RT sialography[39].

Salivary gland organs

Salivary gland embryology

The salivary glands and other branched tubular organs like the respiratory system and many internal glands are all formed with branching morphogenesis or organogenesis[40], which is known as the interplay of epithelial or endothelial with the nearby mesenchyme to induce and remodel epithelium into multicellular tubular networks.

An embryo's outermost layer is the ectoderm. Salivary gland is an ectoderm-derived structure (ectodermal appendages) with ectodermal precursors differentiating into organ-specific stem cells to start the dynamic process to form the tissue morphology[40-42] of the salivary gland. Salivary glands start from ectodermal placodes. Because optimal acinus surface area ensures enough saliva daily, salivary gland branching starts in mice at E11 to E16 days[43] and humans E4th to E12th weeks of pregnancy[44]. Single buds become bulbs and continuously develop during glandular differentiation, resulting in treelike extensions (tubes) and lobulation (Figure 4). A hollow duct then occurs, and terminal buds become functional acinus. Thus, saliva can be produced under fully nerve-stimulated after birth for human. Representative developmental stages are summarized in Table 5 and Figure 4.

Table 5. Development of salivary glands.

Stages of development		Characteristics
I	Ectodermal placodes thicken	Adjacent mesenchyme has inductive signals.
II	Bud formation	Condensed mesenchyme condensed to form endothelial plexus (single epithelial bud).
III	Epithelial cord proliferation	This single epithelial bud goes through proliferation and cleft[44] and outgrow into tubes.
IV	Continuous branching and lobule formation	Parasympathetic nerves participate in tubulogenesis[43,45,46] to ensure nerve and tubes are parallel developing.
V	Canalization	Krt 19 positive ductal cells will proliferate and condense in the midline to fuse into microlumen.
VI	Cytodifferentiation	Multicytodifferentiation form end-buds, with the connective tissue encapsuling and blood vessels formation. Myoepithelial cells appear from the external epithelial layer and can contract under innervation regulations.

Complex sequences of morphogenetics suggest multiple intrinsic and extrinsic signalling pathways are tightly coordinated spatiotemporally, such as glial cell-line derived neurotrophic growth factor (GDNF) family, WNT signalling family, and basement membrane proteins families (like network forming collagens, fibronectin, and laminins)[40].

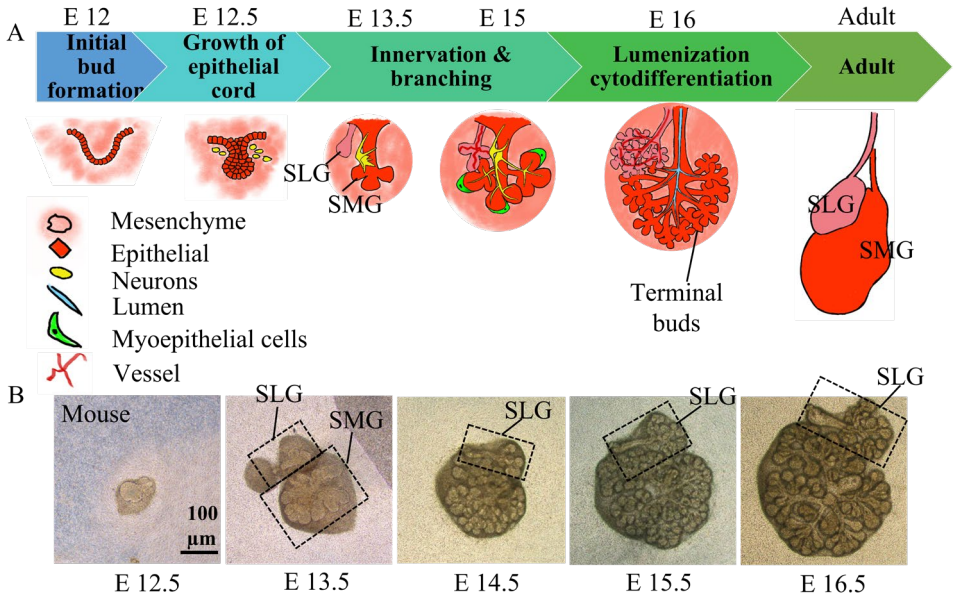

Figure 4. Schematical branching morphogenesis for mouse submandibular and sublingual glands.

(A) Schematic images demonstrate the embryonic submandibular and sublingual glands developmental stages of mouse as E, embryonic days. SMG, submandibular gland. SLG, sublingual gland. (B) Gross observation of mouse submandibular and sublingual glands using bright field microscope in 4 days of ex vivo organ culture. Scale bar: 100 µm. Figure 4A created by the author and Figure 4B, DONG et al. unpublished data. Copyright by the author.

Major and minor salivary glands

Saliva bathes the oral cavity primarily as a mixture of secretions from the major salivary glands (parotid, submandibular, sublingual) and innumerable minor glands (labial, buccal, palatine, and lingual). Detailed comparison and introductions about the major and minor salivary glands in terms of sizes, classifications based on the saliva that they secrete, gland locations (Figure 5), saliva output, duct numbers and openings, innervation distribution and gland functions are listed in Table 6.

The major salivary glands are highly vascularized. The external carotid artery supplies blood to the parotid gland. The facial artery, which is a branch of the external carotid artery, supplies blood to the submandibular gland.

There are more lymph nodes in and around the parotid glands. Roughly 90 % of nodes are located within the glandular tissue for parotid glands. For submandibular gland, they are located between the gland and its fascia.

Parasympathetic nerves primarily stimulate electrolyte secretion, whereas sympathetic stimulation is primary for protein secretion, but these two systems often interact. Sympathetic innervation also regulates blood flow to glands, local inflammation, immunity, and biogenesis. The major salivary glands are highly innervated, so they rest at night and minor glands[47] produce a small amount of saliva continuously to lubricate mouth.

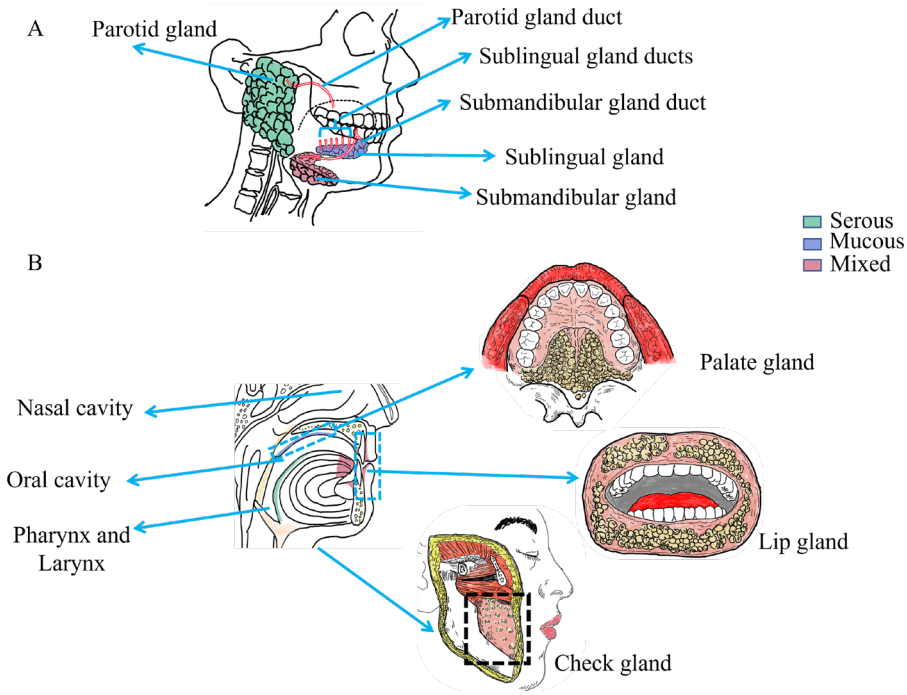

Figure 5. Salivary glands location and types

This diagram illustrates the location and glandular types of major and minor salivary glands. (A) The location and types of major salivary glands includes parotid glands, submandibular glands, and sublingual glands, with their duct openings in the mouth. (B) The location and types of minor salivary glands locating everywhere beneath the epithelium in almost all parts of the oral cavity and oropharynx, with their short ducts opening directly into mouth. Examples that listed here are palate glands, lip glands, and cheek glands. Created by the author. Copyright by the author.

Table 6. Introduction to different salivary glands.

Gland categories and names		Gland types	Bilaterally or not	Size	Locations	Salivary output	Excretory duct	Capsule	Neuronal activity control	Nerve responsibility	Function
Major salivary glands	Parotid gland	Serous gland	Paired	Largest major salivary glands (15 - 30 g)	Between ramus of mandible and sternocleidomastoid-mastoid muscle	50 % of the total daily salivary output[48]	Stensen's duct*1	Encapsulated by connective tissue	Para-sympathetic nerves	For secretion of watery, electrolyte-rich and low protein saliva.	To produce digestive and protective saliva
	Submandibular gland	Mixed gland	Paired	Second largest (7 - 15 g)	Beneath the tongue	Up to 70 %	Wharton's duct*2		Para-sympathetic and sympathetic nerves	For two types of saliva secretion.	
	Sublingual gland	Mucous gland	Paired	Smallest (2 - 4 g)	Beneath the sublingual fold	5 % portion	Several ductal*3		Sympathetic nerves	For producing thicker, protein-rich saliva.	
Minor salivary gland		Mixed gland	Not paired, in patches	Approximately 800 - 1000 individual glands	Scattered around the mucosa in the upper aero-digestive tract, including nasal cavity, oral cavity, pharynx, and larynx	Approximately 1 % or less	Each gland has one opening	Not surrounded	No		To lubricate walls of oral cavity

*1Parotid gland duct: Opens on the buccal wall at the level of maxillary second molar.*2Submandibular gland duct: Opens at sublingular papilla under tongue.

*3Sublingual gland duct: Openings along the sublingual folds.

Salivary gland histology

Salivary glands contain two main components: glandular secretory tissues (parenchyma) and connective tissue (stroma) that surround parenchyma (generally shown in Figure 6). The parenchyma of salivary gland is encapsulated outside by connective tissue and separated into lobes by connective tissue septa, which are further subdivided into lobules. Each lobule is made up of numerous rounded glandular terminal bulbs as secretory units and arborized ductal parts. Three types of secretory acinus are serous acinus (secreting proteins in watery saliva), mucous acinus (secretes viscous fluid), and mixed acinus (forms serous demilune). All salivary glands are mainly made up of a mixture of acinar cells, ductal cells, and myoepithelial cells[49] (shown in Figure 6). Table 7 shows major cellular biomarkers in different histological components, respectively.

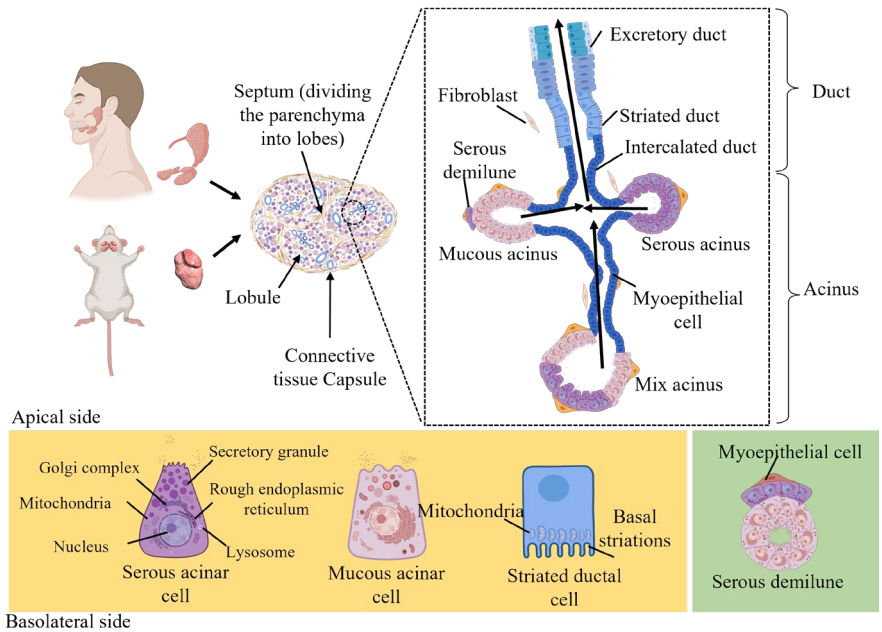

Figure 6. The architecture of mouse salivary glands
A diagram of mouse salivary gland histology showing foundamental substructural units like serous acinus, mocous acinus, and mixed serous-mucous acinus with ductal systems. Serous and mucous acinar cells contains mitochondria, rough endoplasmic reticulum (RER), Golgi apparatus, secretory granules. For striated ductal cells, they are columnar with obvious basal striations produced by the infoldings of basal cell membrane, between which are packed numerous mitochondria. Created with BioRender.com.

Table 7. Major cellular biomarkers for different histological components in salivary gland organs.

The Categories of cells		Biomarkers
Secretory function	Acinar epithelial cells	α-amylase NKCC
	Water-producing acinar epithelial cells	Aquaporin 1, 3, 5
Ductal epithelium	Epithelial cells	Cytokeratins (CK 7, CK 15)
Myoepithelial cells		α-SMA
Tight Junctions		Occludens 1 (ZO-1)
Defense against oral bacteria		Cystatin 3, 10 (Cst 3, 10) Mucin 5b (Muc 5b)
Neural innervations	Neurotrophin	NGF
	Neurotransmitter receptor	Muscarinic acetylcholine receptor III (M3R)

Terminal secretory units

The salivary glands can be divided into parotid glands which are composed of serous acinus, sublingual glands, and minor salivary glands with mucous acinus, whereas submandibular glands have mostly serous acinus and some mucous acinus attached to serous demilunes[50,51] (The blind end of a mucous acinus are serous acinar cells that cap this region, forming serous demilune).

Serous acinus predominantly exist in parotid and submandibular glands and exhibit with granular appearances in histology. They secrete thin watery secretions which are rich in enzymes. Serous acini have narrow lumens compared to mucous acini. They are comprised of groups of serous cells that are polygonal in shape with dense, intracytoplasmic, basophilic zymogen enzyme-containing granules. Both the parotid and submandibular gland show darker staining of serous cells compared with mucous cells with standard hematoxylin and eosin (H&E). Alcian Blue and Periodic Acid Schiff staining (PAS) shows that the parotid gland has neutral mucins while the submandibular gland has mixed neutral and acidic mucins. In serous acinar cells, proteins are transported to from rough endoplasmic reticulum to the Golgi apparatus where they are combined with carbohydrates to form mucin.

Mucous acinar are more often found in sublingual glands and the minor salivary glands. They are formed by round mucous cells with mucin and contain a condensed and basally located nucleus and a large lumen. Rough endoplasmic reticulum, Golgi apparatus, and mitochondria, are not readily apparent. They have a diffuse mass of secretory material that is weakly stained in H&E staining and visible with standard light microscopy. Mucin generated by the mucous acini varies from red to purple to royal blue in PAS staining, indicating that it is a mixture of neutral and acidic mucin.

Mixed seromucous acinus are most prevalent in the submandibular (serous predominance) and sublingual (mucous predominance) glands, as well as some minor salivary glands in the lips, cheeks, and anterior tongue. It has a classical

structure on one side with mucous acinus and crescent-shaped caps of serous cells (serous demilunes) (see Figure 7).

Treelike salivary gland ducts

The three main types of ducts in the salivary gland are intercalated, striated, and excretory ducts, forming a treelike ductal delivery system (Figure 6). Intercalated and striated ducts are intralobular ducts and excretory ducts are interlobular ducts.

The acini form from intercalated ducts in parotid and submandibular glands as well as sometimes in sublingual glands. There is a single layer of cuboidal epithelium lining the acini. Compared to primitive acinar and ductal cells of fetal salivary glands, intercalated ductal cells retain primitive characteristics and can differentiate into other secretory cells[52], and may play a role in the pathogenesis of pleomorphic adenomas[53] (which is an epithelial (ductal) neoplasm of the salivary gland characterised by neoplastic proliferation with myoepithelial components, with a potential for malignancy).

Striated ducts are intralobular ducts having an intermediate caliber between intercalated and excretory ducts; they have a columnar epithelium with prominent basal striations along their lumen, formed by mitochondria alternately folding with the folded cell membranes. These folds increase the surface area of the cell membrane, enabling active transport through the duct. Thus, sodium and chloride ions are reduced in isotonic primary saliva by water resorption and ion secretion, while carbonate and potassium ions are increased. The water, protein, and electrolyte secretion inside of saliva is energy-consuming and thus a high concentration of mitochondria is required to provide energy. Striated ducts eventually drain into the interlobular ducts.

The excretory ducts (ED) are formed by the striated ducts that partially merge in the interlobular portions of the parotid and submandibular glands. In ED, pseudostratified epithelium is the predominant type of tissue. Columnar luminal and basal cells may also be present. Only a few species of ED have sequestratory granules located in their apical cytoplasm, but they may also contain a wide range of oxidases, acid hydrolases, and transporters, indicating that these ducts serve more than just facilitating saliva production, but also perform metabolically active roles in glandular function (Figure 7).

Myoepithelial cells

Acini and intercalated ducts of salivary glands, as well as other exocrine organs, contain myoepithelial cells. These are a starfish-shaped cell type derived from basal cells in large ducts and form a basal layer around acinar and ductal cells. In addition to their elongated processes, they contain bundles of contractile myofilaments. As they are an intermediate cell type with features of both epithelial and smooth muscle

cells, they are able to contract rhythmically when parasympathetic or sympathetic stimulations are applied to squeeze secretions into ducts (including intralobular, interlobular, or excretory ducts) before draining into the mouth[54]. Acini cells as well as the underlying parenchyma, are supported by these cells, so when the myofilament component of myoepithelial cells is lost or thinned, as in sialadenosis, the acini lose their mechanical support and secretory granules accumulate intracellularly, resulting in an expansion of these cells. Additionally, they may be able to propagate secretory stimuli or reduce saliva backflow[55].

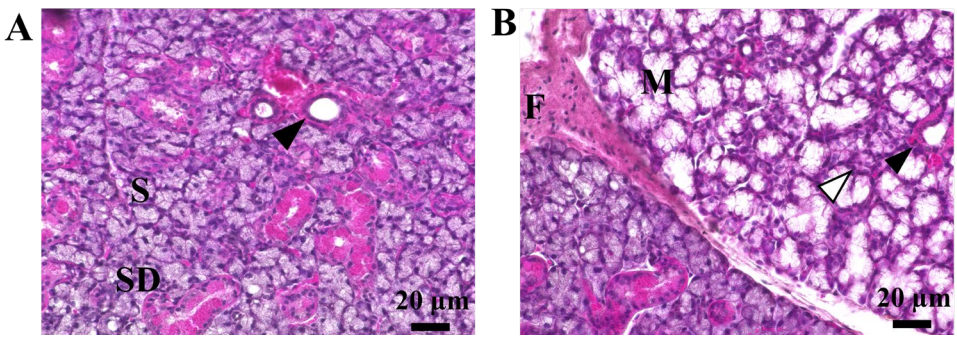

Figure 7. Histological H&E staining for mouse submandibular glands
Submandibular glands from adult mice averaging 7 - 9 weeks old were processed with xylene, embedded in paraffin blocks and stained with H&E. (A) H&E staining of a healthy mouse's submandibular gland shows strongly stained serous acinar cells (S) with a circular or oval gland morphology. Under H&E staining, pale and light stained mucous acinar cells (M) together with strongly stained serous cells (S) form the charactered structurure serous demilunes which are labeled in white arrows in Figure 7B. The fibrous connective tissue between intertubules is called F. The ducts with simple columnar epithelium lining in (A) and (B) are intercalated or striated (striated ducts shorten as SD is shown in black arrows). The scale bar is 20 µm (40 times magnification). Dong et al. unpublished data. Copyright by the author.

Connective stroma tissue

The salivary gland extracellular matrix and stroma (including endothelial and lymphatic vessels) is mainly maintained by fibroblasts but also contains endothelial, lymphatic, nervous cells, adipocytes, macrophages, mast cells, leukocytes, plasma cells, and macrophages. CD34-positive fibroblasts in the stroma are thought to function as immunosurveillance agents[56]. Plasma cells are scattered throughout the stroma, secreting IgA to protect the mucosa from infection. As a surrounding capsule, the stroma separates the gland from the adjacent structures. Along with proteoglycans and glycoproteins, collagen and reticular fibres are embedded in the stroma. Small ganglia can also be found within the gland stroma.

Salivary gland disorders and pathology

A disorder of salivary gland secretory function can occur as a consequence of many types of diseases and treatments[57], including diabetes and Sjögren's syndrome, as well as oral manifestations after systemic drug applications, or complications following radioisotope or irradiation treatment for antineoplastics. Moreover, sialadenitis associated with salivary gland duct stones and other glandular lesions (such as benign or malignant tumours of the salivary glands) can also result in salivary gland dysfunction. Therefore, all of the above circumstances can contribute to salivary gland dysfunction symptoms. Below are a few examples and descriptions of some of the situations.

Complications after irradiation therapy

The parotid glands are naturally included in or close to the target field of irradiation[21] during irradiation therapy for nasopharyngeal carcinoma patients. Irradiation-induced xerostomia is hypothesized to be a multi-factorial clinical manifestation involving damage to major and minor salivary glands and associated nerves and endothelium[58].

Irradiation therapy for head and neck cancer patients includes the parotid gland in irradiation pathway. In clinical radiotherapy, irradiation is given in fractions, such as 2 Gy a day, 5 days a week, for 5 - 7 consecutive weeks. Fractionated radiotherapy reduces irradiation damage to non-malignant tissues[59]. Patients may experience 50 % saliva volume reduction in the first week following radiotherapy[60]. Irradiation-induced xerostomia is believed to be caused by multiple factors, including damage to the salivary glands, nerves, and endothelium. Salivary gland epithelium consists of 80 % acini and 20 % ducts, surrounded by blood vessels, nerves, and fibrous connective tissue. Researchers initially thought that apoptosis of acinar cells caused salivary gland function loss during the acute phase of injury[61,62]. However, further research has shown that acinar cells do not undergo massive apoptosis in the early stage[63]. Therefore, the early stages of irradiation injury cannot be explained by the "apoptosis theory".

According to current understanding of salivary gland dysfunction in different stages of irradiation injury, salivary glands are highly radiosensitive at the acute stage due to interference with signal transduction pathways (muscarinic receptors and aquaporin 5). Consequently, watery secretions are hindered[64]. Later, as time goes on after irradiation, the impact of cumulative exposure to irradiation (IR) will have a combined effect on the acini, ducts, nerves, blood, and stroma interact and further damage to the tissue develops over time[65]. The comprehensive issues that develop with time could include different degree of fibrosis and inflammation, cellular senescence, ongoing parenchymal cell apoptosis, microvascular dysfunction caused by endothelial cell injury, and reduced parasympathetic

function. With the surrounding micro-environment impaired, stem cells can become exhausted and depleted and excess extracellular matrix deposits remain. Ultimately, due to combined alterations on the acini, ducts, nerves, blood, and stroma, fibrosis irreversibly replaces the salivary gland parenchyma and renders the salivary glands incapable of secreting saliva[66] or an altered saliva composition with changed pH and altered bactericidal properties[67] (Figure 8).

With the continuous progress of research, it becomes increasingly apparent that nerves and blood vessels also play a significant role in irradiation injury[68]. Studies have shown, for example, that neuronal apoptosis can occur within 24 - 72 hours after IR and that neurotrophic nutrients (NRTN) stimulate neuronal survival and regeneration in salivary gland explants[69]. Endothelial cell death can occur at least four hours after IR in murine models[70]. The proliferation of endothelial cells may be stimulated by stem cell factor (SCF) and granulocyte colony-stimulating factor (G-CSF) in irradiated glands[65], thereby increasing the production of saliva.

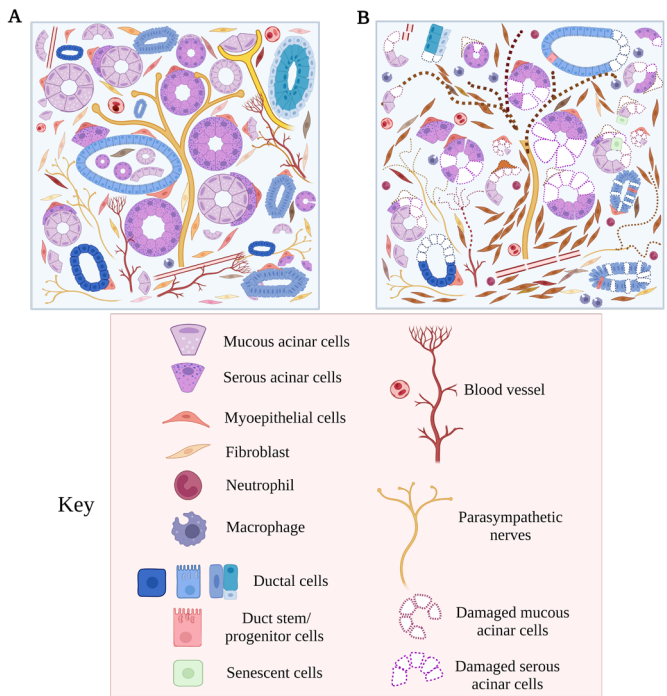

Figure 8. The changes in salivary glands following irradiation injury.
(A) The salivary gland maintains its functional integrity by maintaining the homeostasis of the gland parenchyma. As part of the niche, neural, blood vessel, and mesenchymal microenvironments must maintain a fine balance between self-renewal and differentiation of stem and progenitor cells. (B) Acinar progenitor cells fail and the acini die as a result of therapeutic irradiation in head and neck cancer, while irradiation also damages parasympathetic innervation. As inflammatory cells invade the glandular niche, fibrosis occurs, and the vascular system fails to function, the glandular niche irreversibly fails. Created with BioRender.com.

Sjögren's Syndrome

SS is an autoimmune disease characterized by chronic inflammation of exocrine glands throughout the body, such as the salivary glands and lacrimal glands (LG)[71]. Due to the fact that Sjögren's syndrome is an autoimmune disease, it is also seen in patients with rheumatoid arthritis (RA), systemic lupus erythematosus (SLE), scleroderma, and polymyositis, which may involve additional extraglandular organs such as the lung, kidney, and skin. SS can either occur alone (primary SS, pSS) or in association with other autoimmune diseases (secondary SS, sSS)[72].

Table 8. General accepted criteria to diagnose SS

Number	Categories
I	Ocular symptoms
II	Oral symptom
III	Ocular signs: at least one test is positive
	1. Schirmer's test I, performed without anaesthesia (≤5 mm in 5 minutes)
	2. Rose bengal score or other ocular dye score (≥4 according to van Bijsterveld's scoring system)
IV	Histology: In minor salivary glands (obtained through normal-appearing mucosa), focal lymphocytic sialadenitis, defined as a number of lymphocytic foci (near normal mucous acini and containing more than 50 lymphocytes) per 4 mm^2 of glandular tissue (evaluated by an expert histopathologist).
V	Salivary gland involvement: at least one test is positive
	1. Unstimulated whole salivary flow (≤1.5 mL in 15 minutes)
	2. Parotid sialography showing punctate, cavitary or destructive pattern, reminding for a diffuse sialectasias, no obstruction in the major ducts
	3. Salivary scintigraphy showing delayed uptake and excretion, reduced concentration
VI	Autoantibodies in the serum:
	1. Antibodies to Ro/SSA
	2. Antibodies to La/SSB antigens
	3. Both antibodies

In order to diagnose Sjogren's syndrome[72,73], subjective symptoms such as dry mouth and eyes are highly important reference values. This subjective symptom has significant individual and regional differences in measurement and evaluation, and its specificity is low[74]. An auxiliary diagnosis based on objective and effective examination is therefore required (Table 8). Serological tests for anti-SSA antibodies (Ro) and anti-SSB antibodies (La) (Ro/SSA and La/SSB), physical examination, dry eyes and mouth for a period of three months, positive Schirmer's tests (primarily used to diagnose dry eye syndrome), as well as an unstimulated whole saliva flow test to determine salivary gland function and aid in diagnosis. After salivary gland biopsies, salivary gland histopathology provides the most important diagnostic basis. Sjögren's syndrome has a histological hallmark of focal lymphocytic infiltration. Analysing the infiltrating and focus score (FS)[75] is a key indicator for the diagnosis of this disease. Chronic inflammatory lymphocytic infiltration is defined as a lymphocytic foci contains >50 lymphocytes per 4 mm^2

tissue in minor salivary gland biopsies. With a focus score >1, histologically it can be diagnosed as Sjögren's syndrome. As a conclusion, glandular infiltration of lymphocytes and the presence of anti-SSA autoantibodies are two key indicators of SS, while ocular problems and salivary hypofunction may also be helpful to diagnose SS[73].

The pathogenesis mechanism of Sjögren's syndrome remains unclear. It is generally believed that environmental factors trigger inflammation among individuals with a genetic predisposition to Sjögren's syndrome. Then the exposure to self-antigens, the activation of both B cells and T cells as well as disturbed cytokine networks, and the apoptosis of exocrine gland epithelial cells[76,77] all contribute to the progression of disease. The initial steps in pathogenesis are likely to involve glandular epithelial cells, glandular vascular endothelial cells, or the stromal and dendritic cells that lie beneath them[78]. Stress or infection can trigger the accumulation of apoptotic debris, thereby stimulating plasmacytoid dendritic cells to produce interferon (IFN) type I. Upon accumulating apoptotic debris, plasmacytoid dendritic cells produce interferon type I. In addition to stimulating IFN-primed effector cells, IFN type I also stimulates adjacent target cells by presenting IFN signatures. Neutrophils can further damage tissue by forming extracellular traps, resulting in the production of IFN type I. As autoantibodies trigger netting of IFN-primed neutrophils, RNA-associated autoantibodies (SSA/Ro, SSB/La) will increase, further amplifying the loop. Autoantibodies and RNA form immune complexes in conjunction with self-apoptotic debris. Figure 9 summarizes the pathogenesis. Sjögren's syndrome is characterized by an infiltration of lymphocytes into specific organs and by autoantibodies to SS-A, an antigen found on all nucleated cells. In primary Sjögren's syndrome, dendritic cells trigger T and NKT cells, causing decreased complement solubilization and immune complex accumulation as inflammation exhausts the complement system. IFN-driven pathogenic loops result in a decline in the functional ability of target tissues. In Sjögren's syndrome mice (non-obese diabetic severe combined immunodeficiency mice), epithelial cells and venules undergo changes even without functional lymphocytes[79], which may result from the production of metalloproteinases or secretion of other cytokines from infiltrating immune cells which alter the functional units of the salivary gland. In support of the hypothesis that secreted factors from infiltrating immune cells are responsible for causing salivary gland dysfunction, the glands of these mice do not become dry until T lymphocytes are present. As part of the process of homing lymphocytes into the gland, adhesive proteins are upregulated and chemokines are produced that perpetuate the cycle of lymphocytes and dendritic cells migrating into the gland, further causing damage[80,81]. In addition to dendritic cell abnormalities, organ-specific lymphocytic localization has been suggested as a contributing factor[82]. These cells have been suggested to cause abnormal lymphocyte retention in tissues as well as the production of type 1 interferon, which activates lymphocytes and metallo-proteinases.

There are several advantages to using animal models[83] to study the pathogenesis of SS. Over the past few years, several animal models have been developed that reproduce the key characteristics of primary SS patients, including secretory dysfunction, glandular inflammation, and presence of autoantibodies.

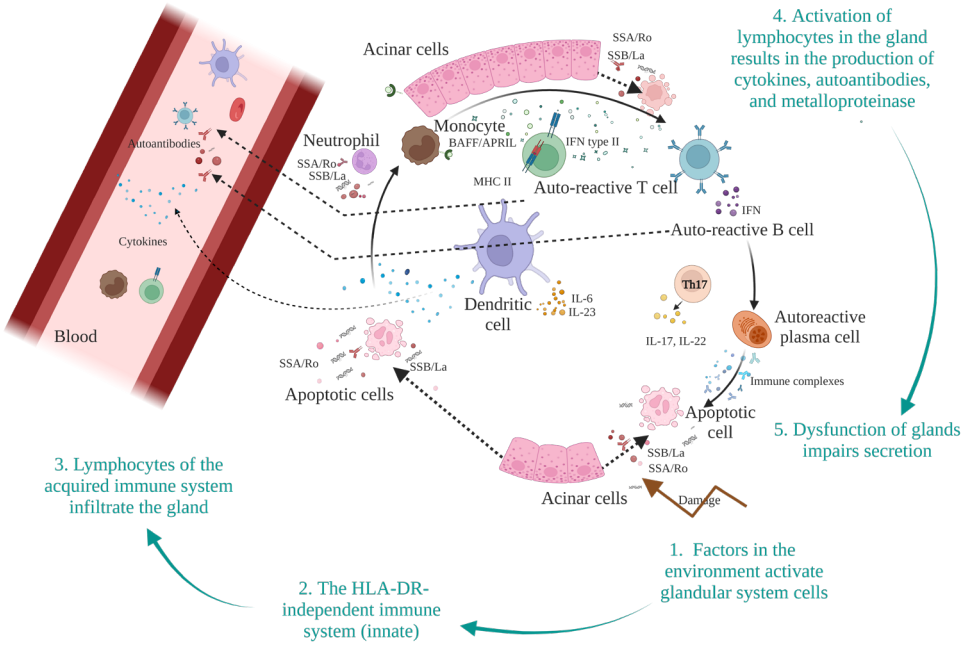

Figure 9. The pathogenesis in primary Sjögren's syndrome is an interferon-mediated self-amplifying multifactorial loop.
Plasmacytoid dendritic cells produce interferon type I when apoptotic debris accumulates. IFN type I stimulates IFN-primed mature effector cells as well as IFN signatures on adjacent target cells following binding. By forming neutrophil extracellular traps, neutrophils can cause further tissue damage, causing IFN type I production as well. RNA-associated autoantibodies (SSA/Ro, SSB/La) will increase as autoantibodies trigger netting of IFN-primed neutrophils, further amplifying the loop. Autoantibodies and RNA form immune complexes in conjunction with self-apoptotic debris. As inflammation exhausts the complement system, complement-mediated solubilization becomes decreased and immune complexes accumulate. In primary Sjögren's syndrome, dendritic cells trigger T and NKT cells. IFN-driven pathogenic loops result in functional decline in target tissues. The T-helper cells are Th17; IL: interleukin; MHC is major histocompatibility complex. The B-cell activating factor is BAFF. Created with BioRender.com.

Salivary gland tumors

Patients with lower lip biting are susceptible to a variety of benign salivary gland neoplasms, the most common of which is mucocele[84]. Malignant salivary gland tumours (MSGT) are very rare diseases (incidence rate 0.5 - 2 per 100,000 people), accounting for 20 % of salivary gland tumours and about 1 - 7 % of head and neck tumours. Each year, approximately 53,000 new cases of salivary gland cancer are

reported worldwide[85]. In accordance with statistics, the incidence rate ranges from 40 to 60 years old, and men are slightly more susceptible than women[86]. The most common malignancies are mucoepidermoid carcinoma (MC) and adenoid cystic carcinoma (ACC)[87]. Parotid gland tumours are the most common form of salivary tumour, but only 25 % of them are malignant. The malignant transformation rate for submandibular glands is 40 % - 45 %, for sublingual glands is 70 % - 90 %, and for minor salivary glands is 50 % - 75 %. The main cause of salivary gland tumours is unknown. The tumours are heterogeneous and can occur from multiple cell types within the tissues (Table 9). In addition to smoking and alcohol consumption, there are some risk factors associated with the etiology of the disease, such as exposure to chemicals and hair dye, exposure to ultraviolet irradiation previously, and a history of immune-suppressive or HPV virus-related diseases. Currently, MSGT is more inclined to utilize immunohistochemical staining and morphological features for diagnosis[88]. It is worth mentioning that protein and molecular analyses[89] of MSGT may reveal genetic changes, which may provide insight into the discovery of new treatments for salivary gland tumours as well as predictive biomarkers[90]. Also understanding the etiology, progression, histology demonstration, and metastasis of malignant salivary gland tumours may facilitate our study on salivary gland regeneration.

Table 9. The most common cancer of salivary glands.

Type	Origin	Most common location	Metastatic	5-year survival rate	Molecular targests and pathway activition
Mucoepidermoid carcinoma[91]	Excretory stem cells	PG	Yes, regional lymphnodes	22-86 %	Notch, Hes1, EGFR, P53,Krt 5
Adenoid cystic carcinoma[92] (ACC)	Intercalated stem cells	minor SG	Yes, lungs	89 %	Notch, TGF-β, c-Kit, Myb, p63
Acinic cell carcinoma[93]	Intercalated stem cells	PG	-	76 %	p63, SOX2
Polymorphous adenocarcinoma[94]	Intercalated ductal cells	minor SG	Rarely perineural lymphnodes	80 %	p63
Squamous cell carcinoma[93]	Excretory stem cells	PG, SMG	Neck region	-	WNT/β-catenin, SOX2
Non-Hodgkin lymphoma[95]	Infiltrating immune cells	PG	Bone Marrow metastatic is common.	69 %	p53, INK4a, RB, mTOR, NF-κB, BCL-1, c-MYC
Pleomorphic adenomas[93,96]	Intercalated stem cells	PG	no	-	Krt5

Animal disease model

The development of experimental animal models has been extended to a wide variety of diseases to simulate clinical situations that cause salivary gland dysfunction[97]. These animal models included irradiation or radioisotopes, ligation of salivary gland ducts, the administration of inflammatory agents to induce inflammation, mechanically injuring salivary gland ducts, or the use of drugs or genetic manipulation. Through the development of these animal models, we have been able to gain a deeper understanding of the disease's pathogenesis, how it progresses and pathological characteristics. Below is a brief summary of the models used to date and major findings (Table 10).

Table 10. An overview of experimental animal models that mimic diseases associated with salivary gland dysfunction.

Model's typel	Methodology for experiments	Pathological targets
Irradiation model	Irradiation using experimental equipment[98].	Loss of salivary gland function due to irradiation.
Radioisotope model	A radioiodine administration[99].	Salivary gland function is reduced as a result of radioactive iodine exposure.
Ductal obstruction (ligation) model	Obstruction of the salivary duct through the use of surgical sutures or aneurysm clips[100].	The condition of obstructive sialadeitis.
Inflammation model	Using animal models of autoimmune diseases[101] or inflammongens.	Sjögren's syndrome, or inflammation caused by bacterial.
Mechanical injury	Using biopsy punches, direct tissue damage is induced[102].	Inflammatory sialadeitis caused by trauma
Systemic diseases or medications	The use of animal models of systemic diseases and/or the application of their therapeutic medications[103].	Diabetes, renal disease, hypertension, and/or their therapeutic interventions may result in salivary gland alterations.

Animal models of irradiation injury are one of the most commonly used animal models of salivary gland dysfunction. Currently, the majority of animal irradiation models used to simulate irradiation therapy for head and neck cancer patients are conducted on mice and rats. At the histopathological and some genetic level, these experimental models present disease-related changes associated with salivary glands. Table 11 presents common animal models for single-dose or fractionated irradiation treatments. The treatment of fractionated irradiation in animals is often simulated as a real treatment for patients receiving fractionated irradiation therapy, which is given in small doses (2 Gy in one dose) over several weeks (6 to 8 weeks). In the majority of the animal models, irradiation of the salivary glands results in extensive deterioration, including acinar atrophy, interstitial fibrosis, loss of glandular parenchyma, ductal hyperplasia, and striated duct dilation, along with decreased AQP5 expression. This largely mimics the pathology of human

irradiation damaged salivary glands. A deterioration in regenerative potential (Shh signal activation) and stem cell expression (Sca-1) is a result of late post-irradiation effects (parasympathetic dysfunction and nonparenchymal tissue damage)[104]. Mice and rats and human model have major genetic differences[105,106]. Recognition of differences between species is therefore necessary to apply the results from rodent models into humans. The following is a comparison of the salivary glands between humans and rodents[107,108] (Table 12).

Table 12. A comparison of the salivary glands between humans and rodent.

	Categories	Human	Rodent
Paroid gland	**Size:**	1st largest	2nd largest
	Histology:	Mainly consist of serous acini	Mainly consist of serous acini
		Prominent intralobular adipose tissue	Less prominent intralobular adipose tissue
	Location:	Antioinferior area of ear	Posteroinferior area of ear
Submandibular gland	**Size:**	2nd largest	1st largest
	Histology:	Both serous and mucous acini	Mixed composition with predominant serous acini
		Marked demilunes	Less/no marked demilunes
		-	Prominent: granular convoluted ubule producing various growth factors
	Location:	Submandibular area	Ventral cervical area
Sublingual gland	**Size:**	Smallest in major glands	Smallest
	Histology:	Mainly consist of mucous acini	Mainly consist of mucous acini
	Location:	Sublingual area	Ventral cervical are

Parotid glands are the largest salivary glands in humans, while submandibular glands are the largest salivary glands in rodents. Minor salivary glands in mice are too small and difficult to dissect for biopsy to be used as a diagnostic tool for Sjogren's syndrome, but human minor salivary glands can be dissected. The location of the major salivary glands is also different between rodents and humans. The submandibular glands are located in the head (i.e., submandibular region) of humans, while submandibular glands of rodents are located in the cervical area. Thus, in rodent models of irradiation, the neighbouring tissue which may also be co-irradiated is very different. Histologically, sexual dimorphism in granular convoluted and intubated cells (GCTs and GIDs, respectively) is demonstrated in mice. This means male submandibular glands have larger and more numerous GCTs than glands in female. These GCTs are composed of serous-like exocrine cells between the intercalated ducts and the striated ducts. While GID cells are found to be located in the female SMG intercalated ducts, there are not found in males[109]. In contrast, human SMG does not have granular convoluted tubules and does not display this sexual dimorphism[110]. Due to their influence on histological features and downstream analyses, careful attention must be paid to these species and sex factors.

Table 11. Irradiated animal model

Animal	Target Gland	Total Dose	Dose Rate	Single or Fraction	Peroid	Experiment Outcomes	Histopathological characteristics
Mice	PG	5 Gy	-	Single	30d, 60d[62,68,111,112]	IGF-1 suppress salivary gland dysfunction after IR.	In the short term, irradiation induces cell mitosis and compensatory proliferation. Strict and intercalated ducts show inflammation. Acinar secretory granules are discharged. In the longer term, mild atrophy of glands. Damage to innervation, blood vessels, stroma.
	SMG	13 Gy/28 Gy	6MV energy X-ray	5d, fractions of 5.6 Gy/d	48h, 72h; 2w, 8w[113]	IL6 pretreatment prevents both senescence and salivary gland hypofunction.	
	PG, SMG, SLG	15 Gy	1.55 Gy/min	Single	10d, 30d, 60d, 120d[114]	TPL or 3-AB attenuated recover salivary fluid secretion.	
Rat	SMG	18 Gy	2 Gy/min	Single	4d, 7d, 28d, and 56d[115]	ALA mediating Nox2 preservation of salivary function	The remaining acinus are disorganized. There is marked acinar atrophy and fibrosis. There is visible, but unevenly distributed loss of acinus.
Minipig	PG, SMG	70 Gy	2 Gy/min	35d, fractions of 2 Gy/d	30d[116]	Irradiation of 70 Gy in minipig show structural and functional injury on salivary glands	Acinar atrophy, fibrosis, and parenchymal loss. Acinar cells are vacuolated, secretory granules are lost. Lymphocytes diffusely infiltrate acinar cells.
Rhesus monkey	PG, SMG	50, 55 Gy (CHART)	2 Gy/min	50 Gy in 20 fraction/4w 55 Gy in 25 fraction/5w 54 Gy in 36 fractions (12d)	16w[117]	Parotid glands are more sensitive to irradiation compared to submandibular glands.	In atrophied acinus lobes, there are many intralobular ducts and marked cytoplasmic granularity. There are also fibrous connective tissue infiltrates between lobes.
Rabbits	PG, SMG	10, 20, 30, 40 Gy	0.4 Gy/min	5, 10, 15, 20 days, fractions of 2 Gy/day	immediately [118]	Parotid myoepithelial cells increase proliferation in dose-dependent way.	HE sections revealed mild to moderate inflammatory cell infiltration in all irradiated groups, and salivary gland myoepithelial cells proliferated more rapidly after irradiation.

Senescence

Endogenous as well as exogenous stresses (e.g., irradiation induced DNA damage, telomere dysfunction, activation of oncogenes, persistent DNA damage) result in senescence, which is characterized by permanent proliferative arrest and inflammatory effects[119]. Senescence can also be a controlled process that occurs during embryonic development as well as is a hallmark of normal aging. The defining characteristic of aging is stable growth arrest, which ensures that damaged and transformed cells do not continue to reproduce[120]. This is achieved by activating a tumour suppressor network of $p16^{INK4}$/Rb and p53/$p21^{CIP1}$.

The drivers to senescence can be many. A combination of impairments, including irradiation, telomere attrition, metabolic and proteostasis dysfunction, carcinogenesis, or oxidative stress, are all other important driver of senescence, leading to DNA damage[121]. As the signalling cascade of the DNA damage response (DDR) is triggered, the deposition of phosphorylated histone H2AX (γH2AX) and 53 binding protein 1 (53BP1) increases, thereby activating the following kinase cascade, eventually leading to p53 activation. This in turn causes cell cycle arrest (shown in Figure 10 and Table 13). The insulin/IGF signalling pathway has been associated with aging and longevity[122], research has demonstrated that IGF1 could together with p21, play a role in signalling pathways that signal cell cycle arrest[123].

Table 13. Most common protein in senescence

Protein or marker	Role in senescence
Senescence-associated β-galactosidase	Increased activity at pH 6.0 in senescent cells
p53	Its activation triggers cell cycle arrest
Rb (retinoblastoma suppressor protein)	Its activation triggers cell cycle arrest
$p21^{CIP1}$	Inhibits cyclin-dependent kinase; downstream of p53
$p16^{INK4A}$	Inhibits pRb phosphorylation and inactivation
Bcl-2	Increase expression of senescent cells, inhibit apoptosis
macro H2A1.1	Macro H2A1 isoform; SAHF marker
H3K9Me2/3 (lysine 9 di- or tri-methylates histone H3)	SAHF markers
HP1 (heterochromatin protein 1)	SAHF markers
Phosphorylated Histone H2A.X (Ser139)	DNA damage markers
MMP3 (matrix metalloproteinase-3)	SASP components
TNF-α (tumor necrosis factor α)	SASP components
IL-6 (Interleukin 6)	SASP components
HMGB1 (High Mobility Group Box B1)	SASP components

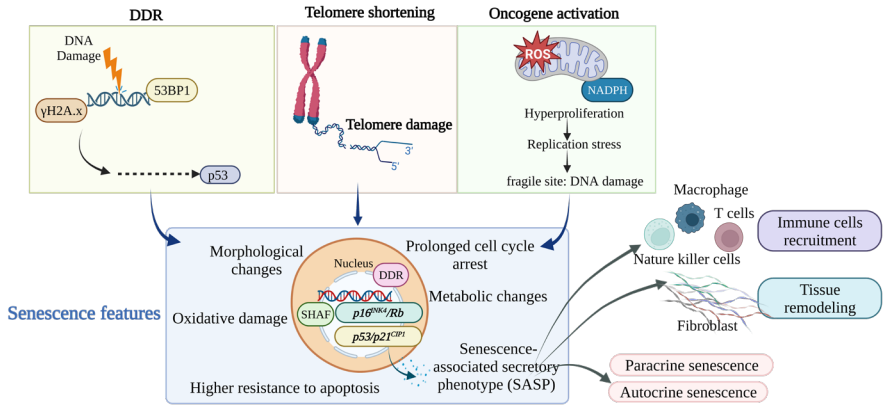

Figure 10. The drivers and phenotypes of cellular senescence and functions of SASP. Created with BioRender.com

In order to identify senescent cells in culture or tissue samples, multiple markers are used because there is no single biomarker for senescent cells[119]. The first and still the most widely used biomarker to detect senescent cells in cultured cells and in fresh tissue samples is the accumulation of a lysosomal enzyme termed 'senescence-associated-β-galactosidase' (SA-β-gal)[124]. Senescent cells also accumulate lipofuscin. Sudan black B staining containing biotin have recently been developed for use as diagnostic tools. In addition to their abnormally enlarged and flattened morphology, senescent cells possess disproportionately large nuclei. Senescent cells normally accumulate two cyclin-dependent kinases known as p21 and p16 that inhibit p53- and RB-mediated tumour suppressor pathways. It has been demonstrated that the expression of p21 and p16 can serve as surrogate markers for senescent cells in mouse models that eliminate senescent cells selectively. As additional markers of senescent cells, nuclear senescence-associated heterochromatin foci are also present, but appear to be specifically associated with aging caused by oncogene activation. Telomere-associated foci may also serve as markers. As a marker for general senescence, the senescence-associated secretory phenotype (SASP), mainly the proinflammatory cytokines interleukin 6 (IL6) and IL8, can also be measured transcriptionally and proteomically (shown in Figure 10).

In multiple organs, irradiation induces senescence. Irradiation can induce senescent cells in salivary gland stem and progenitor cells, suggesting that irradiation-induced salivary gland insufficiency is caused by senescent cells[125]. To eliminate senescent cells, senolytic compounds such as ABT263, with activity against anti-apoptotic proteins BCL-2 could be used. Thus, senolytic therapies may be promising to explore in the future to treat irradiation-induced xerostomia. In addition, irradiation causes bone cell senescence; thus, bone cells in the path of irradiation can become senescent and secrete characteristic SASP factors; this may interfere with bone marrow stem cell differentiation and subsequent phenotypes of

immune cell infiltration into the salivary gland or systemically through paracrine signals[126]. Thus, organ-to-organ communication in the context of senescent cells and their SASP (both through aging and concomitant injury) is an important emerging concept.

Treatment and prevention of dry mouth

There is no cure for dry mouth, only relief from it. Preventative and conservative remedies[27,127] include a quick review of every patient's medication history to determine the cause of xerostomia. If possible, the attending physician will recommend, and quickly alter the patients' medication to see if withdrawal of a specific prescription can relieve symptoms. In addition, cessation of the use of tobacco and alcohol usage are also recommended and can contribute to a reduction in the symptoms of dry mouth[27]. After xerostomia is ultimately diagnosed, only symptomatic or palliative treatments are available; this is independent of partial or complete loss of functioning secretory tissue that remains. The most common and practical method is to prescribe substitutes like mouth humidifiers to locally replace saliva and increase the moisture content of the mouth[128].

Artificial saliva

As a non-Newtonian fluid, artificial saliva is similar to natural human saliva in terms of fluid properties and molecular composition, and it performs most of the same functions that natural saliva does, namely lubricating, moisturizing, remineralizing, and regulating microorganisms[129,130]. Approximately 700 different types of bacteria have been identified in the oral cavity, and the oral microbiome is also constantly changing. As a result of the accumulation of mixed biofilm plaque on teeth, which contains more than 500 species of bacteria, bacteria then colonize the tooth surfaces, resulting in dental caries and periodontal disease and further general health issues as a consequence[131]. Therefore, the use of artificial saliva preparations in patients suffering from xerostomia requires that the antimicrobial properties of saliva can also be restored.

Consequently, artificial saliva is comprised primarily of matrix materials and pre-caries antibacterial auxiliary materials[132]. Among the effective matrix materials[133] are carboxymethylcellulose, glycerol, and mucin combined with xanthan gum or guar gum, whereas antibacterial auxiliary materials include fluoride, xylitol, enzymes, etc.

The development of fully functional artificial saliva is thus complex. Normal saliva is composed of a liquid phase of electrolyte solution, a continuous network structure resembling a scaffold, less water-soluble proteins and saliva molecules suspended within the network structure, phase microorganisms and epithelial cells

suspended within the network structure[134]. The correct adjustment of natural saliva's viscosity and viscoelasticity is a key of the current areas of development for artificial saliva[135]. A great deal of future research is needed to understand how artificial saliva can be developed for xerostomia patients; this will need to be done in parallel to better understanding the fluid and biological functions of natural saliva[136]. There are numerous dosage forms theoretically available for administering artificial saliva, including mouthwash, sprays, gels, and so on. Artificial saliva could thus become a scientific alternative strategy to mouth health and may become a reality in the future, despite some temporary issues like inconvenient portability, poor oral comfort, and less relief time[129].

Salivary gland transfer surgery

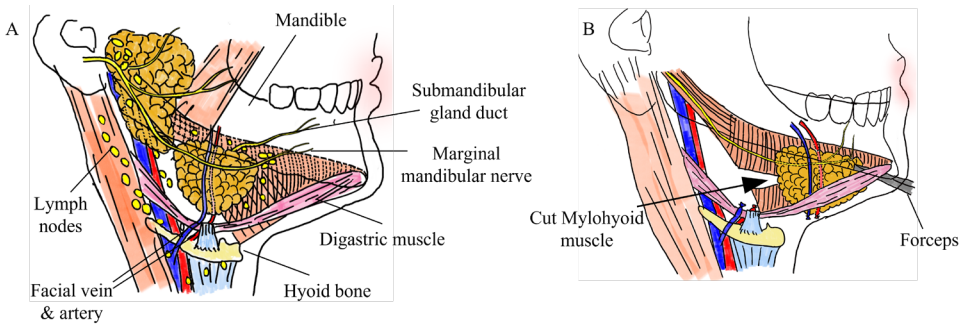

Figure 11. Schematic workflow of submandibular gland transfer.
(A) In the right upper neck, a neck incision is made at a distance of two centimeters below the mandible body in order to expose the surgical submandibular area. (B) The submandibular gland and the anterior belly of digastric muscle is released from the surrounding tissues. The facial artery and vein are ligated and cut near their branches that supplies the gland with blood. Finally, the submandibular gland is repositioned in the submental space. Created by the author. Copyright by the author.

In addition to restoration of salivary gland function after irradiation injury, there are also approaches to prevent damage to the gland from the onset as irradiation for head and neck cancer patients has a known clinical timing. Thus, submandibular gland transfer has emerged as a potential surgical approach to temporarily relocate the submandibular gland to the submental space to shield it from irradiation therapy[137-139] (Figure 11). One study from 12 institutions, 177 patients in a mean follow-up of 22.7 months shows[140] that approximately 80 % of patients who received salivary gland transfer surgery before irradiation therapy did not develop xerostomia (95 % confidence interval, 76.6 - 87.7 %). They observed a similar pattern with unstimulated/stimulated saliva flow rates, with the transfer surgery patients maintaining 79 %/74 % of their pre-surgical values compared to 28 %/17 % for control subjects. The results of this study suggest that salivary gland transfer

surgery could maintain a standardized level of baseline salivary flow rate in one year after irradiation treatment, together with patients' improved perception of saliva amount and consistency.

This surgical transfer procedure can potentially change the way patients with dry mouth are managed[141]. But its validation and promotion are being limited by the requirements for practicing on this surgical procedure and small patient sample sizes. Thus, while it is still in the pilot stages of prospective clinical trials, it may be a promising approach[141-143].

Protective drugs used in radiotherapy

As a cytoprotective drug, amifostine was approved by the FDA (Food and Drug Administration) in 1995[144]. Amifostine improves DNA repair abilities and induces hypoxia in tissue to protect patients undergoing radiotherapy. A meta-analysis conducted by Gu et al[145]. shows that amifostine significantly reduces complications such as mucositis, dry mouth, and dysphagia after radiotherapy for head and neck squamous cell carcinoma without reducing the efficacy of tumour treatment, and its adverse effects on the digestive tract are acceptable. Despite this, some claim amifostine causes more serious adverse reactions, such as nausea, vomiting, hypotension, and even protects tumour cells[146]. Its widespread use therefore depends on the results of future research.

Another commonly used drug, pilocarpine, has also been shown to increase residual salivary gland secretion after radiotherapy as a cholinergic receptor agonist[147]. In addition, Jaguar et al[148] in a phase III study showed that oral bethanechol twice daily reduced salivary gland damage caused by radiotherapy in head and neck tumour patients. Irradiation protective drugs need to be verified by additional clinical studies.

In radiotherapy, active oxygen scavengers may be used as radioprotectors[70]. Furthermore, transient receptor potential type M2 (TRPM2) also mediates the increase in intracellular Ca^{2+} concentration induced by oxidative stress, and one type of radioprotector tetramethylpiperidine restored salivary gland function, suggesting that transient receptor potential M2 type inhibitors may be effective in treating dry mouth[114]. A prospective double-blind randomized controlled trial conducted by Chung et al[149] found that antioxidant supplements (100 U vitamin E and 500 mg vitamin C) improved dry mouth symptoms. Based on a systematic analysis of seven related articles, Fox et al[150] concluded that hyperbaric oxygen improves xerostomia after radiotherapy, but randomized controlled trials are still lacking.

Intensity modulated radiotherapy

Further advancements in radiotherapy may include the use of intensity-modulated radiotherapy (IMRT), which would improve partial salivary gland secretion, as it is

CT-planned radiotherapy with conformal control in three dimensions so that only the tumour is irradiated while maximum protection is provided to the parotid glands[26,151,152]. The functional outcome of IMRT is to better execute the specific irradiation treatment plan created for every individual with HNC, also avoid affecting specific regions containing epithelial stem cells in salivary gland, known to be especially radiosensitive[153].

Gene therapy

Gene therapy for salivary glands was only a theoretical concept in researchers' minds in the early 1990s. However, over the last 30 years, researchers have advanced this idea to small and large animal studies and now to phase I and II clinical trials. Bringing gene therapy for salivary glands into the clinic treatments from the research bench has the potential to achieve long term and effective functional changes.

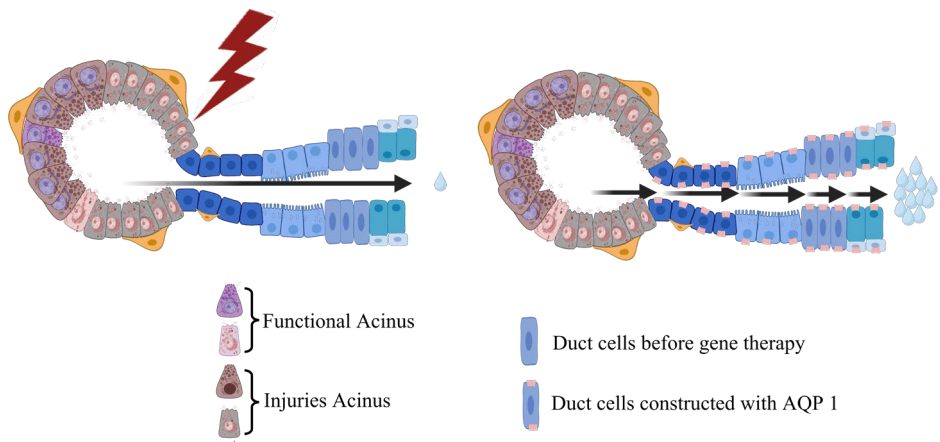

Figure 12. Schematic flow depicting the theory of AdhAQP1-encoded gene therapy.
(A) Some salivary glands are damaged by irradiation and produce less saliva. (B) After gene therapy, the ductal epithelium expresses AQP1, ductal epithelial cells move more water into the ductal lumen. Thus, saliva components have a low osmolarity concentration. Created with BioRender.com.

The most common gene therapy being explored for salivary glands uses recombinant adenovirus serotype 5 vector as gene delivery vehicles to deliver human aquaporin-1 genes (AdhAQP1) to salivary glands' cells (Figure 12). This is an adenovirus that causes only transient gene expression, and thus carries less risk long terms. After the encoding aquaporin 1 protein is expressed on cell membranes, water will move more freely through ductal cells. Animal studies and clinical trials have demonstrated that rejection is reduced in viral vectors, and dry sensations are relieved in the mouth. This response has been shown to last for several years after

the one-time injection of AdhAQP1, which is quite surprising because it is short-expression viral vectors[154-157]. Further research is needed to better understand the longer-term mechanism of action.

Next, with the completion of additional clinical studies, methods to avoid immune reactions and extend long term expression in the salivary glands are needed; identification and optimization of vector doses to deliver the AQP1 gene that elicits only minimal immune responses, as well as to advance gene therapy to a broader population, such as patients with Sjögren's syndrome or other difficulties will be interesting. There may be other cells affected by salivary gland diseases, so gene therapy of functional secretory proteins like AQP1 may not be sufficient to regenerate fully functional salivary glands[158].

Molecular therapy

While gene therapy approaches have shown promise, other approaches have demonstrated potential therapeutic effect by directly delivering therapeutic proteins. The following is only a brief introduction to one representative example.

In the past, apoptosis was considered a major mechanism of irradiation damage to the salivary glands. Irradiation-induced salivary gland cell apoptosis can be inhibited by down-regulating p53 activity in transgenic mice expressing protein kinase B (Akt)[62]. By injecting (IGF-1) or activating endogenous Akt or inhibiting p53 expression, salivary gland apoptosis can be prevented during radiotherapy[68]. IGF-1 administration has been shown to be effective when injected into irradiated FVB mice (1 - 2 Gy/d, 5 days in total) as well into similarly irradiated transgenic mice (myr-Akt1). Aging is also influenced by the Insulin/IGF axis and thus IGF-1 administration may be effective for reversing senescent related salivary gland dysfunction beyond irradiation induced injury. However, due to the wide range of tissues expressing the IGF-1 receptor, IGF-1's effects are diverse and thus off-target effects must be minimized if administered systemically. Alternatively, mechanisms to deliver it locally to salivary glands, such as gels or sprays, could help overcome this problem. IGFs communicate with cells' physiologic environment.

In addition to IGF-1, cyclin-dependent kinase inhibitors[159] may also be used as a preventive treatment for salivary gland dysfunction. In sum, molecular therapies have the benefit of avoiding potential genetic alterations as are possible if viral vectors are used; they have been shown to be a precise and effective targeting strategy for preventing and treating irradiation damage of salivary glands. But the high cost of molecular therapy and the fact that it may need repeat administrations to sustain therapeutic effects may prevent it from being widely used.

Stem cell-based transplantation

Stem cells are thought to play a crucial role in salivary gland formation as well as play an important role in recovery from injury[160]. Stem cell therapy offers the possibility of long-term restoration of salivary gland tissue and secretory function either through modulation of the remaining endogenous stem cells or exogenous delivery of stem cell populations to the damaged tissue[161]. Different types of stem cell therapies are currently under study. Both embryonic stem cell (ESC) and induced pluripotent stem cells (iPSCs) derived salivary gland cells are being explored as replacement therapies. On the other hand, immunomodulatory therapies derived from mesenchymal stem cells (MSC) are also being explored[162]. These MSCs can be derived from different tissues such as dental pulp[163], bone-marrow derived MSCs[164], adipose-derived mesenchymal stem cells[163,165] (ASCs), amniotic membrane mesenchymal stem cells[166], urine-derived mesenchymal stem cells[167], etc).

While ESC applications have shown promise for several diseases, the ethical question of destroying fertilized embryos remains. Therefore, iPSCs can be considered to have less societal resistance to implement. By transferring four transcription factors (Oct4, Sox2, KLF4 and c-Myc) into differentiated somatic cells, human iPSCs[168] can be generated and they completely avoid ethical concerns like ESCs. They also have other advantages which include the ability to select donor somatic cells, avoiding histocompatibility issues with donor/recipient grafts, and the ability to transfer information from the reprogramming process directly into the human body so that damaged or diseased tissues or cells can be repaired in vivo. Teratomas are still possible for iPSCs, and this must be carefully examined with each new protocol and cell type. Progress has been made for deriving salivary gland stem cell from iPSCs[169]. Currently, the use of non-epithelial sourced peripheral blood mononuclear cells[170] (PBMCs) for regenerative medicine is one potential promising concept. A study has shown that intraglandular transplantation of mouse SGs results in gradual restoration of salivary function by reducing inflammatory genes, increasing proliferation, vascularization, increasing acinar and ductal areas, and reducing fibrosis following irradiation[170].

Currently, there have been more studies focused on using the immunomodulatory and angiogenic properties of MSCs as compared to direct cell replacement (producing new cells to replace dead ones). Recently, secreted factors from stem cells[25] and extracellular vesicles (EVs)[171] have become a topic with high research and clinical interest as they avoid concerns about the risks associated with directly injecting stem cells into the human body[168]. Despite the need for further research to confirm safety and efficacy, cell transplantation remains a promising regenerative technique which will be discussed further in this thesis.

Human dental pulp stem cells

Dental pulps are divided into three major parts: a central pulp chamber, pulp horns, and root canals (shown in Figure 13). There are several types of loose connective soft tissues in the dental pulp, including fibroblasts, undifferentiated mesenchymal cells, macrophages, and lymphocytes, with water, proteoglycans, glycoproteins, and collagen matrixes surrounding these cells. A tooth's pulp is highly vascularized and neutrally innervated, ensuring teeth healthy and forming dentin. As we age, the pulp chamber shrinks due to dentine deposition[172].

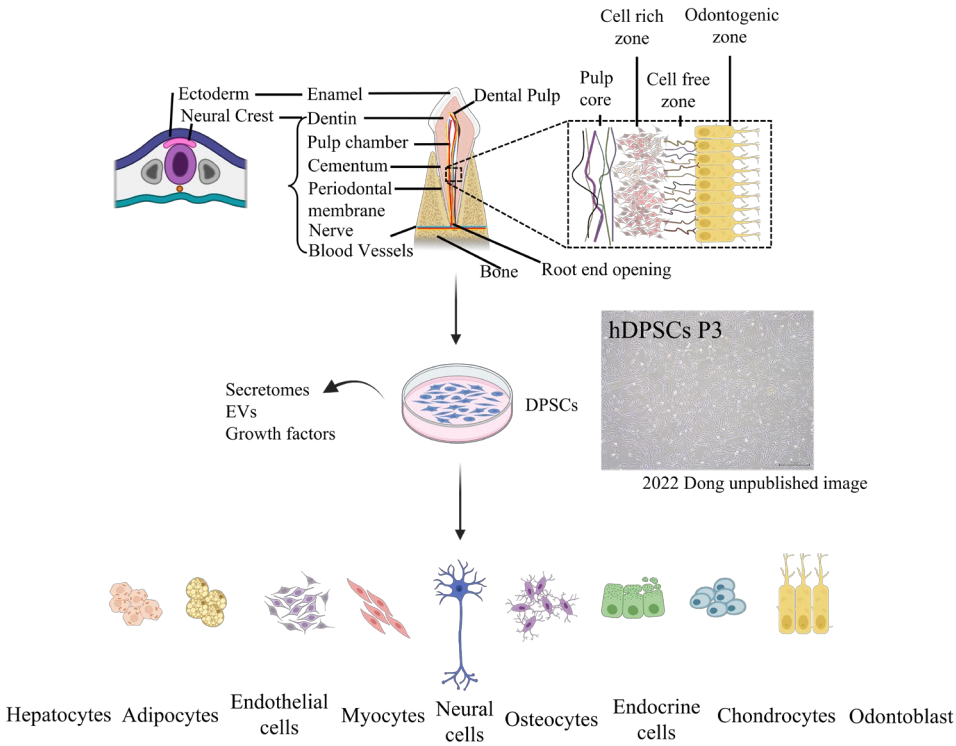

Figure 13. Developmental and anatomical structure of teeth and stem cells derived from dental pulp.
In this diagram, the ectoderm cells contribute to the formation of only the enamel of the teeth, whereas the neural crest cells are responsible for generating the remaining tooth tissues. In addition, it illustrates that dental pulp stem cells are capable of multilineage differentiation because they derive from the neural crest. Created with BioRender.com.

Exfoliating deciduous teeth, orthodontic treated teeth, traumatized teeth, and periodontal disease teeth can be used to obtain dental stem cells[173]. A highly notable feature of hDPSCs is that when compared to other adult stem cells from other tissues, they can be readily sources from medical wastes (dental pulp) after routine

dental surgery. Other advantages include their ability to be stored long-term using cryo-preservation, and potential use as autologous transplants later in life with reduced immune rejections. hDPSCs also are less controversial than ESCs are multipotent owing to their neural crest source[174]. hDPSCs could also be used as a source of iPSCs; therefore, their application prospects are broad[175].

In light of the potential to use dental pulp stem cells for diverse clinical stem cell therapy applications in the future, it is particularly important to separate and expand them with effective and well-characterised markers, store them appropriately with vital viability, and administer them in a clinically manageable way. There may be several populations of stem cells in dental pulp that express surface markers such as CD29, CD44, and CD90[176], which could prove useful for future isolation. Well-defined protocols to expand and cryopreserve teeth, with consideration being given to controlled cooling rates and lower the limitation of cryo-preservant have been established[177,178].

Stem cells in salivary gland

There is a small pool of undifferentiated stem cells in a variety of tissues in most living organisms, termed adult stem cells[179]. However, unlike embryonic stem cells, adult stem cells cannot become any type of cell and only have the capacity to differentiate into a few types of cells contained within the organ in which they reside. Because of their renewal potential, adult stem cells may be a promising source of cells for the reconstruction of damaged organs. They also eliminate ethical concerns associated with human embryonic stem cell research and concerns of teratomas with iPSCs. The identification and characterisation of salivary gland stem cells has been an ongoing interest since their discovery. A list of biomarkers for progenitor cells and stem cells of the salivary gland is provided in Table 14. Several markers have been studied for sorting/isolating these cells, including c-kit (CD117), CD49f, CD29, CD24, and CD133; combinations of these markers can improve accuracy of precise cell populations.

As evidence of their proliferative and differentiation capacity, *in vitro* microspheres of human salivary glands, termed salispheres, can be created using c-Kit-derived cells[190]. After xenografting, these salispheres increased regenerative potential of irradiated salivary glands[191]. A study involving genetic tracing of animal models concluded that SOX2-marked acinar cells differentiated into MUC19-expressing acinar cells after salivary gland irradiation, resulting in the recruitment of acinar cells[192]. Nevertheless, no ductal cells have been shown to be generated from these cells, indicating a fate commitment program[193]. Future salivary gland stem cell applications could involve harvesting salivary gland stem cells during surgery and implanting them after radiotherapy in a scenario envisioned for future use. Through improved cell extraction, culture, transportation, and transplantation, damaged salivary gland epithelial cells may be replaced with healthier salivary gland stem cells in the future.

Table 14. Biomarkers for putative salivary gland progenior/stem cells[180-182].

Category	Cellular surface biomarkers	References
Salivary gland stem cells	C-Kit$^+$	183
	SOX 2	184
	SOX 9	185
	Krt 5	186
	CD 49f	183
	CD 133	183
	CD 24	183
	CD 29	187,188
	Sca-1$^+$	189

Cell free therapy-Extracellular vesicles

The use of human MSCs in clinical trials began in 1993. In the early stages of MSC research, the hope was that MSCs could be used to directly replace lost or damaged cells by these stem cells. A seminal study conducted by Yoshitaka[194] in 2007 demonstrated an improvement in cardiovascular function after administration of MSCs intravenously, along with the secretion of several protective factors from engrafted MSCs, indicating that MSCs function by paracrine effects or secreted factors. Subsequent studies in many other organs and tissues, including cell free supernatants, have confirmed that secreted factors from MSCs contain potent anti-inflammatory, immunomodulatory, and regenerative factors. Furthermore, the advent of ultracentrifuge techniques and their rapid development during the mid-20th century led to the awareness of the presence of extracellular vesicles secreted by stem cells which protects their contents from degradation by the body during transport. Thus, these techniques have encouraged the deeper exploration of extracellular vesicles (EVs) derived from MSCs and other cell types towards future clinical applications.

EVs are membrane-bound lipid bilayer vesicles secreted by cells or body liquid, with strong capacity to delivery bioactive proteins, metabolites, nucleic acids, lipids[195]. In addition to being a novel form of information transfer between cells, EVs can also integrate extracellular information, thus extending the concept of signal transduction. Roughly classified into small extracellular vesicles (sEV) with diameter from 30 - 150 nm and multivesicular bodies (MVBs) and apoptotic bodies, most EVs are smaller than 200 nm. The various isolating method for EVs and their cons/pros respectively are described in Table 15. The family of EVs are separated into three major classes based on their biogenesis: EVs, microvesicles, and apoptotic bodies. The biogenesis and release of extracellular vesicles is under comprehensive regulation by extracellular signals and have significant clinical relevance in both

healthy and sicknesses[196] depicted in Figure 14. For example, due to the characteristic marks left after EVs packing substances, the surface characters and materials contained in EVs can vary based on the source cells. It has also been discovered that nucleic acids contained with EVs can be used to diagnose disease because they can be traced back to the cells that originated them, such as tumour cells. Therefore, EVs can be used as diagnose purpose by forming tumor landscapes and analysing how tumors spread. For therapeutic purposes, the development of engineered EVs and the identification of specific EVs biomarkers are increasing their research prospect, as we may be able to use EVs with specific miRNAs and modified surface proteins for disease specific treatments in the future[197,198].

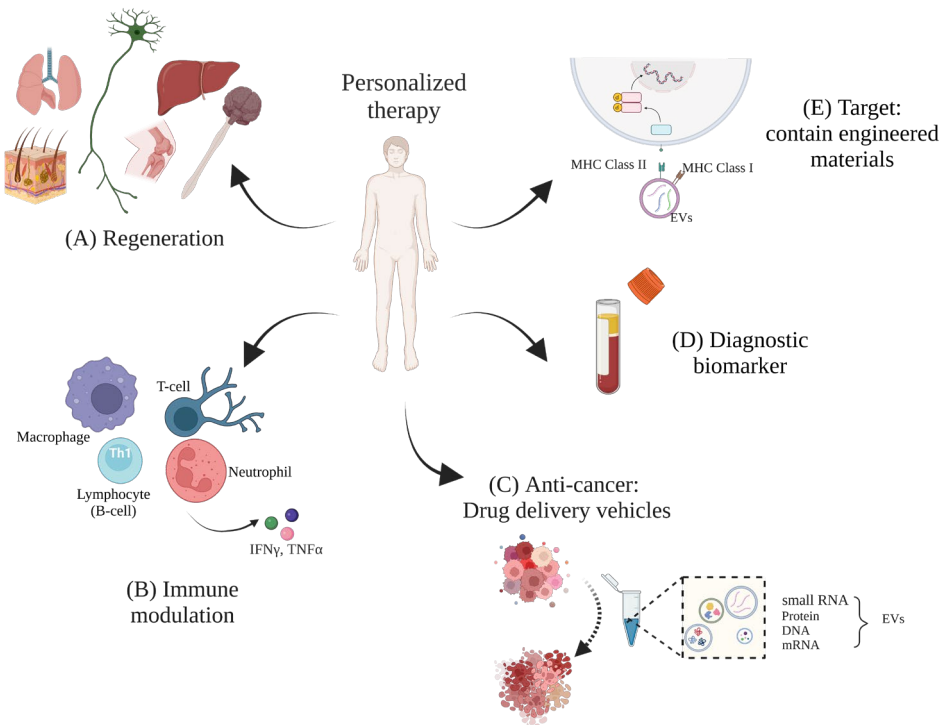

Figure 14. Using EVs as personalized therapy.
Diagram (A-E) shows the wide functions of EVs. (A) EVs play regenerative role in diseases. (B) EVs impact in cellular functionality like immune modulation. (C) EVs work as drug delivery vehicles to against tumor. (D) EVs serves as potential biomolecules in diagnostic tools. (E) EVs load with engineering material to play a targeting role[171]. Created with BioRender.com.

Table 15. Comparision of different EVs isolation techniques.

Techniques	Mechanism	Advantages	Disadvantages
Ultra-centrifugation[199]	Size, density	Gold standard method, minimal reagents and expertise required	Time comsuming, nonspecific purification, decrease in biological activity.
Ultrafiltration[200]	Size, molecular weight	Rapid,	Particle size heterogeneity; EVs loss due to attaching to membranes
Immuno-isolation[201]	Affinity	High purity, rapid,	Not suitable to larger scales.
Polymer-based precipitaiton[196]	Solubility, surface charge	High yield	Low purity (with free proteins contamination).
Microfluidics-based[202]	Affinity, density, electrophoretic	Rapid, high purity, high efficiency	Not-suitable for larger scale.
Membrane-based[203]	Surface properties	High affinity, rapid	Low purity.

Tissue engineering regenerative medicine (TERM)

As defined by Langer in 1993[204], tissue engineering (TE) is the process of replacing or regenerating human tissue or organs using combinations of cells, scaffolds, and growth factors with the goal of restoring or fabricating normal function or replace with transplanted organ. Regenerative medicine is not only restricted to tissue engineering but also includes cell-based therapy, gene therapy, nanomedicine, and TE strategies and so on. These fields are merging as tissue engineering and regenerative medicine (TERM)[205] since they have similar missions and concerns.

Scaffolds, serving as structural matrices, can be manufactured with synthetic materials engineered to contain cell binding sites or together with extracellular matrix components and inductive growth factors. They provide structural, biochemical, and biomechanical cues to trigger and regulate cell behaviours and tissue development. Later the scaffold with different cells should be amenable for vascularization upon implantation in vivo to allow integration with the host. In addition to their usage as clinical tissue for transplantation, tissue engineering has also opened up new possibilities for modelling tissue or disease in the lab as well as for studying new therapies. In particular, this allows for the study of disease in human cells or tissue before performing clinical trials. This next section will discuss different *in vitro* models of salivary gland tissue and cells.

Three-dimensional organoids or spheroids

The simplicity of 2D cell culture with one or more cell types makes it the first choice for many scientists. However, there is a limited ability to culture multiple cell types with spatial orientation with this technique. In particular, 2D culture is insufficient for studying tissues and diseases in a dish that depend on the careful coordination

of multiple cell types for tissue function. As a result, 2D culture cannot replicate the interactions of multiple cells in a 3D network where they exist in vivo. Cultures in 2.5D (monolayers on 3D substrates) use additional materials to alter topography, altering cell membrane curvatures, while maintaining a free surface. While diverse substrates have been used, including those with extracellular matrix components (ECM), to better form a microenvironment required for SG morphology, they still do not fully replicate native cell-ECM interaction characteristics. Recent advances in stem cell biology, microfabrication techniques, and tissue engineering have led to the development of a wide array of 3D cell culture platforms, including multicellular spheroids, hydrogel-based culture, bioreactor-based culture, bioprinting, and scaffold-based culture[206,207] (shown in Figure 15). However, no 3D strategy has not been able to completely recreate a 3D tissue engineered salivary gland. Therefore, animal models are currently viewed as the most practical model for studying salivary glands.

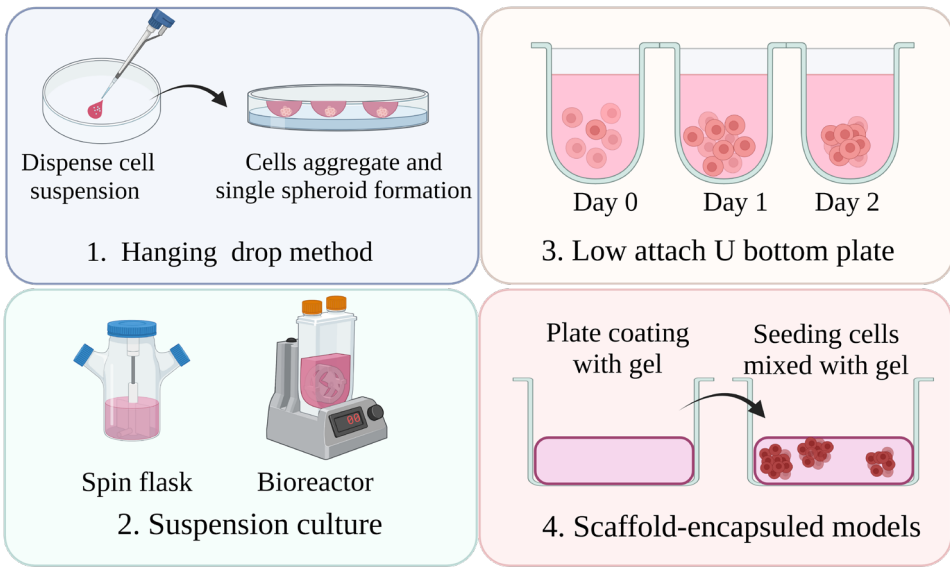

Figure 15. Salivary gland ex vivo models using 3D cultured models. Created with BioRender.com.

Allogeneic tissue specific ECM in tissue engineering

All cells in the human body carry the same genetic material. Therefore, the specification of certain cells and how they function is dictated from the context that surrounds them. This context is called the extracellular matrix niche. Generally speaking, being an abundantly distributed network, ECM is composed of a heterogeneous network of fibrillar proteins between the exterior and cells, including collagen, laminin, fibrin, elastin, fibronectin, GAGs, proteoglycans, and

glycoproteins. Additionally, chondroitin sulfate, heparin sulfate, and sulfonic acids also serve as functional groups that help stabilize tissue mechanics. All these natural "textures" are the source of bioactive cues and growth factors in playing an instructive role to cell fate (by offering cellular signals for tissue specific homeostasis) and a supportive role (as a three-dimensional structural support containing the matrix substrates)[208,209]. The development and usage of 3D stem cell cultures aim to recapitulate this niche. The use of ECM is thus needed to bring the native in-vivo environment to the in-vitro setting, which enables cell models to be significantly more predictive of human physiology and rebuild the clinical transplantation perspective for dangerous patients. Extracellular matrix profiles tailored to specific tissues and adapted to age is found to better summarize the healthy and pathologies for *in vitro* models[210-22]. However, the development of models which recapitulate the ECM niche are challenging to engineer.

Precision-cut salivary gland slices

As an alternative to in vivo animal studies, precision-cut tissue slices (PCTS) model[213-215] have emerged as a promising technique. PCTS are derived by using techniques which can thinly slice native tissue for subsequent *ex vivo* culture. They retain nearly all tissue-derived cell types and the original tissue configuration. PCTS reduce some of the limitations caused by using Matrigel in organoids (which is derived from tumour cells) or other synthetic materials in 2D cultures and organoids as architectural and signal instructions. As a powerful model with a natural in vivo microenvironment, PCTS are thus a promising model which mirrors the natural *in vivo* microenvironment, and further reduces animal usage to allow for safer drug development. Furthermore, they can be derived from excess surgical waste and thus allow testing directly in human tissue. There are many organs in the PCTS system (the liver, the lung, the brain, etc.) and their applications includes physiological research, disease modelling, drug toxicology, and pharmacology[213,214,216,217]. (Figure 16).

While only a few papers have reported on the generation and use of precision-cut salivary gland slices (PCSS)[218-221], their promise is clearly evident, and they can fill an important research need[218-221,229]. Thus far, most studies have used image-based analysis (i.e., antibody or specific staining) which has low throughput. There is thus still room for improvement and thus far there are a limited number of tools available with which to analyse them, in comparison to the tools available for other PCTS. Slice preparation is extremely challenging, especially for murine PCSS which has further limited the number of labs which use this model. Only one study has thus far analysed transcriptional changes during culture, which was done in human PCSS due to the fact that more material was available[219]. As a result, it is less clear how pathways are activated during normal culture as well as how well pathological processes are replicated in slices. New techniques, including the use of ‘omics’

technologies and advanced and state-of-art imaging techniques are urgently needed to allow further usage of this promising *in vitro* model.

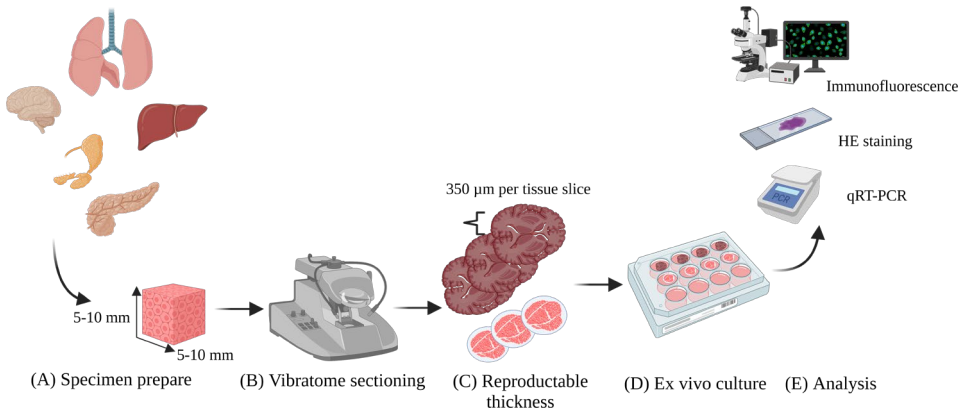

Figure 16. Generating PCSS tissue pieces by vibrotome.
This diagram illustrates how precision-cut tissue slices (PCSS) are prepared, cultured, and analyzed. The insets (A) through (E) show a technical drawing (not to scale) depicting the workflow for culturing different organs as precision-cut tissue slices. Created with Biorender.com.

Advanced in vitro imaging techniques

Light sheet fluorescence microscopy (LSFM) imaging

While light-based imaging has been a standard technique for over 100 years in both research and clinical diagnosis, the majority of research is conducted on thin sections of tissue so that the light can penetrate it. Furthermore, these techniques are time consuming because they require illumination with small points of light. An emerging technique is light sheet-based microscopy. With light sheet microscopy, a thin slice of the sample is illuminated with laser light to create fluorescence images and can be used on thick sections if the tissue is optically cleared[222]. The fluorescence signal and images of the observed region are captured using a wide-field fluorescence microscope placed perpendicular to the light-sheet (Figure 17). The 3D optical sectioning technique is significantly faster than other fluorescent imaging techniques due to its orthogonal arrangement, which decouples illumination from detection[223].

Compared to confocal microscopy imaging, light-sheet microscopy imaging offers fast, high resolution, true volume, and in-depth imaging with the following major advantages: low photobleaching, minimal phototoxicity, the ability to image transparent tissues at cellular and subcellular levels at high spatial and temporal

resolutions and the ability to generate serial optical tissue sections that allow for 3D reconstruction of tissue structures[224]. The unique capabilities of light sheet microscopes allow for the acquisition of challenging specimens as well. At the same time, this fast-moving technology poses many technical difficulties and challenges, such as the preparation of samples, the development of pattern recognition software for data interpretation, and the handling of data deluges and data interpretation. However, these challenges are being overcome with more research undertaken in this area and light sheet microscopy is currently advancing research in a wide range of fields[225].

For example, it has proven invaluable for studying embryonic development, as it can provide quantifiable data on morphogenetic processes[226] and overall features of cells and tissues as entire, intact organisms can be studied. Quantitative mapping of large biological systems can also be achieved through a light sheet microscope. A thin, clarified coronal slab of the human brain has been visualized, as well as hydra[227] body shape changes. By analysing clinical specimens rapidly, light sheet microscopy[228] is also capable of informing treatment decisions. However, thus far, there are no reported images of salivary glands from any mammals. The development of techniques for tissue preparation for light sheet microscopy are thus urgently needed.

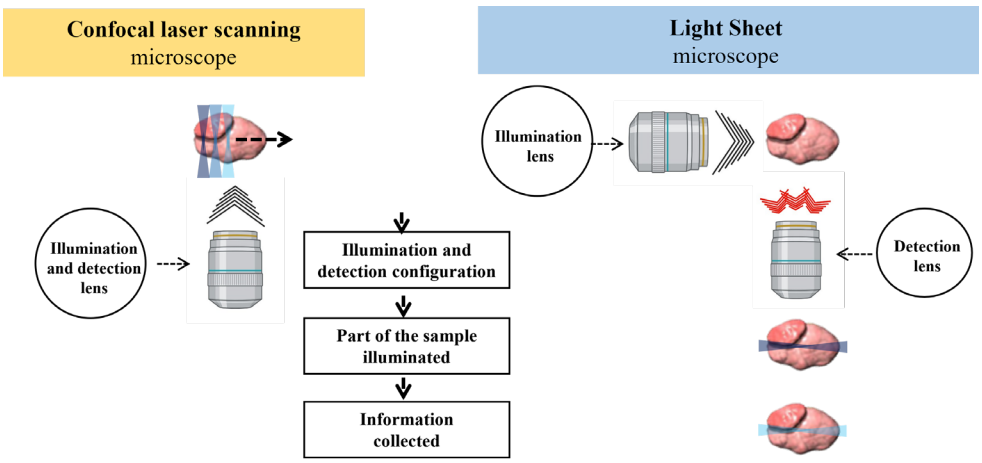

Figure 17. The principles of light sheet microscopy are illustrated in the following schematic with comparision to confocal microscope. Created by the author. Copyright by the author.

New developments in pathology and image-based analysis

Historically, histological analysis has been used in science and medicine for over 900 years since its inception[230]. The basic procedure is that the pathologist cuts the tissue into thin sections, stains them, and examines the samples under a microscope.

It is possible to diagnose, monitor, predict survival rates, and provide personalized treatment based on pathological images, which contain rich phenotypic information. The role of histology has always been important, especially for diagnosing and treating cancer, which is currently a major concern[231].

Histological analysis is relatively simple to operate, easy to understand, and many persons can perform it after suitable training. However, this method has several disadvantages, including the high variability in results, the influence of chemicals and laboratory operations, and the time-consuming and cumbersome nature of the process. The process of processing and staining samples in traditional histology also uses toxic chemicals[232], which are harmful to the environment and there is an urgent need to find alternatives which are safer for the environment and pathologist/researcher. Pathologists and researchers will also interpret results differently based on their levels of experience and subjective factors (such as the selection of the specimen or regions of interest). In this case, the interpretation of results can vary greatly, and may even result in false negative results that affect a patient's treatment plan or be inconsistent with the research results. Thus, while histology is a longstanding technique, innovation is needed. The emergence of sustainable histology, virtual pathology, and artificial intelligence in pathology have all become very significant turning points in modern pathology.

Sustainable histology

Pathologists collect, fix, dehydrate, transparentize, embed, section, stain, and mount samples during their daily work in the pathology department. Gradient ethanol dehydrates the tissue before entering the waxing step which allows thin sectioning (most commonly paraffin), but ethanol and paraffin are not compatible, so a solvent is required as a bridge, since it is miscible with both ethanol and liquid paraffin. The most typical tissue clearing agent used in histopathology is xylene. It has a benzene ring and is an aromatic hydrocarbon compound. In experimental and clinical studies, xylene[233] has been found to accumulate in the kidneys, bone marrow, and other organs, and can be absorbed through the skin, respiratory tract, and digestive tract. Xylene can cause autonomic dysfunction and decrease hematopoietic function, while affecting the ecosystem irreversibly. To replace xylene in histological staining, a new environmentally friendly agent is needed. This area has received increased attention and alternatives have been explored such as alcohols (e.g., isopropanol[234]) or limonene based compounds[235]. Several products have now entered commercialization but are known to have limitations. Importantly, all corresponding tools (e.g., antibodies), need to be revalidated with changes of protocols. Thus, despite health and environment benefits, there is a general resistance to research and implement these changes. The development and implementation of bio-environmentally friendly tissue dewaxing/clearing reagent to replace xylene in pathological technical work is nonetheless needed. It is important to confirm firstly whether the pathological sections of different organs with different diseases will remain of sufficient quality and whether clinical pathological diagnosis

and research requirements will be met. Thus, new environmentally friendly clearing and dewaxing agents not only needs to meet the laboratory's and hospitals' environmental requirements, but also protect pathologists from physical injury.

Histological scoring

Even highly trained pathologists and researchers have subjective experience when evaluating tissues, and pathology-assisted clinical diagnosis can be very complicated due to histopathological appearances in staining. Furthermore, detecting the differences between some disease groups can require highly specialized training. In the case of the common research setting, there may be a limited number of highly trained persons who can evaluate histological sections. The use of histological scoring or grading[236] is one way to help reduce subjective judgments in both the clinic and research because it increases objective evaluations and can further be used to achieve semi-quantitative analysis and comparison. There have been several mature scoring systems used in scientific research, such as those for mouse osteoarthritis models[237]. It is also widely used in clinical work to assess mitosis in the process of histopathological grading of breast cancer. There are several critical principles which should be used to develop histological scoring systems[238]. First, scoring criteria should be chosen based on the ability to define, repeat, and correlate histological manifestations with clinical or laboratory induced diseases. The importance of tissue sampling cannot be overstated, and it must be explained clearly how a sample is obtained and defined. Understanding the principles behind the creation of histological scores is essential for creating meaningful histological scores applicable to target disease organs, tissues, and models.

Aims of the thesis

As a whole, the objective of this thesis is to establish methods to evaluate salivary gland regeneration and functional restoration with cell-free therapy as well as tissue-engineering strategies, with the following sub-aims.

1. Identify the isolation and identification of EVs from hDPSCs (Paper I).
2. Investigate the pathological features of salivary gland hypofunction in two main salivary gland diseases (irradiation and autoimmune-induced damage) by animal modelling (Paper I & III).
3. Evaluate the potential of hDPSCs-derived EVs therapy in salivary gland hypofunction and the possible mechanisms behind (Paper I & III).
4. Explore the possibility of implementing an ex vivo organotypic precision-cut salivary gland slices (PCSS) model for modelling disease and functional evaluation of salivary gland (Paper II).
5. Examine the feasibility of advanced imaging like using sustainable tissue processing method without xylene for histological staining and three-dimensional visualization through light sheet fluorescent imaging for an advanced imaging assessment of salivary gland's tissue and diseases (Paper IV).

Materials and Methods

Animal (murine) usage

Paper I

Thirty-six female ICR mice bred at the Nagoya University School of Medicine were used in this study. The mice were 7 - 9 weeks of age at the time of experimentation and weighed 20 - 30 g. All mice were housed (four mice per cage) under well-controlled conditions with a temperature of 23 ± 3 °C, relative humidity of 54 ± 5 %, and 12 hour light-dark cycle with free access to food and water.

Paper II

All procedures performed on live animals were approved by the Ethical Committee at Lund University when conducting animal research. 8 - 12-week-old mice C57BL/6J mice (Mus Musculus) were housed with free access to water and food and euthanized for organ harvest by injecting a 3:1 ketamine/xylazine (v/v) solution intraperitoneally for every 20 grams of body weight. Fresh salivary gland samples were extracted and immediately placed in an ice-cold PBS or physiological saline solution (PSS)[218] (see manuscript Paper II for detailed components).

Paper III

The animal experiments for Paper II were approved by the Nagoya University School of Medicine Animal Care and Use Committee (No. 31427, 20274, M210183-001) in accordance with the Guidelines for Animal Experimentation of Nagoya University School of Medicine). 7-week-old female NOD/Jcl (NOD) and Jcl:ICR (ICR) mice (CLEA Japan, Inc) were housed with wood tip bedding and maintained under specific pathogen-free conditions. Animals were housed 4 per cage and received normal food and filtered water.

In vitro cell culture of hDPSCs and EVs characteristics

The cell is hDPSCs. We as a whole lab bought this cell line years ago. It is from Lonza coded PT-5025 from Basel, Switzerland. According to manufacturers' protocol, this cell line is cultured in Dulbecco's Modified Eagle Medium (Sigma-Aldrich, St. Louis, MO, USA). The medium only have additives like 10 % fetal bovine serum (GE Healthcare Bioscience, Little Chalfont, UK). We culture cells at 37 °C in 5 % CO_2 incubator. For cells at Passage five, until they grow to 90 % confluency, we could extract EVs from them. Detailed procedures are described in published articles previously[23] with a schematic workflow shown in Figure 18B. Briefly, 3×10^6 cells were initially seeded and cultured in 250 mL medium. Cells were washed twice with phosphate-buffered saline (PBS), and the culture medium (CM) was replaced with Advanced DMEM (FBS free; Thermo Fisher Scientific). After 48 hour of incubation, the cell viability was 99 % as detected using trypan blue exclusion assay. The CM was collected and centrifuged at 2,000 × g for 10 min at 4 °C, and the supernatant was filtered through a 0.22 μm filter (Merck Millipore) to remove cellular debris. The CM was centrifuged at 100,000 × g using an ultracentrifuge (Optima L-100; Beckman Coulter) and a swing rotor (SW 41Ti; Beckman Coulter) for 70 min at 4 °C; this step was repeated four times. The pellets were ultracentrifuged at 100,000 × g in PBS. The concentration of EVs was measured by estimating the concentration of protein in the putative EVs fraction, using the Qubit Protein Assay Kit with Qubit 2.0 Fluorometer (Thermo Fisher Scientific). The EVs pellets were resuspended in 500 μL PBS. The concentration of proteins within EVs was approximately 30 μg/mL as measured by Qubit. The EVs were stored at - 80 °C (shown in Figure 18B).

The isolated hDPSC-sEV were visualized by transmission electron microscopy (JEM-1400PLUS, JEOL, Tokyo, Japan), as described previously[242]. The particle size distribution of hDPSC-sEV was analysed using the Particle Size Analyzer ELSZ-2 (Otsuka Electronics, Osaka, Japan) following the manufacturer's protocol. For western blot analysis, please see Paper I for detailed full steps. Briefly, 200 μL Pierce™ RIPA Buffer (Thermo Fisher Scientific, Waltham, MA, USA) was used to mix with sEV solution. Samples were then run on an SDS page gel, transferred to membranes, and then staining with primary and second antibodies for visualization. Purified sEV were fluorescently labelled using a PKH26 Red Fluorescent Labelling Kit (Sigma-Aldrich; 4 mM) (shown in Figure 18C), following the manufacturer's instructions, for histological imaging.

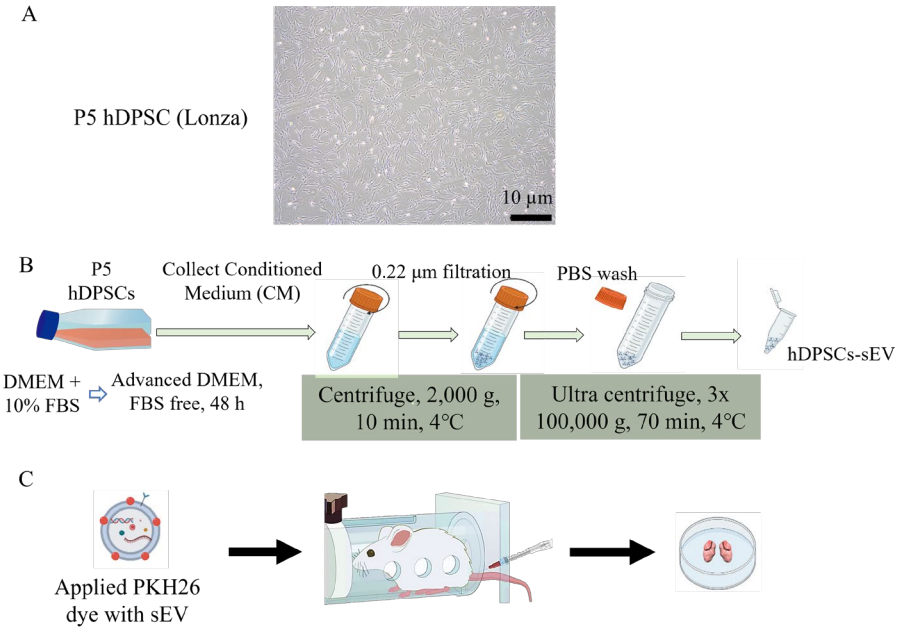

Figure 18. The workflow to identify small extracellular vesicles (sEV) and their uptake by cells. (A) Cell culture of human dental pulp stem cell (hDPSCs) to passage 5 until 90 % confluency. Scale bar: 10 µm. DONG et al. unpublished data. Copyright by the author. (B) General diagram showing the extraction process of hDPSC-sEV. Created by the author. Copyright by the author. (C) Workflow of how to apply PKH26 to identify cellular uptake of sEV. Created with BioRender.com.

Irradiation and NOD model and mouse treatment

Irradiation model

The submandibular glands of mice were irradiated after anesthetization using intraperitoneal administration of ketamine and xylazine mixture (0.3 µL/g body weight) to immobilize them during IR. Single irradiation doses at 25 Gy were delivered only to the middle neck region using an X-ray irradiator (MBR-1520R-3; Hitachi Power Solutions, Tokyo, Japan); the mice were shielded with lead blocks. IR was performed at a dose rate of approximately 3 Gy/min. All mice were randomly assigned to three groups (n = 4 mice in each group): control (no IR, only PBS administration in the following 18 days); 25 Gy+PBS (0.5 mL PBS was injected into the tail vein of irradiated mice); and 25 Gy+sEV (5 µg/0.5 mL hDPSC-sEV were injected into the tail vein of irradiated mice). Injections were performed three times per week for 2 weeks consecutively. All animals were euthanized on day

18 after IR, and the bilateral submandibular glands were carefully dissected. After washing the submandibular glands with 0.9 % saline, the organ wet weight was measured. The change in weight was calculated as follows: weight change (%) = organ wet weight (g)/mouse body weight (g).

Precision-cut salivary gland slices (PCSS) organotypic culture

The method to prepare after organ harvesting (Figure 19A and B) and conduct tissue slicing through vibratome and culture in incubator (Figure 19C to G) is shown in the following workflow. The detailed full method is described in Paper II. Briefly, 3 % low gelling temperature agarose was prepared (A9414, Sigma-Aldrich, USA) (Figure 19A) and poured into a syringe-mould made from a sterile 5 mL syringe with the top cut off (Figure 19C). Next, intact, whole single salivary glands were then placed vertically onto the retracted syringe plunger and immersed in the liquid agarose and allowed to cool at 4°C (Figure 19D). Once solidified, the agarose block was removed and attached to the substrate holder using a few drops of SuperGlue and then sliced with a PBS or PSS solution in a 7000smz-2 vibratome (Campden Instruments, UK) (Figure 19F and G). A vibratome (Campden Instruments) was then used to cut salivary glands into 300 µm thick sections. (Figure 19G). PCSS were cultured in McCoy's 5A Medium (L-glutamine and sodium bicarbonate) or RPMI with 0.05 mM β-mercaptoethanol, 10 % FBS (Fetal Bovine Serum) and 1 % Pen/Strep (Sigma-Aldrich, USA) in an incubator held at 37 °C, 95 % O_2 and 5 % CO_2 (Figure 19H). PCSS tissue was cultured for up to five days with medium changes occurring daily.[218,219].

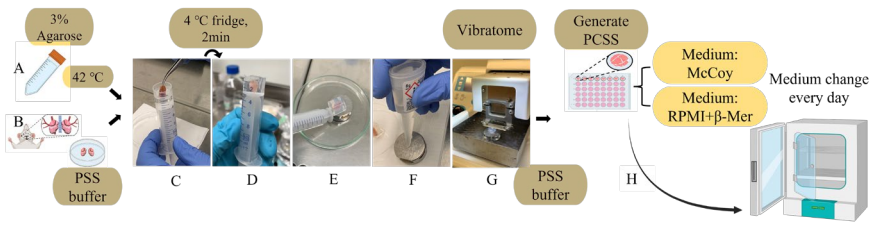

Figure 19. Schematic overview of generating PCSS tissue pieces from mouse salivary glands and culture. (A) 3 % agarose prepared and kept at 42 °C. (B) The harvested salivary glands (submandibular and sublingual) were kept in cold PSS. (C) A manually made syringe-mold was made with 3% agarose pouring in, so agarose is embedded to encapsulate mouse salivary glands. (D) put the mold in 4 °C fridge. (E) Take out the agarose block and glue it on the substrate holder (F). (G) Vibratome slicing at 300 µm thickness and (H) culture in incubator. Additional details described in the Materials and Methods. Created by the author. Copyright by the author.

Irradiate on PCSS

PCSS samples were placed in a 48-well plate where each row was designated to receive single doses of irradiation at 1 Gy, 5 Gy, 10 Gy, and 15 Gy. In order to block neighbouring rows from cumulative irradiation doses, lead strips were used. Irradiation was delivered using a well-established XenX x-ray irradiator platform at the Lund University, Department of Medical Irradiation Physics. Detailed and full steps are described in manuscript Paper II.

NOD model

Eight-week-old female NOD mice were randomly assigned into one of two groups (hDPSC-EVs and PBS; n=9 in each group). Mice received weekly tail-vein injections of 10 μg hDPSC-EVs in 200 μL PBS/mouse for 14 weeks with regular blood glucose monitoring. Mice were anesthetized and sacrificed 8 weeks later. Bilateral submandibular glands were excised and subjected to standard histological processing. Fluorescent labelling of purified EVs was performed using PKH26 Red Fluorescent Labelling Kit (Sigma-Aldrich; 4 μM), following the manufacturer's instructions. Further details are described in Paper III.

Measurement of stimulated saliva flow

For Paper I and Paper III, the method of collecting stimulated saliva flow is the same. Briefly, each mouse was weighed and administered 1 mg/kg (body weight) pilocarpine (P6503, Sigma-Aldrich, concentration: 1 mg/mL) subcutaneously. The saliva of each mouse was collected within 15 min (Paper I) or 10 min (Paper III) and stored in a 0.5 mL microcentrifuge tube; the saliva volume was measured by gravimetric analysis (saliva density was presumed to be 1 g/mL). The SFR was calculated as follows: SFR (μL/min/g) = saliva volume/mouse body weight/time. For Paper III, the mice were anesthetized at different time points with described details.

Primary epithelial cell isolation by MACS

Using Multi Tissue Dissociation kit 1 (Miltenyi Biotec, Germany), minced submandibular gland tissues were dissociated and homogenized. Using gentleMACS (Miltenyi Biotec, Germany), we selected SGECs with Miltenyi mouse CD 326 (epithelial cell adhesion molecule; EpCAM) by MicroBeads (130-105-958)[240].

Sphere-formation assay and cellular senescence detection

EpCAM-positive cells were isolated and cultured as described by Beucler and Miller 2019 in a previous report[241]. For detailed descriptions and steps, please see Paper III. Briefly, well plates were coated with basement membrane matrix (BMM; R&D Systems, USA) after suspending the cells in BEGM Lonza, Switzerland. On days 2, 5, and 8, cells were soaked in paraformaldehyde for 4 %, and incubated one-hour with SPiDER-βGal staining solution SG03 (Dojindo Laboratories, Japan) with further fluorescence observation and analysis. No xylene is used in all immunofluorescences.

Metabolic Assay (WST-1)

WST-1 assays (Roche, Sigma-Aldrich, USA) were used to assess PCSS metabolism and proliferation. At 1, 3, and 5 days, PCSS tissue slices were incubated in 200 µL culture medium adding WST-1 (dilution in 1:10) according to manufactures' instruction. The optical density of the formazan solution was measured after 3 hours at 37 °C incubation in a plate reader (Epoch, Biotek) at 440 nm. For detailed workflow, measurement mode and calculation method, please see Figure 20 and correlated method description in Paper II.

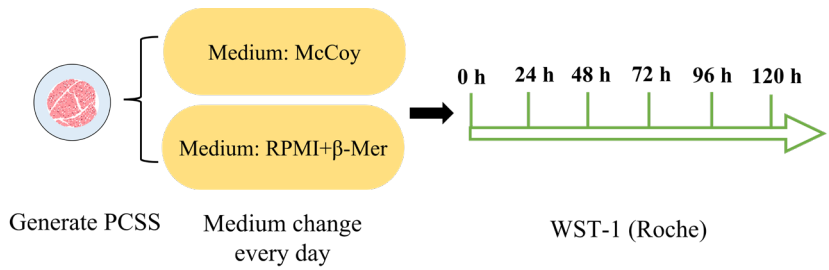

Figure 20. Schematic overview of experimental setup for WST-1 assay for PCSS samples at various time points. Created by the author. Copyright by the author.

α-amylase-activity assay

α-Amylase activity was used to determine if starch could be broken down into sugar molecules by its activity. In this experiment, the α-Amylase Assay Kit (Colorimetric, ab102523) was used on the collected medium supernatant following sectioning and PCSS culture for 12 hours and 48 hours. The supernatant medium was centrifuged for 10 minutes at 1500 rpm and stored at - 20°C. In a kinetic mode,

absorbance was read at OD = 405 nm with a colorimetric multimode plate reader (Cytation 5, BioTek, USA) at 37 °C. α-amylase activity (mU/mL) was calculated using the following formula: α-amylase activity = $\frac{B}{\Delta T \times V} \times D$. For detailed explanation about measurement and the interpretation about the formula, please see Paper II (The overall schematic for the assay is shown in Figure 21).

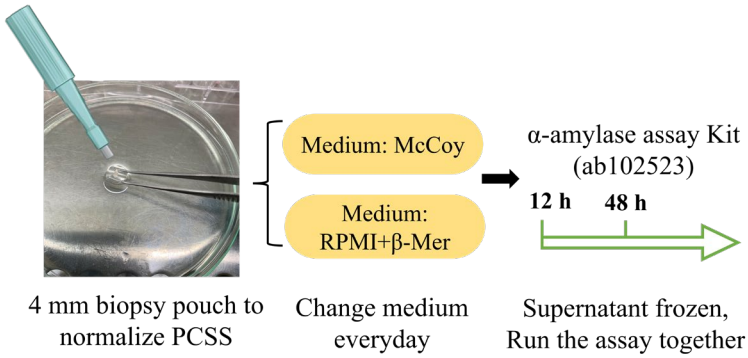

Figure 21. Schematic overview of experimental setup for α-amylase-activity assay for PCSS samples at 12 hour and 48 hour post sectioning. Created by the author. Copyright by the author.

Assay of superoxide anion scavenging activity

The superoxide anions were measured using an SOD Assay Kit (Dojindo Laboratories), according to the manufacturer's protocol. This assay indicates whether superoxide dismutase (SOD) has a strong or weak ability to remove superoxide anions (shown in Figure 22).

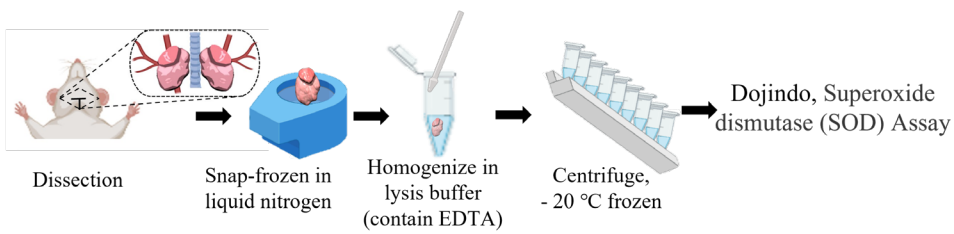

Figure 22. Schematic flowchart of how SOD assays are conducted on animal tissue samples. Remove blood from animal tissues by thoroughly washing them with physiological saline. Wet weight should be measured after wiping off moisture with filter paper. The tissue was disrupted with a histo-homogenizer. Then add 4 to 9 times the wet weight of sucrose buffer (0.25 moles sucrose, 10 mmol/LTris-HCl buffer pH 7.4, 1 mole/L EDTA). Afterwards, use the supernatant for subsquent steps and measurement. Created by the author. Copyright by the author.

Histological analysis and xylene-free tissue processing

For Paper I

Tissue fixation and processing was performed according to conventional techniques using xylene (described in Table 16, the third column) based protocols[239,243].

Table 16. Schedule overview of histological processing with and without xylene.

	Xylene-free tissue processing	Tissue processing with Xylene
1. Fixation	use 10 % neutral buffered formalin overnight and keep in PBS in 4 ℃	
2. Tissue Handling	cut in appropriate size, put in right labelled cassettes, keep in fresh PBS	
3. Dehydration	50 % EtOH, 1 hour	50 % EtOH, 1 hour
	70 % EtOH, 1 hour	70 % EtOH, 1 hour
	80 % EtOH, 1 hour	80 % EtOH, 1 hour
	80 % EtOH, 1 hour	90 % EtOH, 1 hour
	100 % EtOH:100 %ISO (80 mL: 20 mL), 1 hour	95 % EtOH, 1 hour
	100 % EtOH:100 %ISO (80 mL: 20 mL), 1 hour	100 % EtOH, 1 hour
		100 % EtOH, 1 hour
		100 % EtOH, 1 hour
4. Clearing	xylene, 1 hour	100 % Isopropanol, 1 hour
	xylene, 1 hour	100 % Isopropanol, 1 hour
	Xylene, 1 hour	100 % Isopropanol, 1 hour
5. Paraffin Infiltration	Paraffin 1st, 1 hour	
	Paraffin 2nd, overnight	

Firstly, the tissues were fixed overnight and sliced into 4-µm-thick sections using a Microtome and placed on a glass slide. Hematoxylin and eosin (Muto Pure Chemicals, Tokyo, Japan) staining was conducted according to previous protocols[243] in Nagoya University using paraffin-embedded specimens, and also include steps that use xylene to clear before the final mouthing steps.

Immunohistochemistry was conducted according to previous protocols[243] in Nagoya University using paraffin-embedded specimens, and also include steps that use xylene to clear before the final mounting steps. Briefly, immunohistochemistry was performed using the Vectastain ABC Kit (Vector Laboratories, Burlingame, CA, USA). After dewaxing and incubation with primary anti-AQP5 antibody (1:250, Ab3559, Sigma-Aldrich) overnight at 4 ℃, the sections were treated with specific biotinylated secondary antibodies, Vectastain ABC Reagent, diamino-benzidine chromogen, and hematoxylin blue. Tissue images were captured with a fluorescence microscope (BZ9000, Keyence, Osaka, Japan). The percentage of acinar cells was calculated by two independent examiners. Ten fields per

gland/mouse were selected and ImageJ Software (National Institutes of Health, Bethesda, MD, USA) was used for image analysis.

Immunofluorescence was done according to previous protocol[239]. Xylene is not used in immunofluorescence. The frozen tissue sections were incubated with iced acetone overnight and 10-µm-thick coronal sections were prepared using a cryostat (CM3050S, Leica Biosystems, Wetzlar, Germany). Immunofluorescence staining was performed according to the manufacturer's instructions. The sections were incubated with 0.5 % Triton X-100 for 15 min and 3 % bovine serum albumin for 1 hour. Primary antibodies were incubated overnight: E-cadherin antibody (AF748, R&D Systems, Minneapolis, MN, USA), senescence-associated (SA)-β-galactosidase (SPiDER-βGal, SG03, Dojindo, Kumamoto, Japan), phospho-histone H2A.X antibody (2577, Cell Signalling Technology, Danvers, MA, USA), anti-aquaporin5 antibody (Ab3559, Sigma-Aldrich), and anti-keratin-5 antibody (Krt5, 905503, BioLegend, San Diego, CA, USA). After washing, secondary antibodies were incubated for 30 min at 37 °C: donkey anti-rabbit Alexa Fluor 594 (ab150076, Abcam, Cambridge, UK), donkey antirabbit Alexa Fluor 488 (ab1608521, Abcam), chicken anti-goat Alexa Fluor 488 (ab1613906, Abcam), and chicken anti-goat Alexa Fluor 647 (ab1129666, Abcam). Hoechst 33258 (Thermo Fisher Scientific) was stained for 1 min, a confocal laser scanning microscope (A1Rsi, Nikon, Tokyo, Japan) was used to observe the samples.

For Paper II and IV

Paper II and IV use a xylene-free tissue processing procedure where isopropanol replaces xylene (described in Table 16, the second column). Xylene was however used for deparaffinization and mounting steps in Papers II and IV for H&E staining[244]. Tissue was fixed overnight in a 10 % neutral buffered formalin solution, and then replaced with fresh PBS solution the following day and stored at 4 °C. Using an Automated Spin Tissue Processor STP-120, we first programmed the xylene-free tissue-processing-protocol for the steps of dehydration, clearing, and paraffin infiltration for salivary gland (Table 16). Due to the fact that xylene is a health and environmental hazard, isopropanol was used to replace xylene[245]. The use of xylene-free protocols is also important in order to more readily compare antibody staining and morphology of paraffin embedded sections to those generated with light sheet fluorescence imaging (LSFM) (Paper II), as tissue processing, staining, and clearing for LSFM is an alcohol-based procedure (i.e., methanol) without the use of xylene. Xylene has been previously shown to alter antibody-based immunostaining[245]. The Tissue Processor was programmed to stir at a speed of 60 rotations per minute during the entire procedure and to change rotational direction every 60 seconds. To ensure complete infiltration of the paraffin into the entire tissue thickness, the dehydrated and cleared tissues in cassettes must be automatically transferred to the final containers within the tissue processor

containing molten paraffin at 65 °C controlled temperature during the final two steps.

For performing the subsequent tissue sectioning, a microtome was used to cut 5 µm thick sections after paraffin embedding into solidified paraffin blocks. Floating sections were transferred to pre-warmed water baths at 37 °C and placed on histological glass slides for overnight drying. According to the published protocol[244], H&E staining and imaging was then carried out.

For Paper III

In tissue processing steps before paraffin infiltration and before stain, xylene was used (described in Table 16, the third column). For hematoxylin and eosin (H&E; Muto Pure Chemicals, Japan) and Sudan black B (SBB; FUJIFILM Wako, Japan) staining, paraffin-blocks were used. In the trully staining stage to stain hematoxylin and eosin and Sudan black B, xylene was used to clear before the final mounting steps according to previous protocols in Nagoya University[239,243]. For the senescence-associated β-galactosidase immunofluorescent staining, frozen sections of the salivary gland tissue were used, and xylene is not used in immunofluorescence. For the detailed protocol, please see manuscript Paper III.

Real-time RT-PCR

For Paper I and III

For reverse transcription (RT)-quantitative PCR (qPCR), TRIzol reagent (Thermo Fisher Scientific) and ReverTra Ace qPCR RT Master Mix (Toyobo, Osaka, Japan) was used. RT-qPCR was done with THUNDERBIRD SYBR qPCR Mix (Toyobo). Gene expression fold-changes were calculated relative to the control group using **. For the detailed protocol, please see manuscript Paper III.

For Paper II

For PCSS, we firstly optimized a protocol previously optimized for precision cut lung slices (PCLS) that could isolate high quantity and quality RNA from the limited sample amounts generated with PCSS samples[246].

RNA has been isolated from human salivary gland slices RNA for quantitative real-time polymerase chain reaction (qRT-PCR)[219], where there is not a huge limitation in the amount of sample in human PCSS as compared to murine PCSS. The amount of material available for RNA isolation and subsequently PCR is limited due to murine salivary gland slices being much smaller than human salivary

gland slices and thus we first needed to develop a protocol. Furthermore, PCSS agarose can be retained between lobules over time and the residual agarose in organotypic slices can interfere with high-quality RNA isolation[246]. Initially, we aimed to optimize a protocol for separating RNA from murine PCSS samples containing agarose (Figure 23). To simulate residual agarose, we coated native murine salivary gland tissues with agarose. We then modified a TRIzol-based RNA extraction protocol and compared it with agarose-free native salivary gland samples of similar size (Figure 23). To homogenize the PCSS, a Qiagen TissueLyser II was used with stainless steel beads of 5 mm in TRIzol for three times for one minute each, and then for two more times until there are no obvious pieces of tissue in each tube. We found that inclusion of agarose did not affect A_{260}/A_{280} or A_{260}/A_{230} ratios (Please see Figure 4A in manuscript II) and thus that this protocol was suitable for evaluating isolation of RNA from murine PCSS.

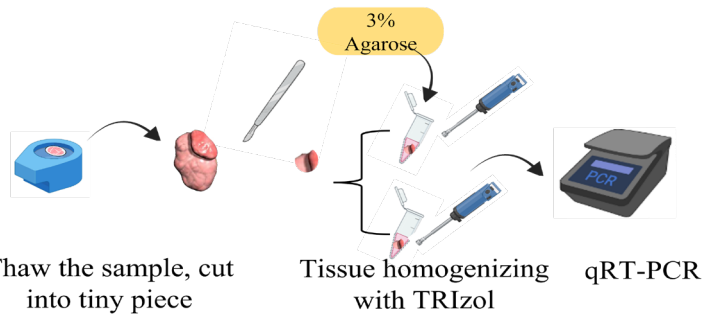

Figure 23. A workflow to mimic PCSS samples in RNA isolation and Nanodrop analysis.
We isolate RNA from PCSS samples obtained from mice by either adding or not adding agarose to salivary gland organ samples after they have been cut into PCSS size samples. Created by the author. Copyright by the author.

After we confirmed that TRIzol can be used to isolate RNA from mouse native salivary glands follow this protocol, then we evaluated RNA's potential for downstream analysis. A three-day culturing of snap frozen PCSS samples (prepared in McCoy and RPMI medium) was used to assess RNA purity and concentration (Figure 24). When PCSS cultures were cultured in McCoy or RPMI media, there was no apparent relationship between high quality RNA yields (A_{260}/A_{280} and A_{260}/A_{230}) and McCoy or RPMI medium usage. We found that samples with higher RNA concentrations yielded good quality A_{260}/A_{280} and A_{260}/A_{230} samples. For RNA concentrations less than 100 ng/µL, A_{260}/A_{280} purity values were around 2.0, but A_{260}/A_{230} ratios were lower (Please see Figure 4B in manuscript Paper II).

Further analysis revealed that A_{260}/A_{280} ratios were to be of good quality, ranging around 2.0 and not significantly differing between groups of two media and over time. This modified TRIzol protocol, therefore, was used for isolating RNA from PCSS derived from murine tissues with high A_{260}/A_{280} ratios (Please see Figure 4C

in manuscript Paper II). In contrast to the samples from native glands, the majority of RNA samples from PCSS had an A_{260}/A_{230} ratio below the recommended value (i.e., 2.1) (Please see Figure 4D in manuscript Paper II). This contrasts with our pilot experiments. This may be due to the limited amount of tissue used for RNA isolation from PCSS samples. A low A_{230} indicates contamination that absorbs at 230 nm, such as carbohydrates, salts (guanidine salts), phenol, etc. The lower quality limit for RNA preparation for downstream applications is not known and depends on the contaminant. Therefore, we next tested whether RNA samples with high and low A_{260}/A_{230} have the same amplification and primer efficiency in qRT-PCR. RNA is converted to cDNA and then amplified for next generation sequencing. Thus, evaluation of RNA quality using reverse transcribed qPCR can also give a preliminary indication if our RNA quality is suitable for multiple downstream assays using cDNA.

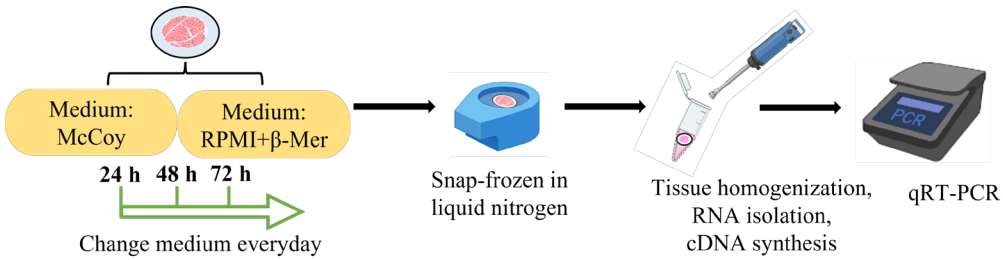

Figure 24. A three-day culture of PCSS samples in different media was performed RNA isolation and Nanodrop analysis.
This is a schematic showing that we culture PCSS for three days in McCoy and RPMI medium to assess the RNA purity and concentration. Created by the author. Copyright by the author.

Two representative PCSS samples were tested to see if they could effectively amplify a housekeeping gene, *Hprt*, previously determined to have a primary efficiency of 90 - 110 % in native tissue (Figure 25). After converting RNA into cDNA, we generated a series of cDNA concentrations from representative PCSS isolated RNA ranging from 1 to 1:256 (Figure 25) and performed qRT-PCR. Using simple linear regression analysis, we found that primer efficiency for cDNA was within acceptable limits for low and high A_{260}/A_{230} groups (Please see Figure 5B and Supplemental Table 3 in manuscript Paper II). Moreover, melt temperatures were consistent across all dilutions and A_{260}/A_{230} at high ratio and low ratios. The melting temperatures of primer have not changed significantly (see Figure 5C in manuscript Paper II). This phenomenon is not for the samples that diluted at 1:256, they have a slight rightward shifts of around 0.5 °C. It was therefore demonstrated that PCSS RNA samples with low A_{260}/A_{230} ratios can be used in qRT-PCR.

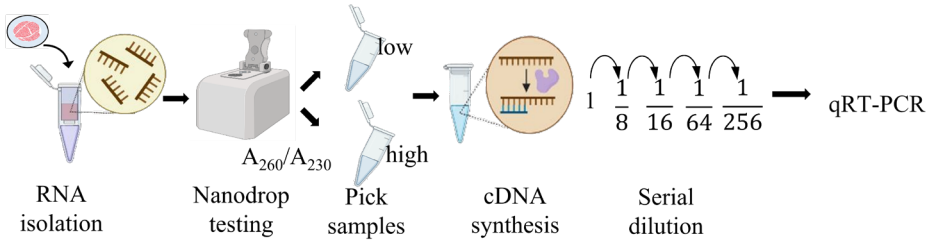

Figure 25. Low A_{260}/A_{230} purity RNA isolated from PCSS was applied to qRT-PCR with acceptable primer efficiency for the common housekeeping gene (mouse HPRT).
The schematic workflow to extract RNA and make a series of dilution and run qRT-PCR after cDNA synthesis. Created with BioRender.com.

Following validation, RNA isolation was done as briefly described below. The entire description is in Paper II. TRIzol homogenates were then mixed with chloroform 5:1 (vol/vol) and RNA was isolated using a published protocol used before for PCLS[246]. After evaluating the RNA concentration by Nanodrop, iScript™ Reverse Transcription Supermix Kit (Bio-Rad, USA) was used to generate cDNA. qRT-PCR was done using SsoAdvanced Universal SYBR Green Supermix (Bio-Rad, USA) and custom designed and previously validated primers. For more details, please see Paper II for a fully description on the working flow.

Light-sheet fluorescence microscopy

Thus far, there is no published work which has described light sheet imaging on whole native salivary gland samples from mouse or human or PCSS tissue pieces. Therefore, our aim is to establish and optimize a workflow for it.

Using tissue clearing techniques previously established in the lab for lung tissue (Alsafadi et al. *in preparation*), we want to know whether tissue clearing could be done on salivary gland organs and their tissue slices PCSS, according to a protocol described earlier[249]. During this modified iDISCO protocol and imaging, dehydration and delipidation are performed using a series of methanol and other organic solvents, along with final incubation in a medium with a RI equivalent to image structures. Due to its nontoxic nature and in alignment with a more sustainable chemical use, we selected ethyl cinnamate as our preferred solvent over previously described organic solvents for RI matching to produce optically clear tissue[248] (Figure 26).

After clearing salivary gland tissue, the samples were submerged in an organic solvent (ethyl cinnamate) and placed into the imaging chamber of a light sheet fluorescence microscopy (LSFM, Ultramicroscope Blaze, Miltenyi Biotec). Autofluorescence (excitation/emission: 488/525 nm) imaging was performed in

dual-side fusion mode and a 4x dipping objective, the samples were sequentially evaluated using SyGlass, a virtual reality software (PCSS after 24 hours).

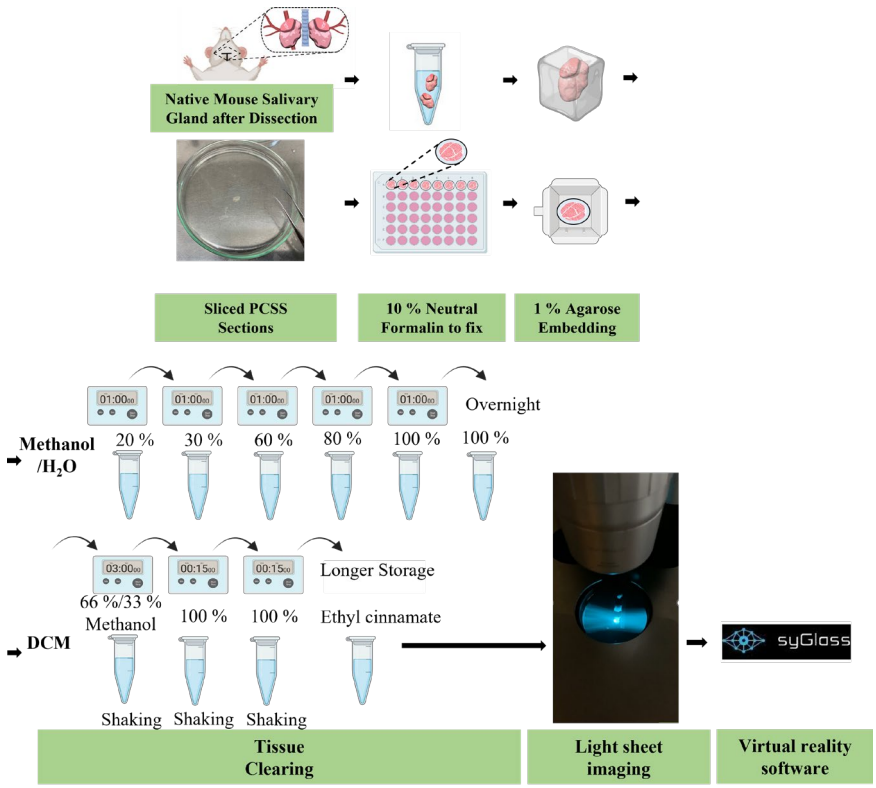

Figure 26. Fluorescence imaging by light sheet microscope after tissue clearing was shown in the following schematic. Created by the author. Copyright by the author.

Statistical analysis

All data are presented as the mean ± standard deviation. At least three independent experiments were done. GraphPad Prism 9 software (GraphPad Software Inc., USA) was used for all statistical analysis. Student's t-test was used to determine the P value in two group comparisons with normally distributed data. Multiple comparison post-test was combined with one-way analysis of variance to determine differences between multiple groups. Differences were considered statistically significant at $P < 0.05$. Please see Paper I, II, III and IV for complete details, including a discussion of the statistical approaches relevant to semi-quantitative scoring in Paper IV.

Summary of Results and Discussion

This thesis examined the potential of stem cell-derived therapy for two major salivary gland diseases which are acute irradiated salivary gland dysfunction and chronic immune-related salivary gland hypofunction (Paper I & III). As a result of the development and implementation of precision-cut salivary gland slices (PCSS), a bioengineered model was built in Paper II to model disease and evaluate salivary gland regeneration. Furthermore, this thesis aimed to extend the application of sustainable histology, without the use of xylene and semi-quantitative histological scoring system (Paper IV), as well as a more environmentally friendly light sheet fluorescence microscopy approach using ethyl cinnamate as the organic solvent, for future application to salivary gland research.

Paper I

EVs could be generated from hDPSCs

An analysis of transmission electron microscopy revealed that the diameter of hDPSC-sEV was 60 - 120 nm, which was in accordance with the results of particle size distribution analysis (Figure 1A and B for Paper I). Positive adhesion of gold colloids was observed to these sEVs (Figure 1A for Paper I). As indicated by Western blotting (Figure 1C for Paper I), exosomal markers CD9, CD63, and CD81 were positively expressed, but α-tubulin was only detected in cells rather than hDPSC-sEV. It was observed that mice were sacrificed 1 days following administration with hDPSC-sEV (5 μg/0.5 mL) labelled with PKH26 (Figure 1D for Paper I) via the mouse tail vein (three times per week for two weeks). Micrographs of the 25 Gy+sEV group revealed that PKH26-labeled sEV were taken upby submandibular gland epithelial cells (Figure 1D for Paper I).

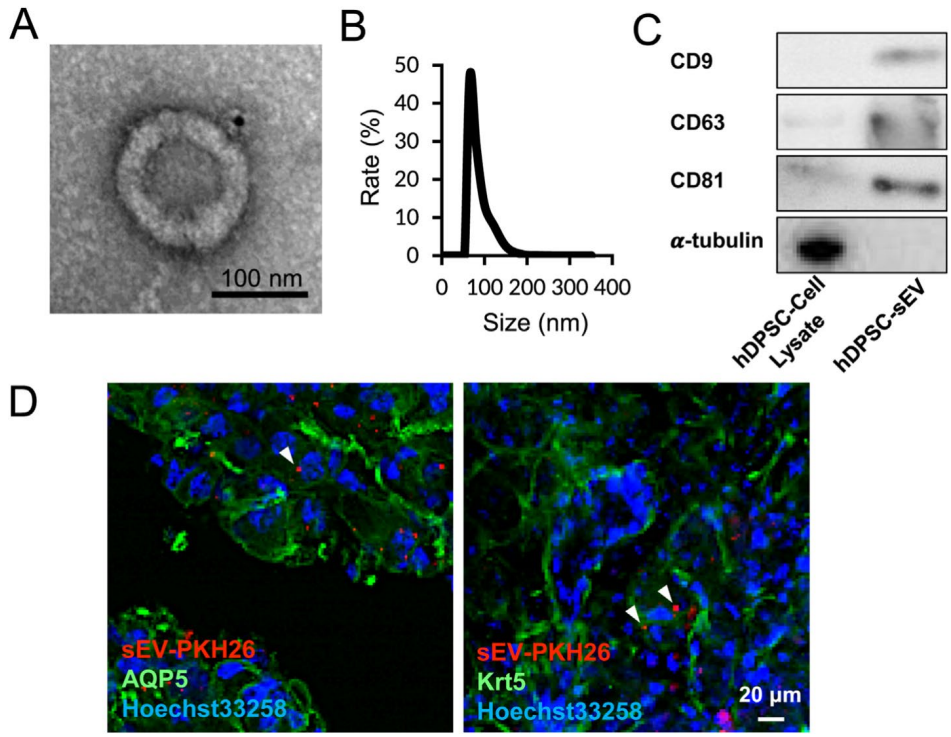

Figure 1 for Paper I. Identification of small extracellular vesicles (sEV) and their uptake by cells. (A) Immunogold labeling of human dental pulp stem cell-derived sEV (hDPSC-sEV) with CD9 antibody visualized by transmission electron microscopy. Scale bar: 100 nm. (B) hDPSC-sEV particle size distribution was measured. (C) Exosomal marker expression in sEV was determined by western blotting, with α-tubulin expression as a reference. (D) Analysis of cellular uptake of sEV. Hoechst 33258 was used to stain cell nuclei (blue). Scale bar: 20 μm.

Characterisation of isolated EVs

With differential centrifugation, cells, large vesicles, and debris are removed while EVs are precipitated. Owing to its simplicity and high yields, this method is suitable and commonly used for our group to separate EVs from biological fluids. The most obvious disadvantage for our frequent usage is being time-consuming and multiple rounds of centrifugation will impact purity[249]. Regardless of the method used for EVs isolation, it is difficult to achieve extremely high purity, and non-EVs impurities will still remain. For example, neither ultracentrifugation nor gradient density centrifugation can remove low-density lipoprotein particles in serum well, so we used serum-free medium when producing EVs and being able to starve cells also helps us to eliminate the interference of serum. It is necessary to show the characteristics of the "EVs" samples we obtained.

In order to identify EVs, their existence, purity, and integrity are considered; therefore, multiple experiments and analyses are needed to confirm one another.

By using electron microscope imaging (scanning electron microscope, SEM and transmission electron microscopy, TEM), we were able to detect the existence and integrity of individual EVs under high magnification. This method is highly sensitive and can identify EVs of different sizes. However, its disadvantages include high requirements for sample preparation and pre-treatment, the inability to accurately measure the concentration of EVs, and the electron microscope can also show partial scenes of nanoparticles which may also be mycoplasma and lysosomes (because they are very similar to EVs under electron-microscope).

The population characteristics of EVs numbers and diameters can be confirmed by particle size analysis. Although this method is accuracy, rapidity, and repeatability, we cannot reliably detect the sample is EVs. Also, particle size detection cannot reflect the particle shape, making it impossible to confirm the existence and integrity of EVs.

Consequently, we used the third method of WB to confirm the presence of EVs by detecting exosomal protein markers presented at the protein level. Common exosomal markers include CD63, CD9, etc. However, CD63 is not unique to EVs; it is also found in cell debris and lysosomes. Thus, WB can only confirm the existence of EVs components, but cannot confirm the quantity and integrity of EVs.

Therefore, we chose to follow the guidelines issued by the International Association of Extracellular Vesicles[250], and used three experiments to jointly identify EVs, that is, the classic structure similar to EVs existed in the sample observed by electron microscopy, and WB found that the samples contained EVs markers. For the number of EVs, the number of particles and the statistical diameter distribution are measured by Nanoparticle tracking analysis (NTA) experiments, and samples are evaluated at the particle population level.

Therefore, the results of these three experiments in our results are all normal (the classical structure was seen by electron microscopy, the marker enrichment of EVs was detected by WB, and the diameter distribution measured by NTA conforms to the definition of EVs). So, we are sure that we have successfully isolated and purified hDPSC-EVs. Moreover, what we obtained was the result of immunoelectron microscopy combined with CD9 antibody labelling, so we are more perfect in the method of identifying EVs.

In vivo irradiation model shows decreased salivary output and no remarkable improvement on SFR shown after sEV administration

During pre-experiments, mice were irradiated at gradient IR doses of 10, 15, and 25 Gy, resulting in a progressive decrease in body weight and wet weight of the submandibular glands as compared to mice that were irradiated at 0 Gy. Weights in each group also decreased with increasing IR doses. In the 25 Gy group, the weight change was 0.4 %, in the 0 Gy group, 0.6 % (Please see Figure S1 in the published Paper I).

Based on IR as shown in Figure 2A, the total SFR of bilateral submandibular glands decreased significantly after stimulation (Figure 2B for Paper I). In contrast to the 25 Gy+PBS group (Figure 2B for Paper I), no significant improvement in SFR was observed in 25 Gy+sEV group. The histological analysis revealed that enlarged acinar cells with hyperchromatic nuclei were present (Figure 2C for Paper I), which were rare in the control and 25 Gy+sEV groups.

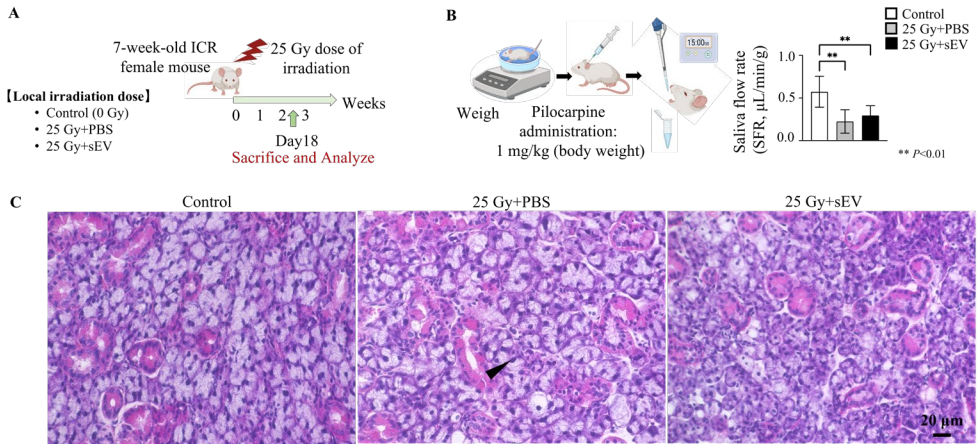

Figure 2 for Paper I. The establishment of the in vivo model was shown.
(A) An overview of the experiment design was provided. (B) SFR was calculated for each mouse (n = 4 per group, 1 data per sample) (**P <0.01*). (C) A histological evaluation was performed by using H&E staining (scale bar, 20 μm) (40 x magnification). Hyperchromatic nuclei were depicted by black arrows.

DNA damage correlates to irradiation and the need for histological scoring

DNA is the majority of the genetic material in the cell. The nucleus of a tumor cell is often larger and has a higher nucleoplasmic ratio than a normal cell's nucleus. Deformities of the nucleus include elongation, jagged edges, depressions, long buds, lobes, and crescents. Area ratio (nuclear enlargement/nuclear area of normal cells) and nuclear outline thickening are important cell morphology indicators.

There are three phases to an irradiation effect: physical, chemical, and biological. The time of physical processes is quite short, the interaction between wave and particle irradiation and atoms in the exposed tissues, then ions are formed. Then completely chemical phase begins. Inorganic molecules are cleaved, and reactive radicals are generated. All subsequent processes are included in the biological phase, which can last for several decades. It involves a chain reaction between inorganic radicals and biomolecules. There is significant relevance to DNA damage in the form of base damage, sugar changes, and DNA protein cross-links as well as single and double strand breaks. So, irradiation should be accompanied by the changed morphology and structure of DNA that could be detected by histological analysis.

In our study, our identification method for nuclear enlargement is, however, extremely subjective and lacks objective quantitative or semi-quantitative analysis. Due to our subjective and unsystematic way to evaluate how large is the enlarged nucleus of submandibular glands and their abnormal proliferation, we are unable to demonstrate the correlation between irradiation damage and the cellular changes on nucleus of submandibular glands cells, which is why pH2A.X was used as an indicator of DNA damage response in later experiments. Also, this implies that the establishment or optimization of histological evaluation, classification, and grading methods to detect nuclear changes caused by irradiation is what we need to do in the future. The development of such a methodology, as outlined in Paper IV in this thesis, can be used as a template to develop this further.

Irradiation induces cellular senescence in submandibular glands and hDPSC-sEV reduces the number of senescent cells

SA-β-galactosidase is a marker for senescence. The number of SA-β-galactosidase-positive cells increased significantly in the 25 Gy+PBS group, which was substantially reduced (**$P < 0.01$) in the 25 Gy+sEV and control groups (Figure 3A and B for Paper I). pH2A.X is a representative protein that is highly expressed during the DNA damage response (DDR). PBS group had a greater number of cells positive for both SA-β-galactosidase and pH2A.X, as compared to the sEV and control groups. Additionally, pH2A.X-positive cell nuclei damage occurred in both the acinar and ductal compartments of the submandibular glands (Figure 3C and D for Paper I). The 25 Gy+PBS group also displayed increased expression of genes involved in cellular senescence (*$p16^{INK4a}$, p21*) and SASP factors (*MMP3)* (*$p16^{INK4a}$, MMP3,* **$P < 0.01$; *p21*, *$P < 0.05$). The administration of sEV, on the other hand, significantly reduced the expression of senescence genes and inflammatory cytokines (*$p16^{INK4a}$ and MMP3*, **$P < 0.01$; *p21*, *$P < 0.05$). For the targets of senescence and hDPSC-sEV among the irradiated submandibular gland cells, Krt5 was expressed explicitly in ductal epithelial cells. In the 25 Gy+PBS group, senescence was co-stained with ductal epithelial cells positive to Krt5 (Figure 3F for Paper I, **$P < 0.01$), whereas in the 25 Gy+sEV group, this was relatively rare (Figure 3G for Paper I, **$P < 0.01$).

Limitations for markers of senescence

There is a difference between aging and cellular senescence. As we age, our bodies begin to undergo a progressive decline which can occur throughout our lives, including during embryogenesis. The number of senescent cells increases as we age. The term cellular senescence refers to a stable state of cell cycle arrest in which proliferating cells become resistant to growth-promoting factors. Several damaging stimuli can trigger senescence, including telomere shortening (replicative senescence), DNA damage (DNA damage-induced senescence), and oncogenic

signalling (oncogene-induced senescence). The morphological and metabolic characteristics of senescent cells are characterized by changes in gene expression, chromatin remodelling, and a pro-inflammatory phenotype known as senescence-associated secretory phenotype (SASP). Another hallmark of senescent cells is extensive chromatin remodelling and altered gene expression, most notably the formation of senescence-associated heterochromatin clusters (SAHF). These facultative heterochromatin loci play a role in the silencing of pro-proliferative genes, including E2F target genes such as cyclin A. Typically, senescent cells contain 30 - 50 SAHF, characterized by DAPI bright staining, macroH2A, heterochromatin protein 1 (HP1), and lysine 9 dimethylated or trimethylated histone H3 (H3K9Me2/3) immunoreactivity. Despite the frequent observation of SAHF during senescence, some cells appear to be senescent without SAHF, so we have not checked for SAHF. This should be done in future work.

Senescence can be destructive or regenerative in xerostomia following irradiation therapy

IR is known to contribute to DNA double-strand breaks or genomic instability, which elicits DDR signals. DDR fuels reactive oxygen species generation and enhances $p16^{INK4a}$ tumour suppressor expression. $p16^{INK4a}$ restrains progression from G1 to S phase of the cell cycle. Persistent DDR signalling also activates SASP. *p21* can interfere with cell division. Rapid phosphorylation occurring at Ser139 of H2A.X after DNA impairment is required to halt the cell cycle[251]. SASP comprises numerous proinflammatory cytokines, proteases, growth factors, and chemokines such as *MMP3*, which can stabilize cell cycle arrest. Our 25 Gy+PBS group also showed predominant overexpression of pH2A.X, senescence genes, and SASP factors after IR damage.

The biological role of aging is complex, and both protective[252] and deleterious effects of senescent cells have been described, mainly depending on the physiological environment. Senescence, for example, is important for development and wound healing. Senescence also prevents the replication of cells containing damaged DNA, which serves to prevent tumours from developing. Even though senescence may have evolved as a means to prevent malignant transformation of damaged cells, it may also lead to many age-related pathologies, including cancer, tissue degeneration, excessive scarring, and inflammatory disorders. The role that senescence plays in chronic pathology changes of irradiation damage in submandibular gland organs is important to clarify. It is presently not known whether senescence in irradiated submandibular gland exaggerates fibrosis or whether senescence helps to regenerate the functional acinar of submandibular glands. Understanding the role of senescence in every stage of irradiated submandibular gland is necessary for designing and evaluating therapies.

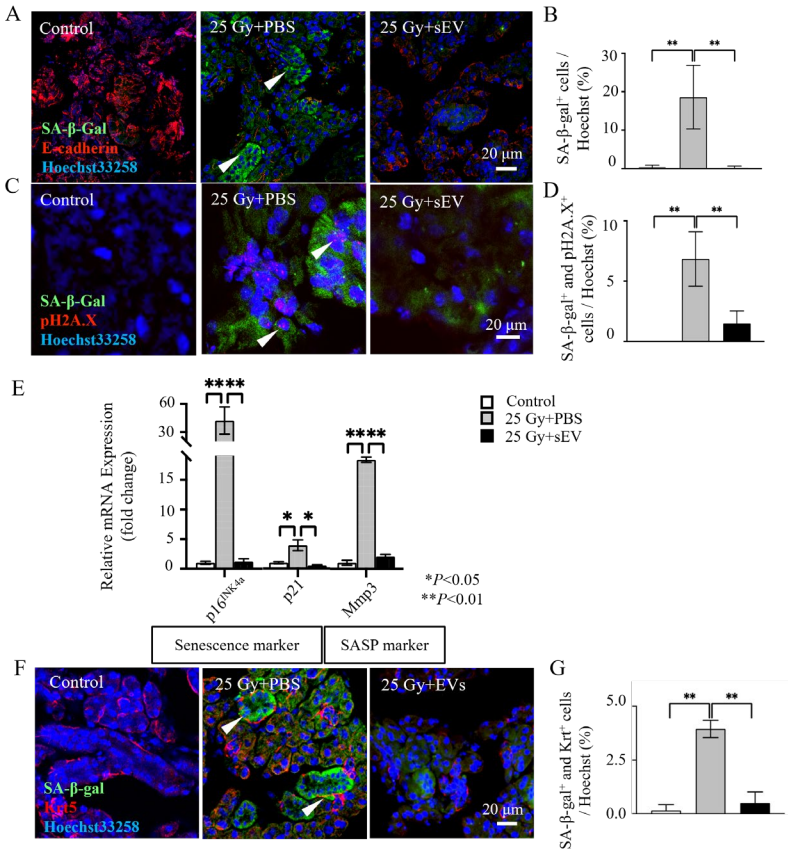

Figure 3 for Paper I. The role of sEV in cellular senescence was demonstrated.
(A) Senescence-associated (SA)-β-galactosidase-positive cells were stained with E-cadherin and Hoechst 33258 for immunofluorescence staining. Scale bar: 20 μm (n = 4 per group, 3 images per sample). (B) Percentage of SA-β-galactosidase-positive cells in the PBS and sEV groups are depicted (n = 4 per group, 3 replicates per sample) (**P <0.01*). All data are presented as the mean ± standard deviation and analyzed by two independent examiners blindly. (C) An immunofluorescence image of SA-β-galactosidase (green) co-staining with pH2A.X (red). Scale bar was 20 μm. (D) The number of pH2A.X and SA-β-galactosidase double positive cells was calculated (**P < 0.01*). (E) An analysis of the gene expression of senescence-associated genes was conducted at 18 days post-IR (*P < 0.05*, **P < 0.01*). (F) Immunostaining for Krt5 (red) and SA-β-galactosidase (green). Scale bar: 20 μm. (G) The number of Krt5 positive cells that are double-positive for SA-β-galactosidase (**P < 0.01*).

EVs play a role by reversing the oxidative microenvironment

As a result of IR, the 25 Gy+sEV group showed higher levels of SOD activity as compared to the 25 Gy+PBS group (Figure 4 for Paper I). This suggests that the 25 Gy+sEV group had a greater capacity to scavenge reactive oxygen species than the 25 Gy+PBS group.

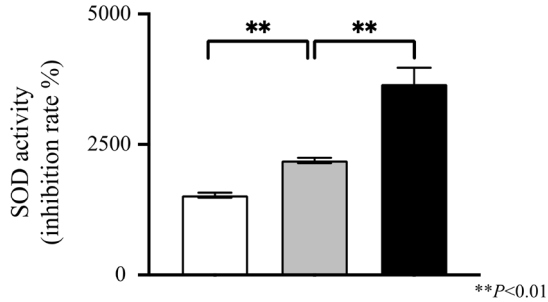

Figure 4 for Paper I.The effect of sEV on oxidative stress in the submandibular gland was shown. All data represent the mean ± standard deviation from three independent experiments (***P <0.01*).

EVs and reactive oxygen metabolites

Additionally, we observed that hDPSCs may possess the ability to perform reactive oxygen metabolism, which can be transmitted by sEVs. EVs derived from mice with 2 Gy irradiation were found to transmit the cellular antioxidant system of donor mice to bystander mice, thereby increasing circulating reactive oxygen metabolite levels systematically in bystander mice[253]. It is widely accepted that the potential molecular (mRNA/miRNA/protein) shuttled by EVs (derived from healthy cells) may be responsible for the therapeutic effects of EVs[254]. There is therefore a need for further research into which miRNA fragments transmitted by hDPSC-sEV exert the advantages of reactive oxygen metabolites (will discuss more in "Future Perspectives" with discussion on mitochondrial) and how they react with the pathological senescence process of submandibular glands' stem cells and ductal cells.

As a limitation of this study, we did not explore the long-term impact of cellular senescence and the long-term role of hDPSC-sEV. The use of small animals in disease modelling is another limitation.

Paper II

Metabolic activity exists in murine PCSS model at 0 hour of ex vivo culturing.

The first step was to embed the excised salivary glands in agarose, then conduct slicing on a vibratome. Slices were then cultured in McCoy's 5A or RPMI+β-mercaptoethanol (Please see Figure 1D in manuscript Paper II) to compare. Learning from the experience of previous work[221], we created our own workflow to generate multiple, serial sections of precise thickness (300 μm). Multiple lobules

were visible along with blood vessels and ducts within these slices (Please see Figure 1A and B and C in manuscript Paper II).

Next, we are interested that PCSS were viable after vibratome slicing or not. We found that PCSS has metabolic activity in both McCoy's 5A and RPMI+β-mercaptoethanol at 0 hour after slicing (Please see Figure 1E in manuscript Paper II).

Murine PCSS exhibit metabolic activity up to 96 hours.

In the 96 hours of culture, all PCSS initiated strong metabolic activity. It was evident that at no point were there any statistically significant differences between the two culture mediums (Please see Figure 2A and B in manuscript Paper II), which has been observed in other precision cut organ systems generated by our group[242].

Generation of an organotypic PCSS culture system with a vibratome

In terms of the current workflow of generating PCSS, one question is how to generate PCSS of precision and consistent thickness. Thickness of 30 - 50 µm has reported in published papers for direct observation. The precise thickness of salivary gland is hard to obtain because salivary gland is not a hard tissue, and it is super soft organ with fibrotic texture tissue. It is important to note that, solidified agarose that is embedded around salivary glands provides a support structure. It is possible to injure organs when the vibratome performs a mechanical slicing process because of the amount of connective tissue present. For this method to become more widely used, many more practical small tips should be compared between laboratories. For many soft tissues, such as the salivary gland, PCTS (Precision-cut tissue slices) are generated by embedding the excised tissue in low melting agarose which matches the mechanical environment of the native tissue. This allows for the vibrating blade to cut through the tissue evenly. However, the salivary gland has connective tissue both within and outside the organ which are more difficult to cut due to their composition. Alternative techniques like cutting first with a tissue biopsy punch might help avoid these problems but are difficult to do for small organs.

The second major limitation is until now, the most optimal cutting conditions and culture system for PCSS tissue pieces is unknown. In this thesis, we tried two different cutting buffers and did not see any major changes. We also only cut with one major orientation (vertical) and one slice thickness. In preliminary studies, we tested if we could cut PCSS of different thicknesses using our approach. While we could cut 100 µm PCSS, this is a limited amount of material for some downstream assays, so we did not continue with testing this condition. However, thin slices are optimal for imaging applications so future studies should look into the role of slice thickness. With regard to cell culture conditions, depending on the researcher's question, different cell types within the PCSS might be of more interest. Different culture conditions, such as air-liquid-interface, are known to greatly impact

organotypic slices and this should be evaluated for PCSS. In addition, we have learned a lot from primary cell cultures and organoid culture of primary salivary gland epithelial cells. They are known to require specific growth factors to maintain them but none of these factors are included in the majority of medias used. Currently, fetal bovine serum is used in different concentrations due to the fact that it provides a range of growth factors. However, more studies are needed to understand what components should be there. For some studies, it might be enough to preserve acinar cells to study saliva production where in other studies, both nervous and acinar cells should be preserved. Different media formulations might also be necessary for extended culture time. All of this depends on what the model is used for and what sort of readouts the researchers will use.

Culture supernatant of PCSS has physiological α-amylase secretory function during the first 48 hours of culture.

Secretion of enzymatically active α-amylase is central to normal saliva function[219]. Previous studies have used secretion of active α-amylase activity as a marker of tissue level function in PCSS although[219]. α-amylase activity was determined by measuring the ability of PCSS supernatants to cleave the substrate ethylidene-pNP-G7 over time. This substrate releases nitrophenol (NP) which can then be read using kinetic measurements (Please see more details in Paper II in Figure 3A and B). α-amylase activity was apparent due to the continuous increase in the amount of NP during the 1 hour assay period. As expected, the ddH_2O group had no active functional α-amylase secretion while the positive control confirms that the assay is functioning as expected. In comparing McCoy 5A and RPMI+β-mercaptoethanol medium, we saw trends towards increased secretion of functional α-amylase in the McCoy media (Please see Figure 3C for manuscript Paper II), but no statistical analysis was performed due to it only being done on two animals. McCoy's 5A medium has not been used for PCSS before but is known to be commonly used for culturing diverse epithelial cell types (such as α-amylase producing acinar cells)[256-258]. Because of this observation, we next wanted to check what cell types are still present during the culture with different mediums.

McCoy's 5A medium maintains diverse epithelial and mesenchymal phenotypes.

After developing a workflow to isolate high-quality and quantity RNA from PCSS, we used qPCR to evaluate how cell populations change over time in the PCSS model. In our study, we tested two culture mediums and two initial cutting mediums (PBS versus PSS). It is not known how these impact the cell types which are present in PCSS. PCSS models can be used in many different ways, so it's important to know this. The qRT-PCR method was used to study changes in epithelial markers (*Aqp5*

in acinar cells and *Krt5* in ductal cells). In addition, extracellular matrix, and mesenchymal markers Collagen1a1 (*Col1a1*) and Fibronectin (*Fn*) were also studied. It is recommended that PCSS cultures be carried out for 72 hours.

The use of PBS and PSS as a cutting bath medium did not seem to change any of the markers we assessed after culture in McCoy's 5A medium (*Aqp5*, *Krt5*, *Col1a1*, and *Fn*) (Please see Figure 6 in manuscript Paper II). Next, we compared the changes in *Krt5*. This is belonging to a group of well-known markers that represent epithelial cell types in PCSS over time. *Krt5* increased over the first 72 hours with McCoy's 5A medium but only increased for the first 48h with RPMI media (Please see Supplemental Figure 1 in manuscript Paper II). *Aqp5* decrease during the first 48 hours with McCoy's 5A medium but recovered to baseline levels at 72 hours. This indicates restoration of *Aqp5* expression which may come from newly produced *Aqp5* or from cells differentiating into *Aqp5* cells. *Aqp5* decreased over time in RPMI media, with only small increases in one sample at 72 hours (Please see Supplemental Figure 1 in manuscript Paper II).

Fibroblasts are known to be relatively easy to isolate and culture in comparison to epithelial, endothelial, and nervous cells. Other PCTS tissues have seen that fibroblasts can increase over time in these models due to the culture conditions. Using type 1 collagen (collagen 1a1) and fibronectin as markers, we observed increases in both *Col1a1* and *Fn* over time in PCSS for both medias (Please see Figure 6 and Supplemental Figure 1 in manuscript Paper II). This might indicate fibroblast proliferation and should be checked in the future. This can also be a limitation of the model if fibroblasts overgrow.

In conclusion, McCoy's 5A media has several advantages over RPMI. PCSS cultured in McCoy's 5A increases functional α-amylase expression and also results in increased expression of key markers for epithelial cell types. We therefore only used McCoy's 5A for the remainder of Paper II.

McCoy's 5A culture media retains the general structural integrity and neuro-innervation distribution in mouse PCSS

Bright field images of PCSS over 72 hours showed relatively intact PCSS, including retention of the parenchyma and a typical capsule structure. We could also observe intact blood vessels within the tissue slice. This confirms the integrity over culture time (Please see Figure 7A in manuscript Paper II).

We then stained cryosections of PCSS with antibodies against E-cadherin for epithelial cells and β-IV-tubulin for neurons. It was evident that E-cadherin and intracellular tubulin were both expressed over the 48-hour culture period, and both levels were similar to native cells. Hence, McCoy's 5A is effective in maintaining epithelial as well as neuronal cells in PCSS culture (see Figure 7B and 7C in the manuscript paper II).

Three-dimensional imaging is feasible for PCSS and native salivary gland using light sheet microscopy.

In spite of the fact that thin sections of PCSS allow more throughput and the visualization of multiple markers, thin sections do not give the ability to visualize how cells related to one another in 3D within the PCSS. Previous studies in PCSS have used thin slices (as thin as 50 μm) and imaged using confocal imaging. The light scattering that occurs in thicker tissues as well as the long times needed for imaging, which can result in photobleaching. This makes conventional light-based techniques inefficient for visualizing PCSS. LSFM is an emerging technique which has been used to image thick tissues, including up to whole organs which are a few centimetres thick. This is achieved due to advances in optical clearing which then allows an entire sheet of light to pass through the sample. Therefore, we chose to apply this emerging imaging technique to PCSS.

There are several different tissue clearing techniques available for making native tissues optically transparent and currently this must be determined experimentally. We used a modified iDISCO optical clearing protocol (Please see Figure 8A in manuscript Paper II), due to success in our lab in parallel projects on lung tissue. After the modified iDISCO protocol, the tissue appears extremely transparent (Please see Figure 8B in manuscript Paper II), even in air, but the overall structure of the tissue was still preserved. Due to refractive index matching, the tissue appears even more transparent when it was submerged in ethyl cinnamate solution which is the final organic solvent we used (Please see Figure 8B in manuscript Paper II).

After clearing native salivary gland tissue, autofluorescence imaging was performed with a light sheet microscope. Analysis of large 3D images is challenging to do on 2D computer screens and therefore we used a virtual reality software, SyGlass, with virtual reality glasses for visualization. We compiled all of the light sheet imaging computationally (i.e., transformed 2D data into 3D) for both native salivary glands and PCSS and were visualized in VR (virtual reality) with this software. Then we could compare their architecture pre (i.e., native) and post slices (PCSS cultured 24 hours after slicing). We found that both the native salivary gland and PCSS tissue pieces can be easily image by LSFM and look similar (Detailed figures are shown in Figure 8C, and the detailed videos are shown in Supplemental Video 1A and B in manuscript Paper II). Accordingly, light sheet imaging of PCSS closely resembles the classic H&E staining of native salivary gland tissue. This indicates the tissue architecture is maintained after dehydration, delipidation and optical clearing. (Please refer to Figure 8D in the manuscript Paper II for further information). Next, we examined PCSS cultured over time and found that lobule positions appeared in different locations after 24 hours (as shown in Figure 8D and Supplemental Video 1 in manuscript Paper II). We also observed similar changes in lobule architecture in PCSS with increased culture time (For more information, please see Figure 7A in manuscript Paper II). Future work will include antibody-

based staining to identify the location and relative location of different cell types in different conditions.

Paper III

NOD mice are a suitable animal model for Sjögren's Syndrome

Here we examined whether hDPSC-EVs prevented NOD mice from developing salivary gland dysfunction. A significant reduction of foci per 4 mm^2 was observed in the hDPSC-EVs group versus the PBS group in 22-week-old NOD mice with lymphocyte infiltration revealed by H&E staining of the submandibular glands (Please see Figure 2C and D in manuscript Paper III). In hDPSC-EVs group, salivary flow rate was significantly higher than in PBS group (Please see Figure 2B in manuscript Paper III). A microscope examination of the salivary glands 1 hour following the administration of PKH26-labeled EVs revealed the presence of EVs in the submandibular gland tissue (Please see Figure 2E in manuscript Paper III).

Discuss the use of NOD mice as a model for pSS

The ability of animal models to replicate many of the key characteristics of primary pSS patients, including secretory dysfunction, glandular inflammation, and autoantibodies, has been demonstrated to be useful in studying pSS pathogenesis. So, they are still the most widely used and applicable model to this disease that currently available. It can be divided into two categories based on how disease is induced in animals with primary SS-like symptoms: induced models, which are induced in animals by artificial means[259], and genetic models, in which the animals develop disease symptoms by mutation or modification to their genes[260]. Until now, a total of 20 mouse models have been developed for SS, including both induced and genetic models.

The mice serve as the most commonly used model for human autoimmune diseases because of their short lifespan, high fertility, genetic similarity, and ease of genome manipulation[261,262]. pSS patients tend to develop glandular[263] (sialadenitis and dacryoadenitis) and extraglandular manifestations as well as B-cell malignancies. pSS patients fall into two groups: those with mild disease, such as dry eyes or mouth, and those with severe systemic disease, such as severe interstitial lung disease. But the mouse models of pSS don't often exhibit systematic symptoms similar to those of pSS in human; most mice only develop mild symptoms. This may because most mouse models are caused by antigen immunity, viral infections, or a single genetic variation, while human pSS is a complex disease caused by a combination of genetic and environmental factors. So, in order to better mimic human pSS, novel and more representative disease models will be needed. Therefore, there is still no ideal mouse model.

Until now, NOD and derived murine models are the most widely used to study immune pathogenesis and develop potential therapeutics for human SS. NOD mice spontaneously develop diabetes and symptoms similar to secondary SS. Like human SS patients[264-266], NOD models produce low levels of anti-SSA, anti-SSB, and anti-muscarinic acetylcholine receptor type III (M3R) autoantibodies. Our understanding of SS has been greatly enhanced by NOD. For example, NOD-derived models reproduce key symptoms in patients without diabetes with SS, suggesting that diabetic symptoms and glandular dysfunction may develop independently. There are multiple insulin-dependent diabetes (IDD) loci in NOD mice that contribute to SS-like development is what we just know[267]. Moreover, blocking CD40-CD40L interaction reduced lymphocyte infiltration and glandular ectopic lymphoid structures (ELS) in a NOD model, providing a therapeutic strategy which may be used in the future[268].

Consequently, we could ensure that our NOD mice have automatically developed into SS at 22 weeks of age with H&E staining showing lymphocytic infiltration at around grade 5 and saliva flow rate obviously decreasing.

EVs play an important role in reducing senescence in NOD mice submandibular gland epithelium at 22 weeks

Multiple markers of cellular senescence must be defined, as no single marker has been established for proof of cellular senescence yet. In paraffin sections of 22-week-old NOD mice, SBB-positive cells have been observed, which indicates the progression of cellular lipid metabolism (Please see Figure 3A in manuscript Paper III). SA-β-galactosidase-positive cells were seen in fresh frozen section samples of 22-week-old NOD mice (Please see Figure 3B in manuscript Paper III). Compared with ICR and hDPSC-EVs, PBS showed more pronounced effects with the expression of SA-β-galactosidase. Our histological analysis revealed that SGECs, particularly those in the ductal epithelium, underwent senescence. Although for the immune cells, it is also interesting to test whether they are senescence or not in this model, but this was not the aim of the current research. Therefore, we performed a quantitative analysis of mRNA expression in the epithelial cells of mouse submandibular glands. In the PBS group, AQP5 expression was significantly decreased while in the hDPSC-EVs group, it was increased. For $p16^{INK4a}$, $p19^{ARF}$, $p21^{CIP1}$, and *p53*, the opposite trend was observed. Several inflammatory cytokines known to be released by senescent cells (SASP) were also found to follow this pattern (See Figure 3C in manuscript Paper III).

In vivo tracking techniques for EVs

In both Paper I and III, EVs were administered through the tail vein. There are some limitations to this approach, including the fact that most EVs will be up taken by the liver and spleen and may not be taken by our targeted tissues. This will result in a

different outcome depending on the mechanism by which EVs are involved in diseased bodies (primarily through immunomodulation or by locating in targeted tissues and regenerating damaged cells directly). The animal model used in Paper III is related to the whole body and has an immune system dysfunction, it is even more challenging to understand how EVs administration may reduce SS. In our opinion, EVs should be better understood as to their biodistribution in our body after administration, how their fate changes as a result, and how their final contribution to disease development will be affected. This issue is one key issue to be addressed if we aimed to use EVs in human body in the future.

To study this question, it is essential to integrate in vivo tracking techniques based on EVs imaging as early as possible in the development of EVs. This prompted us to study the tracking technology and labelling methods of EVs, as well as the method of engineering EVs that are specifically designed for therapeutic purposes in order to improve the level of on-target EVs and to summarize the reasons for off-targets.

Since optical imaging (OI) is simple, cost-effective, and time-efficient, it is the most popular imaging technique for tracking EVs biodistribution over time. For example, bioluminescent imaging uses light generated by natural biological processes, such as luciferase-substrate reactions, to provide rapid imaging after substrate injection with a low signal-to-noise ratio. Its limitation is a lack of depth penetration of tissue. It is therefore only used in preclinical settings (for whole-body imaging of animals). There are also other optical techniques such as fluorescence imaging (tracking EVs using lipophilic fluorescent dyes or give plasmids or viruses that already fused with fluorescent proteins such as GFP and bioproteins for exosome membrane such as CD63)[269]. In contrast, there are imaging methods that are not subject to preclinical limitations, such as computed tomography (CT)[270], magnetic resonance imaging (MRI); the photoacoustic imaging (PAI) which uses ultrasound imaging and optical imaging to image EVs. Nuclear imaging like positron emission tomography (PET) and single photon emission computed tomography (SPECT) which could obtain 3D images and if combined with anatomical imaging such as CT or MRI, could improves its ability to localize EVs. All of these imaging methods allow whole-body imaging with unlimited depth penetration of the imaging signal[271]. Thus, are suitable for clinical scenarios.

For me and Koma's model, tracing EVs might provide an additional insight into how EVs function in reducing senescence in NOD mice.

Importance of SBB staining

In order to conduct clinicopathological studies, reliable, convenient, and easy-to-use biomarkers of aging are essential[272,273]. The most widely used biomarker for the detection of cellular senescence is the senescence-associated β-galactosidase activity (SA-β-gal) at suboptimal pH conditions[124]. However, it has a number of disadvantages, including the requirement for fresh frozen tissue to be processed rapidly in order to preserve its enzymatic activity. An important marker of aging is

lipofuscin within aging tissues[274,275]. But it is also present intracellularly in degenerative conditions. Due to its simplicity and reproducibility, the SBB stain is well known in histochemistry, as well as frozen samples[276,277]. Positive SBB-lipofuscin reactions are characterized by brown to black granules within cells and blue-black granules within frozen tissues. SBB staining is a useful supplemental staining for SA-β-gal staining.

Salivary glands cells of NOD mice lose the ability to form spheres, but EVs restore this ability and reduce senescence

The sphere-forming ability of mouse SGECs was assessed as per the protocol previously reported by Beucler in 2019. EpCAM-positive epithelial cells showed the ability to form spheres. PBS treated animals showed poor sphere-forming ability ten days after start of culture, while cells from hDPSC-EVs and ICR group showed high sphere-forming ability (Please refer to Figure 4A and 4B in manuscript Paper III). SA-β-gal staining of spheres revealed a higher percentage of positive cells in the PBS group than in the hDPSC-EVs or ICR groups (Figure 4C in manuscript Paper III).

Paper IV

Establishment of xylene-free tissue processing

There are two main aspects discussed in this article. Our first component of Paper IV is to process lung samples from large animal-based acute lung injury models using a xylene-free histological processing method followed by H&E staining. As a result, we found that this method of tissue processing and H&E staining is feasible. Through xylene-free tissue processing, we were able to produce large numbers of tissue sections that stained with assured quality (as defined by both research and clinical pathologists in our lab) (see Figure 1 and 2 for Paper IV for an overview of the histological process employed for Paper IV and also for paper II).

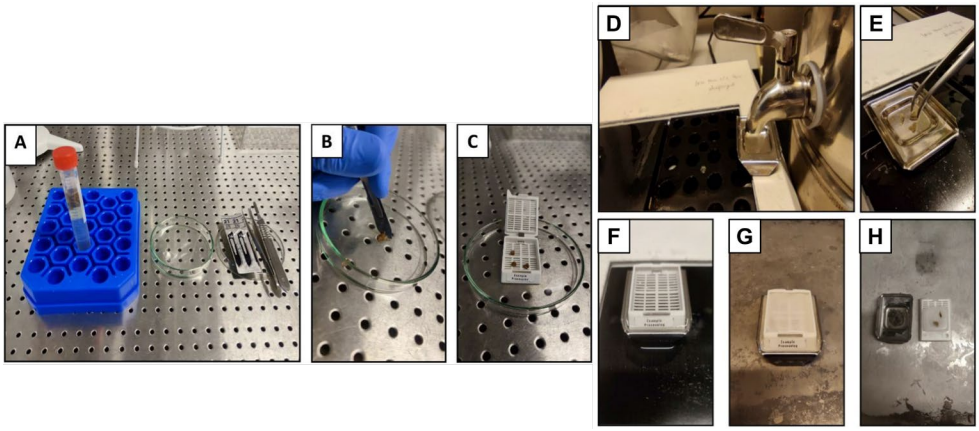

Figure 1 for Paper IV. The procedures of histological processing.
(A)-(C) shows biopsy pre-treatment. (D)-(H) shows tissue processing and until the paraffin embedding.

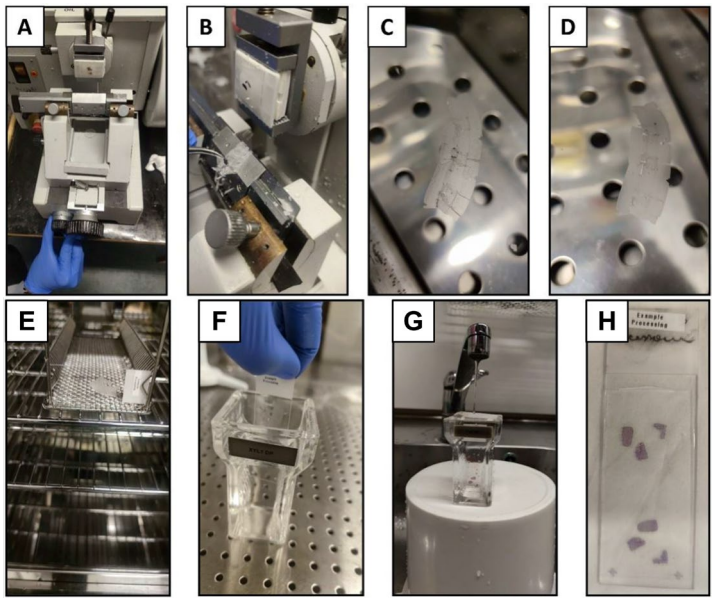

Figure 2 for Paper IV. The procedure to do sectioning on paraffin blocks and do H&E staining follow steps from (A) to (H).
(A) (B) Sections are made with a microtome; (C) (D) Tissue is transferred and relaxed in a water bath that set at 40 ℃; (E) 65 ℃ oven are used to prepare for paraffin removal; (F) All subsequent steps should be performed in the jars; (G) Wash the slide carefully and prevent tissue sections become detached; (H) Mount the slide with a stain to allow it to be stored for a longer period of time.

The second aspect of Paper IV sought to validate the feasibility of grading, interpreting, and evaluating acute lung injury using the set of histological scoring system that we developed. Using a large number of lung samples taken from large animal models of acute lung injury to validate, we found that the overall histological scores were mostly unrelated to the scorer's ability, and the scoring results were reproducible, despite some of the scorers being unfamiliar with the pathological phenomenon caused by acute lung injury. Thus, a well-described histological scoring system can be reliable when evaluating acute lung injury in large animals. This is important because not all laboratories have access to large amounts of people with experience in evaluating histology. If persons with extensive experience and limited experience score differently with a scoring system, then this indicates the scoring values ranging from 0 to 8 and the seven histological features set by this histological scoring system are not completely objective and independent (because the histological scores are affected by other factors, such as the experience of people who read the slides). Such differences would cause challenges in the practical use of that scoring system. Thus, the histological scoring system published in Paper IV is a reliable, objective, and reproducible system (Please see Figure 7 - 11 and Table 1 in Paper IV).

Relation of Paper IV to this thesis

Despite the focus of paper IV being on lung histology, both main aspects of Paper IV are relevant to this thesis. For the first aspect of Paper IV, the use of xylene-free methods for histological processing should be advocated for any research (if after validation, there is no impact on histology results caused by xylene-free processing), whether for the sake of protecting the environment, or for the sake of creating a safe and healthy laboratory (disposal of xylene will bring pressure on various aspects such as ecological environment and societal waste disposal mechanism). This of course means a few more works to do and to think. The idea of sustainable scientific research using xylene-free histological processing deserves everyone's support, advocacy, and physical practices in this area, despite the additional challenges with regard to time and resources it may initially bring. The toxicity of xylene is well-known and thus both research and clinical environments should start now to think, and practice scientific research in a way that is friendly to the future and to the nature. Scientific research cannot be used to justify excessive use of dangerous chemicals for both researchers and the environment. On the contrary, protecting the environment and protecting our homes should be the starting point of scientific research.

Xylene-free tissue processing was used for mouse native salivary glands and PCSS models to produce H&E staining. As a point of comparison, the H&E-stained results obtained at Nagoya University in Paper I and III using xylene in histological processing can be used. We found that the use of isopropanol instead of xylene as the tissue clearing agent prior to paraffin infiltration did not result in obvious

destruction of salivary gland tissues. In addition, we found no significant differences in H&E staining results between xylene and xylene-free processing. However, this alone is not conclusive and further studies are needed to validate and compare the performance of this xylene-free protocol in immunohistochemical and other classic histology staining. Oral pathologists could be consulted to help list criteria or observation indicators to formally compare these protocols. More samples should be tested and with additional species (not only mouse salivary glands but also human salivary glands can be used for verification), to further verify that xylene-free tissue processing is feasible for salivary glands histology (both native tissue and PCSS model). A xylene-free histological processing and staining method will become a very important and advanced method of histological detection and observation for PCSS, assuming the same importance as light-sheet fluorescence microscopy. In addition, and as discussed in the methods section of this thesis, LSFM based protocols are devoid of xylene. As it is known that xylene can alter antibody staining, it is important to have histological pipelines that are xylene free to best predict if antibodies can work. This is another very important aspect of Paper IV.

For the second aspect of Paper IV, as we can see from Figure 9 in Paper IV, this histology score was performed with multiple individuals with different experience in lung histopathology. Access to large numbers of persons with high expertise is only possible at large or focused research centres and thus may not be available to all researchers. There are only a few reports in the literature which describe histological scoring of salivary glands and thus the development of rigorous histological scoring systems for salivary gland tissue after irradiation injury or even in Sjögren's syndrome will be important to pursue in the future. As development of such robust scoring systems takes extensive time and needs to be validated in a centre with wide ranging expertise in histological evaluation or through international collaborative efforts of experts, it was beyond the scope of this research thesis. However, the experience in developing and applying this to lung histology will aid in quickly transferring this knowledge to the salivary field. We have already noted some potential features which could be evaluated such as including evaluation of cellular nuclear changes, which can be particularly challenging. The enlightenment given to us by Figure 9 in Paper IV is that we can actually use researchers and medical workers with different histological expertise in our laboratory in Nagoya University to help us develop this histological scoring system for salivary gland nuclear changes after irradiation, for example.

Conclusion and Future Perspectives

Dry mouth symptoms result from damaged secretory elements in the salivary glands. We found that senescence is a potential, targetable disease mechanism in irradiated submandibular glands and Sjögren's syndrome mice which can be alleviated by utilizing EVs therapy from hDPSCs. We also demonstrated the feasibility of using a precision-cut salivary gland slice culture model with the potential for diverse state of the art endpoints. Future work will focus on implementing histological analysis of these models (such as semiquantitative scoring as done in Paper IV) to grade salivary gland diseases and regeneration. Thus, this thesis work demonstrates a pipeline from in vitro/ex vivo (e.g., PCSS) and in vivo (murine models) to study disease mechanisms of salivary gland disorders with advanced modelling to evaluate new regenerative medicine therapies such as cell-free treatment and tissue engineering treatments.

For Paper I and Paper III

Conclusion

For Paper I, we explored new therapies for patients suffering from dry mouth (also known as xerostomia, characterized by compromised saliva flow) following irradiation therapy for head and neck cancer. To examine this, we established a murine model of submandibular gland damage via irradiation in Nagoya that found reduced submandibular gland secretion. The immunofluorescence and qRT-PCR results showed an increase in senescent-associated cells and *p21* expression in irradiated submandibular glands. These could be reduced by hDPSC-sEV treatment, with a limitation in salivary output recovery. These research findings could contribute to the further development of stem cell-free therapies for treating submandibular gland dysfunction after irradiation therapy using hDPSC-sEV.

For Paper III, we examined the effects of hDPSC-EVs on SS, specifically cellular senescence in SGECs with non-obese diabetic (NOD) mice. The non-obese diabetic mice spontaneously develop SS-like symptoms over time. NOD mice were injected with hDPSC-EVs, and PBS was used as a control. Compared to other previous studies, hDPSC-EVs were able to maintain salivary gland function and had a significantly lower incidence of lymphocytic infiltration. Sudan Black B positive

cells were detected in SGECs of the PBS group, but not hDPSC-EVs treated groups or ICR groups. For PBS treated NOD mice, SGECs have significantly reduced sphere-forming ability. Therefore, we can conclude that hDPSC-EVs administration prevents glandular dysfunction caused by SS in salivary gland epithelial cells and confers resistance to cellular senescence.

Overall, based on our findings in Paper I and Paper III, we concluded that EVs derived from hDPSCs can reduce senescence in a mouse salivary gland irradiation model as well as in an animal model of Sjögren's syndrome accompanied by xerostomia. This may prove beneficial to patients suffering from xerostomia in the future.

Future perspectives

RNA-sequencing for microRNAs within EVs

The mechanism of how EVs could restore saliva secretion directly by, for example, regenerating submandibular cells or to modulate irradiation-induced immune-inflammatory responses, remains unknown. This should be explored more on the exact way of how EVs play its role (directly or indirectly). In terms of this, comprehensive characterization of microRNA that EVs are carrying could be determined by RNA sequencing, for example. This could lead to insights regarding potential mechanism of action. Then we need to screen to explore which miRNA segment is influencing salivary gland organ function via experiments such as adenovirus transfection technology to deliver specific miRNA.

Determining EVs long term effectiveness on salivary glands' function after irradiation damage and translation towards the clinic through large animal models

In addition, we hope to study the long-term mechanism of submandibular gland responses to irradiation as well. One major difference between rodent and human salivary glands is the location of the submandibular and sublingual gland in the cervical versus oral cavity. Therefore, it is more challenging to explore local delivery mechanisms such as gels or sprays in rodent models. Therefore, large animal models with oral anatomy more similar to humans, such as dogs and minipigs, could be more suitable to simulate the long-term clinical effects of intravenous or in situ injections of EVs derived from human cells.

Histology scoring for evaluation: is it necessary and how to achieve it?

In both Paper I and Paper III, subjective assessment of histology was used. Semi-quantitative or automated image analysis is important for more objectively using histological data. One potential future direction is to establish or optimize a semi-quantitative histological evaluation and grading method similar to Paper IV but for

salivary glands. Some features such as lymphocytic infiltration, changes in nuclear shape (e.g., changes caused by irradiation) have been previously described as subjective and descriptive changes in this thesis and could be readily implemented. However, there are a diversity of histological features present (e.g., fibrosis) and it will be important to first consult previous relevant articles, summarize the changes in the morphology and structure of the nucleus after irradiation or other injuries (e.g., Sjögren's) to identify relevant features correlated with disease to examine in H&E histological staining. At the same time, we have to recognize whether low-dose irradiation and high-dose irradiation will have varying effects on the nucleus, both short- and long-term. The change of the nucleus will also have many aspects and dimensions, including the shape and size of the nucleus, the ratio of nucleoplasm to cytoplasm, the size of the nucleolus, the shape and thickness of the nuclear membrane, the number and structure of surrounding chromatin, the number of mitotic events, etc. Therefore, it may be necessary to closely focus on the analysis and summary of "histological H&E staining" by combining different computational analyses, including the use of automated imaging or machine learning, which is the second step. The third step should be repeated verification and further optimization on a large number of irradiation-damaged submandibular glands samples (from human is the best). For now, mice are fine as target species for disease modelling, but due to their small size and also the existing histological differences for salivary glands between mice and human species, larger animal models should be explored in the future if surgical approaches are to be validated through animal models. The methodology to build histological scoring system for nuclei enlargement in larger animals after irradiation could be similar to small animals but will have some differences due to the organ size and species-specific differences; this will also need to be explored.

What is the role of senescence in salivary gland hypofunction?

For the role of senescence, it has been demonstrated that cellular senescence and SASP play a disease-causing role in the pathological changes of many diseases (including our results). However, as senescence also promotes proliferation, it would be great to know when proliferation will occur and whether or not it is low-dose irradiation that triggers it. Therefore, this may be an excellent avenue for clarifying the role that senescence plays in irradiation pathophysiology. It may also be useful to this question if we detect more immediate responses (like 1 hour to 4 hour after irradiation) of submandibular gland tissues after irradiation exposure. Excessive and unbalanced senescence has been associated with the formation of over-fibrosis and unbalanced inflammation. Inflammation development in SS is a well-established and important mechanism. Therefore, we would like to understand the inflammation mediated by senescence and its phenotype factors in Paper III. Fibrosis is a final stage of salivary gland pathology, in which fibroblasts and the extracellular matrix they produce tend to replace all of the functional secretory units of the gland. The role that senescence plays in chronic pathology changes of

irradiation damage in salivary gland organ are thus far not completely understood. Will senescence in irradiated salivary gland exaggerate fibrosis or does some senescence help to regenerate the functional acinar of salivary gland? The role of senescence at every stage of irradiated salivary gland will be important to clarify. It is therefore necessary to conduct further studies in order to determine the precise influence and mechanism of senescence on the submandibular glands in the presence of irradiation-induced impairment and the consequent loss of function.

Are hDPSC-EVs better than other EVs sources in Paper I and Paper III?

Hopefully, in the future, we will be able to determine whether EVs derived from human dental pulp stem cells are different from those derived from bone marrow stem cells. In addition to their different anatomical location, it has been observed that hDPSCs proliferation is significantly higher than that of bone marrow stromal cells. Over subsequent passages, it has also been observed that hDPSCs retain their high proliferation ability[278]. However, it is still unknown whether the EVs secreted by the two stem cell sources have similar effects to salivary gland diseases or not. Therefore, it will be important to fill in this gap in the near future with experiments that directly compare the role of the cell of origin for the EVs.

Will local administration or systematic administration of EVs be different? Is longer sustained delivery of EVs needed?

For salivary glands, the local administration of EVs could be to inject EVs directly into the glands. It also has another way of local administration for EVs, that is, retrograde perfusion of EVs through the submandibular gland duct of mice or rats. Corresponding to the application that can be carried out in the human body in the future is the retrograde perfusion of the human parotid gland through the parotid duct.

The animal models used in Paper I and Paper III are both systemically administered EVs. It is generally thought that EVs produce their biological effects through their internalization by target cells through the endocytic pathway, therefore EVs could show their role in the target specific organs[279]. Additionally, studies have shown that intravenous, intraperitoneal, or subcutaneous injections[280] of EVs will cause the EVs to enter the bloodstream and accumulate mainly in the liver and spleen. As a result, the EVs are rapidly cleared from the bloodstream and excreted. In spite of the route and source of the cells and the administration method, this effect is independent. Therefore, in our studies of Paper I and Paper III, there is a high probability that only a small part of the EVs we injected from the tail vein of mice reached the salivary glands. This leads us to think that the real reason why the salivary gland secretion function in Paper I did not recover after EVs treatment. Is it because the effective concentration of EVs in the target organ is low after being absorbed in systemic reticuloendothelial system[281], and also the action time of EVs is short? Or is it due to the sources of EVs is from human dental pulp stem cells? Or is it because 18 days after radiotherapy is the acute window period of irradiation-

induced salivary gland hypofunction, so there is a special pathogenic mechanism in this stage that EVs cannot work?

We intend to verify this data first, which means evaluating whether systemic administration of EVs results in poor targeting of EVs and low persistence in target organs for our models of salivary gland irradiation injury and Sjögren's syndrome injury.

As a second step, we will compare salivary gland function in our animal model after local and systemic administrations of EVs. This will allow us to determine which method is more effective in the treatment of the disease. This will also allow us to gain a better understanding of how EVs function.

It is important to clarify that in our actual laboratory conditions, the production of EVs is not an easy process due to the fact that they cannot be manufactured on a large scale, they are costly, and they are difficult to maintain high purity and stable quality. Thus, we can conduct a third step, which is to incorporate an additional group with EVs that were loaded with biodegradable and porous hydrogels[282] and place the gel directly on or near the diseased sites of salivary glands. By doing so, we could further compare and judge whether Paper I and III is caused by the premature clearance of EVs or not. In addition, we may also need to check whether it is worthwhile to study other EVs-sustained-delivery systems.

Whether mitochondrial transfer from hDPSC-EVs plays a role in Paper I and III

A previous study has shown that mitochondrial transfer by EVs is at least partially responsible for the therapeutic action of EVs that derived from mesenchymal stromal cells in other organs[283], and that mitochondrial function can be restored as a viable therapeutic target for the restoration of salivary gland function following irradiation therapy[284]. Therefore, future studies should examine whether hDPSC-EVs can transfer mitochondria from stem cells. And whether this has the possible to explain why in Paper I and III, the therapeutic effect of hDPSC-Vs could alleviate and prevent the long-lasting effects of senescence.

How to build salivary gland irradiation in vivo model? Can it be standardized?

From Table 11 of this thesis, we can know that there are a lot of choices for the establishment of irradiation-induced salivary gland injury models for in vivo research. For these models, there are many differences in such aspects as animal species, single or multiple exposures, the total dose, the fractional dose and how to set different time points to give fractional irradiation, irradiation rate, the observation time (1 month, 3 months or 6 months or more), and what are the observation indicators for the histological performance of different models, whether they echo each other or change due to species.

The question is whether there is a gold standard method for building irradiated salivary glands injury on animal models? For instance, what type of irradiator should be used, what irradiation rate should be set, what irradiation dose should be given? What is the best criterion for evaluating irradiation effect: the total dose, the

irradiation rate, or does irradiation damage need to be evaluated comprehensively based on various irradiation indicators (voltage, current, distance, linear or not linear irradiation, whether the body other parts have been shielded except salivary gland?)

Therefore, taking mice as an example, if these irradiation-related parameters are not the standard for establishing a model of irradiation-damaged salivary glands in mice, then we can also rely on some histological manifestations to judge whether irradiaiton is damaging mice salivary gland. This can be done through assessing murine histological staining using histological scoring and grading methods. The histological characteristics of the irradiated mice salivary glands could be summarized and verified repeatedly to establish a histological diagnosis regulation for irradiation damaged salivary glands in mice.

Further clarification of how to best assess the biological and physiological impact caused by irradiation is also needed. For example, should stimulated or unstimulated saliva flow of irradiated mice be used as an indicator? How much of a decrease in stimulated or unstimulated saliva flow following irradiation indicates injury? This quantitative index, after repeated verification, can be used as a bio-physiological indicator to assist in determining whether irradiation has indeed damaged the salivary glands (for mice).

Currently, two indicators are more widely recognized by the scientific community. One is the slowing of saliva flow rate, and the other is the histological results. For the former, there is no generally accepted number, and the data about reduced saliva flow rate used in the diagnosis of xerostomia in humans cannot be applied to animal models. For the latter, long-term histological changes have well-recognized histological features, such as fibrosis, acinar atrophy, and lymphatic infiltration. But for short-term histological changes after irradiation, there are few reports (only some reports like changed cellular nuclear[285] and enhanced cell proliferation[286]). Therefore, how to judge the successful establishment of the salivary gland injury model requires further thinking. There is however an ongoing systemic review on the use of MSCs in animal models of irradiation that may at least partially help to assess how different groups are defining injury and recovery[287]. The major measurement techniques that this systemic review will address are SFR as well as morphological and immunohistochemical effects. Other fields have addressed this issue through the use of consensus reports of pre-clinical and clinical experts to best standardize animal models. Such an approach could be useful for the salivary gland field to follow.

How about applying EVs to the PCSS model?

One of the great advantages of applying EVs to PCSS is that there would be less use of animals. The 3R principles (replacement, reduction, and refinement) are important to apply in the principles of animal experiments. Using the PCSS model, we can better meet the requirement of 3R and reduce animal ethical problems. One salivary gland (submandibular gland and sublingual gland together) from one mouse can produce about 18 PCSS with a thickness of 300 μm, and one mouse has a pair

of salivary gland (submandibular gland and sublingual gland together). Therefore, more than 30 conditions can be tested, and this allows many experiments on different levels. On the other hand, if animal experiments are carried out, each group must have at least three mice depending on the type of endpoints measured, and some experiments even need to increase the number of mice as only one animal can be used per endpoint (e.g., whole LSFM). Therefore, in terms of the principle of animal ethics, PCSS is a good choice to supplement traditional animal research.

The second aspect in which PCSS is superior to animal models is that PCSS is easy to manipulate and handle in a laboratory. Animal experiments require much more resources per experiment as there is a need to raise animals, dissect animals, and a large number of samples need to be recorded and processed for experiments, which take use of many laboratory space, manpower and material resources. This is not always available at all places.

However, the experimental design of applying EVs on PCSS model to validate the efficacy of EVs should consider the following aspects.

First, what is the method of EVs delivery we aim to mimic in PCSS? Is it to deliver via a hydrogel or gel which can be applied to the salivary gland of patients? In that case, EVs could be loaded into a gel or hydrogel, and then applied to the PCSS surface to allow them to come into contact with one another. We might also consider to use an insert that allows us to mimic the air-liquid interface of the oral cavity when cultivating ex vivo? In the clinical scenario, EVs can be directly injected into the parotid glands through cutting the skin and open the salivary gland capsule using minimally invasive surgery, then implant a hydrogel, where EVs are embedded, inside the glandular tissue and then suture the wound. A second method is to use retrograde catheter perfusion of EVs through the parotid gland duct to deliver EVs into the salivary glands' acinus and ducts. A third method is administrating EVs through local or whole-body intravenous injection. Maxillofacial bones have very rich blood supply, and therefore it is possible to choose one artery or vein to do this. The method of giving EVs to PCSS in ex vivo culture in lab cannot fully simulate all these scenarios in clinical practices in the future, but the model could be used to mimic some delivery conditions.

Secondly, although PCSS model retains the microenvironment of all the original cells, extracellular matrix dynamics, blood, nerves, and lymphatic conditions of the organ in its original orientation, it lacks a systemic immune system. This is a major limitation which makes it challenging for us to explore the interaction of EVs and the body's systemic immunity. However, if PCTS are generated from diseased samples, it is possible that the deregulated immune system accompanies it. The Lund University lab has previously shown this in PCLS derived from normal versus chronic lung diseases[246]. For example, taking the salivary glands of patients with Sjögren's syndrome as samples should bring lymphocytes with them. We can then, make PCSS using the vibratome and then administer EVs. Such a scenario could also be applied to animals who have received irradiation or our animal model of Sjögren's syndrome. Such an experimental design is perhaps needed, especially for

cases such as Sjögren's syndrome, because SS are closely related to the activation of systemic immunity.

The third aspect which needs further work is the culture conditions of PCSS. This should be further optimized before we apply EVs to PCSS. Thus far, there is no consensus on the culture medium which should be used for PCSS, the types of growth factors or small molecules which should be added, or the concentration of serum added for PCSS. In addition, whether the culture method is static or dynamic, whether an air-liquid interface mimicking the air-liquid interface of the duct should be used, how long can we culture PCSS (i.e., how do cell subtypes and ECM change in PCSS during ex vivo culture), etc. At least some of these factors need to be further clarified before EVs are applied to PCSS.

To give just one example, serum is known to contain EVs. Therefore, serum free formulations may be necessary for testing the impact of EVs on. However, whether it is feasible to culture PCSS ex vivo without serum, and what changes will happen at the cellular level are unknown. Lack of serum may alter cellular phenotypes or even alter ECM production by fibroblasts. How this experimental condition will alter the analysis of EVs in PCSS are therefore unknown. The ability to conduct small-scale pre-experiments to test different experimental conditions before using large scale PCSS samples is therefore needed.

One of the main methods developed in this thesis that can help us with the above questions is that we now have a method to extract high-quality and sufficient RNA samples from small amounts of PCSS which can be used for RNA-sequencing. As our group has previously described, bulk RNA sequencing can be used to predict cell diversity under different conditions. We also have a method for clearing and imaging PCSS through light sheet microscopy. These are both useful tools to help us continue to clarify the deeper transcriptional and morphological changes which occur in ex vivo culture of PCSS and which can be used to evaluate potential therapies, such as EVs.

The above are only some reflections on the advantages and disadvantages of the current setup we have established and should be considered before applying EVs to PCSS.

For Paper II

Conclusion

Paper II sought to advance precision-cut salivary gland slices (PCSS) as an ex vivo model for salivary gland research. After optimizing workflows, PCSS were detected to be metabolically and functionally active for two days in ex vivo. By using qRT-PCR, we demonstrated how salivary gland phenotypes change dynamically over time in addition to assessing the morphology and histology in fluorescence and 3D

visualization. We also found that the PCSS model has physiological responses to irradiation induced damage, similar to a previous study[221]. While murine PCSS are a convenient model to use based on the diversity of transgenic animals available and species-specific tools (e.g., antibodies), there has the far been limited development of applying state-of-the-art techniques to analyse them. Thus, we have developed reliable methodologies for generating viable murine PCSS tissue pieces which could retain function and architecture, as well as innovative analysis like qRT-PCR and LSFM for a diverse validation. This can help them serve as a disease model that more closely resembles natural salivary gland biology, thereby paving the way for future studies of salivary gland mechanisms and therapeutic development in human tissues.

Future perspectives

What is the optimal culture medium and culture method for PCSS?

Until now, the culture mediums we have tried including RPMI with β-mercaptoethanol and McCoy's 5A. RPMI with β-mercaptoethanol has been used in PCSS organotypic slices from adult mouse parotid glands[219]. For RPMI medium with β-mercaptoethanol, a previous study found that a subpopulation of the acinar cells of parotid slices can be maintained during short-term culture and retain their morphology and function for up to 2 days[219]. This is a research for mouse parotid slices. Human salivary gland slices were cultured with serum-free hepatocyte-defined medium supplemented with EGF and slices were placed on membrane inserts[221]. They found that it was possible to culture human salivary gland slices for 14 to 30 days to assess the retention of different phenotypic markers using this proposed method. However, all of these studies used subjective selection of the phenotypic markers and no comprehensive technique like RNA-sequencing has been applied.

For McCoy's 5A medium, it is generally used as a general-purpose medium for propagating primary cells, established cell lines, and biopsy tissue explants. It has wide application in bone marrow, skin, breast, lungs, and submaxillary salivary gland tumour epithelial cells line (A253)[288] but has thus far not been used for culture of PCSS.

It is necessary to know the role of different medium components on supporting different cell types. In addition, static or liquid gas surface culture, or dynamic culture is also worth exploring since this determines the mode and efficiency of nutrients and wastes being exchanged between tissue cells and the medium. What growth factors or additives to use is critical to know because the baseline state of the cells or cellular composition of the model may change the expression of some cell phenotypes or change the mechanism of ex vivo culture. This may cause the cells to behave differently from the in vivo situation. For example, whether the PCSS model could be used to study senescence after irradiation and whether the

natural process of fibrosis for PCSS model will be an influential factor for us to study fibrosis in the late SS using this model deserves to think.

Optimization of RNA isolation from PCSS for RNA-sequencing

At the moment, we have only analysed RNA level changes in 4 genes (*Aqp5*, *Krt5*, *Col1a1*, and *Fn*). The transcriptional expression of only 4 genes is insufficient to evaluate the changes in cell expression as well as to predict changes in cellular composition or phenotype. Thus, future studies should be undertaken to perform RNA sequencing in order to gain a general understanding of the changes that occur at cellular and molecular levels during the ex vivo period of 3 - 5 days in this model.

Previous work has shown that bulk RNA sequencing can be computationally deconvoluted to predict changes in cellular level composition by combining bulk RNA datasets with publicly available single cell datasets[246]. This is an economically preferable direction due to the high cost with single cell sequencing and can be a main tool to objectively evaluate the effect of media composition. This can be a suitable solution for our aim of evaluating PCSS. In order to do RNA seq analysis, we are extremely dependent on the extraction of sufficient high-quality RNA from murine PCSS models.

Both sufficient quality and quantity of RNA is important for RNA sequencing studies. In Paper II, RNA quality and quantity was only measured through UV spectrophotometers (Nanodrop). Nanodrop is a traditional method to detect the RNA concentration and purity through measuring A_{260} and A_{280} for RNA samples. Nanodrop has the advantage that it is available in almost every lab, is easy to handle and fast to obtain quantitative data. It has several disadvantages, including its inability to differentiate DNA from RNA and that it can be influenced by contaminants absorbing at the same wavelengths; thus, it is less than ideal for quantifying super diluted RNA.

The lowest concentration of our RNA samples is 40 ng/µL which corresponds to a minimum of 400 ng total RNA. For samples with higher concentration of RNA (like 300 ng/µL), the total RNA is 3 µg. The minimum input for RNA seq can be 100 ng - 1 µg, and as low as 25 ng when samples are of high purity. However, the minimum which Nanodrop can accurately measure is not sensitive enough to reliably calculate these lower amounts of RNA. Alternative techniques with higher sensitivity to specific types of nucleic acids should thus be used. There are several different techniques which determine nucleic acid concentration based on fluorescence intensity using fluorescent dyes which can distinguish dsDNA, ssDNA and RNA. These assays can be used with microplate readers or fluorometers like Qubit[246]. Future work should focus on more precisely quantifying RNA for use in next generation sequencing.

The A_{260}/A_{280} found in these samples was generally around 2.0 (Please see Figure 4C in Paper II). A_{260}/A_{280} ratios of 1.8 to 2.1 indicate highly purified RNA. This means according to Nanodrop, our RNA samples from PCSS have enough purity to do RNA seq. However, this is not the only parameter needed to ensure sufficient

quality of RNA. Future work should focus on analysing the RNA quality using more precise methods such as Bioanalyzers which measure the RNA integrity number (e.g., Agilent 2100 bioanalyzer)[246]. This is especially important for samples with low amounts of RNA, as we have encountered with PCSS. We found that samples with lower RNA concentrations also had lower purity of A_{260}/A_{280} (Please see Figure 4B in Paper II). Thus, it will be important to verify the purity and integrity of RNA prior to performing RNA-sequencing.

Optimization of 3D imaging with light sheet microscopy

It will also be important to continue to explore three-dimensional imaging analysis methods using light-sheet fluorescence microscopy technology. Clinical and experimental irradiation is focused on a particular 3D volume and thus conventional histological analyses may not be representative of the entire tissue volume. Later antibody staining can also be performed to spatially correlate DNA damage with senescent cells, apoptotic cells, and fibrosis development, which will require us to develop and optimize a protocol for antibody penetration on cleared tissues for light sheet microscopy. The antibody incubation period may need to be extended to three days or longer to ensure penetration of the antibodies through the whole construct thickness. Alternative techniques such as pumps, agitation, or electrophoretic based methods may be necessary.

What can we use the PCSS model for?

PCSS offers many distinct benefits with one of the main advantages being that multiple experiments can be conducted on samples obtained from a single animal. As one example, it could be used to explore different types of irradiation. In radiotherapy, Flash irradiation therapy is a new technique[290]. It means using super-high dose of irradiation while reducing the damage to normal tissues but at the same time killing tumours effectively. The reason for this concept is that many tumours still resist conventional irradiation therapy (CRT), and CRT doses are based on the tolerance dose of normal tissues, so to develop super-high doses of radiotherapy (e.g., Flash radiotherapy) to irradiate above 40 Gy/s and the irradiation time is generally less than one second. In radiobiology, the dose rate is one of the most important factors affecting radiotherapy's biological efficacy[291]. The development and implementation of Flash or other advances may make significant changes to future tumour treatment[292]. It is currently in the preclinical stage of experimental research and has just begun to be applied in the first human experiments[293]. Due to the fact that irradiation therapy is an important adjuvant therapy for patients with head and neck cancer and irradiation therapy indeed poses a high risk to normal salivary gland tissue, it will be of interest to see if this different technique of applying irradiation will similarly impact normal salivary glands.

PCSS may be an ideal platform to investigate this. As a first step, it is necessary to determine whether Flash radiotherapy can be applied to PCSS, and then compare how PCSS respond to Flash and common radiotherapy. As we have already applied

conventional irradiation therapy to murine-derived PCSS, we have concluded that our PCSS model exhibits a normal physiological response to irradiation injury (See Figure 9C in manuscript Paper II). As a result, Flash could be used on PCSS models as well, and we will compare Flash's effects with traditional radiotherapy on normal salivary gland tissue. In addition, it will be of interest to further study the effect of Flash on different species in order to see if PCSS can be used to correlate to *in vivo* findings, including in human salivary glands.

Another potential interesting application for PCSS is in the study of salivary gland tumours. During preliminary experiments, we cultured human salivary gland cancer cells (A253) into spheroids using U-shaped low-adsorption well plate for suspension culture (Figure 1 and 2, Perspectives). We found that microspheres can be produced within three days, with retention of cell viability and proliferation capabilities. A253 cells are epithelial cells derived from mucoepidermoid carcinoma of the human submandibular gland. Therefore, the A253 microspheres can be used as a simulation of human salivary gland tumors. We could implant these micro-spheroids or coated with gel on the PCSS model and then apply different types of irradiation therapies or pharmacological approaches.

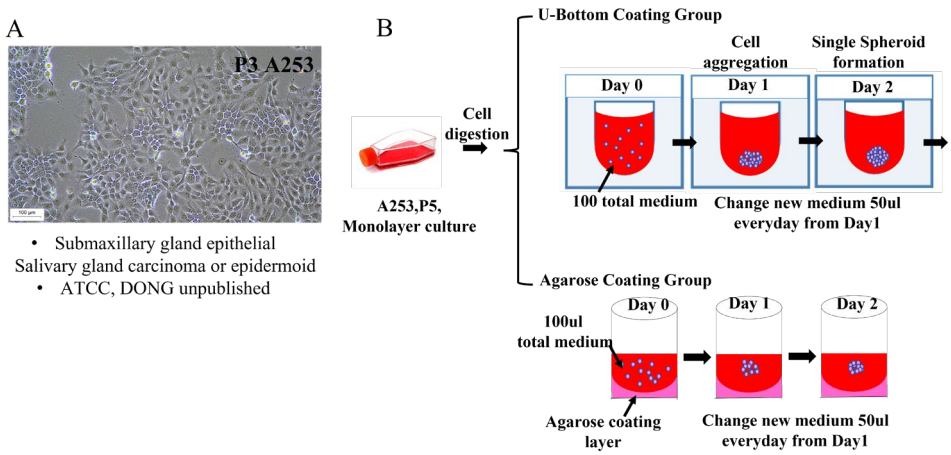

Figure 1 for Paper II in Perspectives. A253 cell culture and spheroid formation workflow.
(A)The culture of submanxillary gland epithelial cells line A253. Dong et al. Unpublished data. Copyright by the author. (B) The schematic workflow shows the use of 96-well plates with special coatings to form single spheroids from single A253 cells, while agarose coating plates were used as negative controls to form spheroids manually. Created by the author.Copyright by the author.

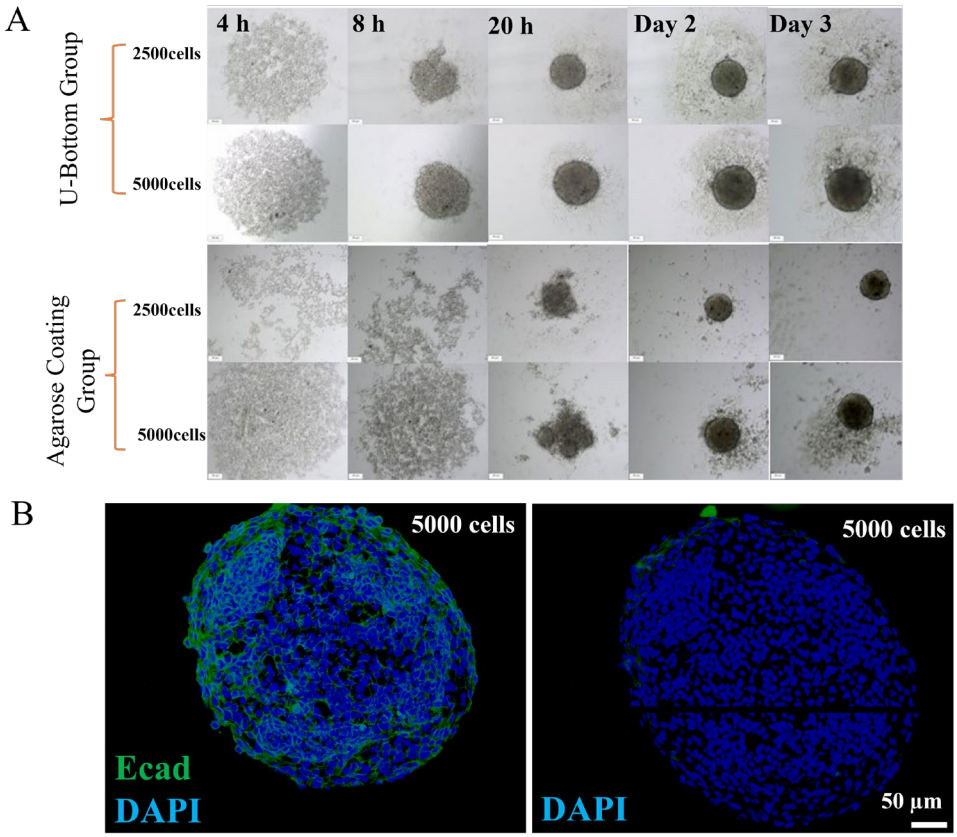

Figure 2 for Paper II in Perspectives. Observations of spheroid under bright field and and fluorescence microscopy.

(A) The morphology observation showing U-Bottom shaped 96-well plate with unique polymer coating could support uniform, rapid (8 hours) and larger spheroid culture with less irregular aggregation and cell satellites, when compared to the manully agarose coating group. (B) Immunofluorescence staining of spheroids showing expression of E-cadherin (For A and B, Dong et al. Unpublished data. Copyright by the author).

Finally, in order to connect the findings of Paper I and Paper II, we hope to apply EVs derived from hDPSCs in the above-mentioned various animals and PCSS models, as well as observing and elucidating the mechanism of action for EVs. The PCSS platform allows use to explore more focused questions such as do EVs exert antioxidant effects? whether the EVs transferring mitochondria as part of their mechanism of action? We could also test to understand the differences between dental pulp stem cells and bone marrow stem cells, as well as the differences between their EVs in this aspect of transferring mitochondria. In the end, we have a long-term vision to use human derived PCSS, which will be critical to use as an in vitro research model to hopefully predict clinical efficacy in humans.

For Paper IV

Conclusion

For Paper IV, our goal was to develop a set of histological scoring system to semi-quantitatively evaluate the degree of tissue damage in the porcine acute lung injury model. Based on the literature and experience, we classified and proposed 7 core observation indicators for judging tissue damage and set up a scoring value from 0 to 8. Then we tested and verified in people with different experience and found that our scoring system is not be affected by the experience of the readers. We found that the use of 7 judgment observation indicators and the setting of 0 - 8 score values produced stable and reliable results. This demonstrates that our histological scoring system can be used to judge the degree of lung injury in large animal acute lung injury models. Therefore, it provides a very reliable and practical histological tool to apply this model to mechanistic research and evaluation of therapies. Moreover, it is feasible to use the xylene-free histological approach to process acutely injured large animal lung tissues, and it does not interfere with the quality of the tissue sections or interpretation of the tissue staining. Because the concept of sustainable development can protect the environment and create a healthy laboratory, it is worthy of extensive promotion and application.

Future perspective

Validate and advance xylene-free tissue processing methods for human salivary glands.

The contribution of Paper IV to this doctoral thesis is in imaging observation, which provides a very novel method and concept that can reduce the use of xylene and protect environment and researchers. We have already performed xylene-free histological processing for salivary gland tissue, followed by H&E staining and the results are shown in Figure 8D in manuscript Paper II. Then as a control, we used xylene-treated tissue processing, obtained paraffin blocks, and then performed H&E staining. We did not find any difference in the xylene-free processing treatment group by this comparison. But whether xylene-free histological processing is feasible, whether it will not interfere with the quality of sections, whether it will not interfere with staining results, need to be answered firstly before promoting it in the field of salivary gland histology.

Future studies should aim to treat neighbouring parts from a single biopsy region of salivary glands with and without xylene for processing, and then perform H&E staining as well as other common stains at the same time to make sure other aspects are consistent. Sample sources such as mice, rats, rabbits, and dogs should also be used as well as healthy and diseased salivary gland tissues to obtain a

comprehensive judgment. This will allow for a more comprehensive understanding of the feasibility of xylene-free histological processing in salivary gland studies.

Development of a histological scoring system for evaluating nuclear changes in salivary gland tissues following irradiation treatment.

For salivary gland research, there is a diversity of histological changes which have been reported for different animal models. For short-term histological changes after irradiation, there are only a few reports which use quantitative or semi-quantitative metrics from histology (only some reports like changed cellular nuclear[284] and enhanced cell proliferation[285]). Therefore, the successful establishment of a histological scoring system for salivary gland injury requires the use of evaluating criteria that are more comprehensive while staying objective. Whether or not aspects such as changes in acini size, as observed in Paper I, or increased deposition of ECM are thus far not clear and may need to be adapted based on the timing and duration of injury studied.

Artificial intelligence in research and clinical pathology

The digitization of pathological slides with a digital microscope after slide staining is an important new advance in research and clinical pathology[294]. Whole slide scanning facilitates data preservation. This has already appeared since 1990 as whole slide images (WSI). However, for the analysis of digital pathological slides, it is an opportunity brought by the rapid development of artificial intelligence technology in recent years, allowing us to use artificial intelligence (Artificial Intelligence, AI) technology to analyse tissue slices more consistently. This makes pathologists' judgments more objective and repeatable by converting them from qualitative to quantitative judgments[295].

In the early days of pathological image analysis, many features were artificially designed by humans. These manual features require professional knowledge and are insufficient to cover all of the features in an image. Using deep learning models to detect, grade, and classify tumours has become a mainstream method for pathological image analysis because of it is powerful in handling increasingly accumulated clinical data and perform quantitative analysis[296]. In this way, deep learning in machines could help pathologists make accurate and fast diagnoses even though facing large datasets. Digital image analysis and computer assisted diagnosis must be a trend of pathological analysis in the future[297]. So, this could also be the future of pathology in salivary gland field, especially for features that may be hard for novice human scorers to perform (e.g., nuclear shape changes).

Overall Conclusion of the Thesis

In xerostomia, salivary secretion is decreased due to changes in the secretory components (acinar, ductal, myoepithelial, and neural). In the study of salivary gland injury and recovery, cell therapy and tissue engineering techniques are receiving increasing attention. In Paper I and Paper III of this doctoral dissertation, stem cell-derived therapy was evaluated in two major salivary gland diseases (acute irradiated salivary gland dysfunction and chronic immune-related salivary glands). Also, this thesis (Paper II) established a workflow for precision-cut mouse salivary gland slices (PCSS) and also developed new analytical options such as qRT-PCR and light-sheet fluorescence microscopy (LSFM) to evaluate this model. The future aim is to use human salivary glands to generate slices and use this model in research related to salivary gland physiology and disease, as well as pharmaceutical and EVs therapy trials. Finally, in this doctoral thesis, a sustainable histological process (Paper IV) for H&E staining is developed to reduce xylene usage in salivary gland tissue processing. Combined with the development and testing of light-sheet fluorescence microscopy workflow on PCSS model, we currently have two relatively advanced strategies for imaging and observing PCSS model. Thus, this work has developed a set of in vitro and in vivo experiments and methods to conduct advanced modelling and systematic diagnosis and category of salivary gland diseases, thus contributing to improved knowledge for salivary gland research and evaluation of potential new therapies such as cell-free and tissue engineering treatments in the future.

Acknowledgements

Dr. Darcy, thank you for accepting me to your lab in my double degree program between Nagoya University and Lund University. Also thank you for all you endeavor to guide me and offer the best learning environment. Thank you for your kindness and support to help me overcome many challenges.

Sakai sensei, thank you for becoming my co-supervisor at the beginning of my PhD and giving me the most fundamental training for research which lay a good foundation for my exchange to Lund University. And thank you for you accompany during my nearly 3 years of doctoral study in Nagoya University and thank you for offering help as a native speaker in the very end moment of graduation.

I am grateful to you, **Ingela**, for always being ready to lend a hand to our research. Also thank you for your sincerity, friendliness, and kindness, always warm and caring for me in a foreign land and give me power to move forward. You picked me up and dropped me off on my first and last day at Lund University. I think this is the most beautiful cycle in the world.

I would like to thank **John** for being my mentor, and I am grateful for your contribution to the light sheet microscopy imaging part of the PCSS project. I also drew upon your findings on PCLS. Your dedication has made all of this possible.

Thanks to **Linda** for you helping me write my Swedish abstract for my doctoral thesis.

In addition, I would like to thank **Kristina** for listening to my ppt report on the eve of my mid-term review, thank you for your enthusiastic feedback and genuine encouragement. I will always remember your encouraging smile.

Hani, thank you for being patient in helping me solve problems during my daily research day in the lab, as well as taking me to collect organs for my animal experimentation. So, thank you, Hani. Your outstanding research also inspires me to do my best.

Thank you, **Iran**, for your enthusiasm, optimism, and sense of humour which always inspire me. Also, thanks for your kindness and thoughtfulness that give me encouragement all the time.

Thank you, **Victoria** for being a female doctoral student, which gives me a great deal of strength. Also, thank you for your hard work on your Ph.D. project, which always motivates me to do my best.

Thanks to **Niko** for your sincerity, friendliness, and kindness, and thank you for your concern for me, always warming my heart like a neighbour's younger brother. During my first weekend as a student at Lund University, you invited me to your house for lunch. You give me a feeling of home in Lund.

I would like to thank **Tania** from **Neurosurgery lab** for your honesty and sincerity, and for often giving me spiritual encouragement. I also thank Tania for your serious and responsible work style. Cultivating organoids together with her is enjoyable.

Thanks for all the teachers and classmates in **WCMM Research School** 2021/22 teaching me so much valuable knowledge and research skills, which is a great experience for me. I would like to thank **Kablian** and thank his belonging lab (Cell mechanobiology leaded by **Vinay** Swaminathan) for designing the academic idea, writing the fund together and watching it progress, and for finally getting it.

I would like to thank the **LBIC** of Lund University, for their help in imaging.

I would like to thank other labs in Lund University, like **Iben**'s neuroscience lab and **Oxana**'s lab about medical microspectroscopy for sharing wild type mice with me. I would like to thank **Liu Na** in Iben's group for contacting me to share her animals.

I would like to thank **Radhika** from the Oxana research group who helped me study for the statistics course. So, thank you, Radhika, I appreciate your help.

My sincere thanks go out to **Fanli** and **Indra** for coming to Dr. Darcy's laboratory. Thank you, Fanli, for introducing your Chinese classmates to me, and thank you to Indra for giving patient and rational suggestions sometimes to me. Preparing flowers and cards on that very early morning for you two is the proudest thing I have done.

I would like to thank **Deniz** for helping me with my research plan while I was still at Nagoya University. I would also like to thank **Simon**, **Emil**, and **Sagar** for introducing your research to me during my first days at Lund University. Thanks to **Ernesto** for teaching me how to use the vacuum centrifuge. So, thank all of you.

Thank you, **Maria**, for being my student and for giving me spiritual sustenance during my first days at Lund University. Thank you for your innocence, simplicity, kindness, and sincerity, that always warm and enrich my heart. After my mid-term check-up, I remembered we cheered together because we finally be able to do the cell experiment portion of your internship project. This has always been a very fond memory in my mind.

Thanks to other students like **Ines**, **Alex, Isabel**, **Elisse** and **Fran**, who worked hard in Dr. Darcy's laboratory. Thank you for your enthusiasm, passion and vitality that always infect me.

My greatest thanks go to Professor **Hibi** for trusting me and recommending the joint degree program at the beginning of my Ph.D. I also appreciate his support during the last graduation period.

I would like to thank **Kasuya** Sensei for admitting me into the Joint degree doctoral program and giving me a chance to study and work hard. I would also like to thank Kasuya Sensei for his continuous concern, enthusiasm, and sincerity to us.

I would like to thank **Sumigama** sensei, as the actual coordinator of this joint degree program. During all the important moments in the 4-year of PhD, he maintained the most care for the students, active and patiently participated and solved questions.

Finally, I would like to thank all the other members of the **Nagoya University International Student Centre**, whose hard work and dedication has enabled the joint degree PhD program to continue even during the COVID-19 pandemic.

I would like to thank **Dr. Olga**, who is the Deputy head of Department of Experimental Medical Science of Lund University, for her kindness and caring for such a long time. Also give my sincere thanks to **Anette Saltin** at the Office of the Faculty of Medicine, Lund University. Thank you so much for your effective work.

It was a pleasure working with **Koma** sensei on salivary gland topic. I also wish to thank Koma sensei for working together to solve scientific difficulties caused by our initial inexperience.

Watanabe sensei, thank you for introducing me to the extraction and identification method for EVs without reservation, I would like to express my sincerely gratitude.

I would like to thank **Sakaguchi** sensei and **Maruyama** sensei for their sincerely helping me overcome many difficulties at lab.

Moreover, I would like to thank **Okabe** sensei for interviewing me before my PhD admission, thank **Yamaguchi** sensei at Nagoya University for lending me unused mice for preliminary experiments, as well as **Urada** sensei for introducing me to the Nagoya University graduation process. For all the other Japanese sensei in our Oral and maxillofacial surgery department, I would like to thank all of them for their understanding and support.

I would also like to thank all the Chinese international students at Nagoya University including **Chang Qi**, **Song Xinman**, **Wang Yilin**, **Chen Hui**, **Liu Kehong, Bian Huiting**, **Yang Ming**, **Li Jinheng**, **Zhang Qingwen**, **Liu Yuqing**, **Xiong Xia**, and **Wang Qinhong** for their sincere relationship and selfless help.

References

1 Carpenter, G. H. The secretion, components, and properties of saliva. *Annu Rev Food Sci Technol* **4**, 267-276, doi:10.1146/annurev-food-030212-182700 (2013).

2 Morgan-Bathke, M., Martin, K. L. & Limesand, K. H.

3 Louro, T. *et al.* Salivary Protein Profile and Food Intake: A Dietary Pattern Analysis. *Journal of Nutrition and Metabolism* **2021**, 6629951, doi:10.1155/2021/6629951 (2021).

4 Pedersen, A. M. L., Sorensen, C. E., Proctor, G. B., Carpenter, G. H. & Ekstrom, J. Salivary secretion in health and disease. *J Oral Rehabil* **45**, 730-746, doi:10.1111/joor.12664 (2018).

5 Laputková, G., Schwartzová, V., Bánovčin, J., Alexovič, M. & Sabo, J. Salivary Protein Roles in Oral Health and as Predictors of Caries Risk. *Open Life Sci* **13**, 174-200, doi:10.1515/biol-2018-0023 (2018).

6 Esteves, C. V. *et al.* Diagnostic potential of saliva proteome analysis: a review and guide to clinical practice. *Braz Oral Res* **33**, e043, doi:10.1590/1807-3107bor-2019.vol33.0043 (2019).

7 Lima, D. P., Diniz, D. G., Moimaz, S. A., Sumida, D. H. & Okamoto, A. C. Saliva: reflection of the body. *Int J Infect Dis* **14**, e184-188, doi:10.1016/j.ijid.2009.04.022 (2010).

8 Boros, I., Keszler, P. & Zelles, T. Study of saliva secretion and the salivary fluoride concentration of the human minor labial glands by a new method. *Arch Oral Biol* **44 Suppl 1**, S59-62, doi:10.1016/s0003-9969(99)90022-5 (1999).

9 Lee, V. M. & Linden, R. W. An olfactory-submandibular salivary reflex in humans. *Exp Physiol* **77**, 221-224, doi:10.1113/expphysiol.1992.sp003578 (1992).

10 Garrett, J. R., Ekström, J. & Anderson, L. C. *Neural mechanisms of salivary gland secretion*. (Karger Medical and Scientific Publishers, 1999).

11 Segawa, A., Terakawa, S., Yamashina, S. & Hopkins, C. R. Exocytosis in living salivary glands: direct visualization by video-enhanced microscopy and confocal laser microscopy. *Eur J Cell Biol* **54**, 322-330 (1991).

12 Hunter, L. Saliva and oral health, 4th edition. *British Dental Journal* **214**, 425-425, doi:10.1038/sj.bdj.2013.421 (2013).

13 Gill, J. Dental Caries: The Disease and its Clinical Management, Third Edition. *British Dental Journal* **221**, 443-443, doi:10.1038/sj.bdj.2016.767 (2016).

14 Dawes, C. & Wong, D. T. W. Role of Saliva and Salivary Diagnostics in the Advancement of Oral Health. *J Dent Res* **98**, 133-141, doi:10.1177/0022034518816961 (2019).

15 Javaid, M. A., Ahmed, A. S., Durand, R. & Tran, S. D. Saliva as a diagnostic tool for oral and systemic diseases. *J Oral Biol Craniofac Res* **6**, 66-75, doi:10.1016/j.jobcr.2015.08.006 (2016).

16 Wong, D. T. Salivaomics. *J Am Dent Assoc* **143**, 19S-24S, doi:10.14219/jada.archive.2012.0339 (2012).

17 Denny, P. *et al.* The proteomes of human parotid and submandibular/sublingual gland salivas collected as the ductal secretions. *J Proteome Res* **7**, 1994-2006, doi:10.1021/pr700764j (2008).

18 Prescher, N. *et al.* Rapid quantitative chairside test for active MMP-8 in gingival crevicular fluid: first clinical data. *Ann N Y Acad Sci* **1098**, 493-495, doi:10.1196/annals.1384.019 (2007).

19 Li, N. *et al.* Longitudinal Monitoring of EGFR and PIK3CA Mutations by Saliva-Based EFIRM in Advanced NSCLC Patients With Local Ablative Therapy and Osimertinib Treatment: Two Case Reports. *Front Oncol* **10**, 1240, doi:10.3389/fonc.2020.01240 (2020).

20 Chaudhuri, A. A., Binkley, M. S., Osmundson, E. C., Alizadeh, A. A. & Diehn, M. Predicting Radiotherapy Responses and Treatment Outcomes Through Analysis of Circulating Tumor DNA. *Semin Radiat Oncol* **25**, 305-312, doi:10.1016/j.semradonc.2015.05.001 (2015).

21 Jensen, S. B., Vissink, A., Limesand, K. H. & Reyland, M. E. Salivary Gland Hypofunction and Xerostomia in Head and Neck Radiation Patients. *J Natl Cancer Inst Monogr*, doi:10.1093/jncimonographs/lgz016 (2019).

22 Chibly, A. M., Nguyen, T. & Limesand, K. H. Palliative Care for Salivary Gland Dysfunction Highlights the Need for Regenerative Therapies: A Review on Radiation and Salivary Gland Stem Cells. *J Palliat Care Med* **4**, doi:10.4172/2165-7386.1000180 (2014).

23 von Bültzingslöwen, I. *et al.* Salivary dysfunction associated with systemic diseases: systematic review and clinical management recommendations. *Oral Surg Oral Med Oral Pathol Oral Radiol Endod* **103 Suppl**, S57.e51-15, doi:10.1016/j.tripleo.2006.11.010 (2007).

24 Wijers, O. B. *et al.* Patients with head and neck cancer cured by radiation therapy: a survey of the dry mouth syndrome in long-term survivors. *Head Neck* **24**, 737-747, doi:10.1002/hed.10129 (2002).

25 Lombaert, I., Movahednia, M. M., Adine, C. & Ferreira, J. N. Concise Review: Salivary Gland Regeneration: Therapeutic Approaches from Stem Cells to Tissue Organoids. *Stem Cells* **35**, 97-105, doi:10.1002/stem.2455 (2017).

26 Wijers, O. B. *et al.* Patients with head and neck cancer cured by radiation therapy: A survey of the dry mouth syndrome in long-term survivors. *Head & Neck* **24**, 737-747, doi:10.1002/hed.10129 (2002).

27 Jensen, S. B. *et al.* A systematic review of salivary gland hypofunction and xerostomia induced by cancer therapies: prevalence, severity and impact on quality of life. *Support Care Cancer* **18**, 1039-1060, doi:10.1007/s00520-010-0827-8 (2010).

28 Li, Y. *et al.* Diagnosis, Prevention, and Treatment of Radiotherapy-Induced Xerostomia: A Review. *J Oncol* **2022**, 7802334, doi:10.1155/2022/7802334 (2022).

29 Memtsa, P. T. *et al.* Validity and reliability of the Greek version of the xerostomia questionnaire in head and neck cancer patients. *Support Care Cancer* **25**, 847-853, doi:10.1007/s00520-016-3471-0 (2017).

30 Hu, J., Andablo-Reyes, E., Mighell, A., Pavitt, S. & Sarkar, A. Dry mouth diagnosis and saliva substitutes-A review from a textural perspective. *J Texture Stud* **52**, 141-156, doi:10.1111/jtxs.12575 (2021).

31 Beetz, I. *et al.* The Groningen Radiotherapy-Induced Xerostomia questionnaire: development and validation of a new questionnaire. *Radiother Oncol* **97**, 127-131, doi:10.1016/j.radonc.2010.05.004 (2010).

32 Navazesh, M. & Christensen, C. M. A comparison of whole mouth resting and stimulated salivary measurement procedures. *J Dent Res* **61**, 1158-1162, doi:10.1177/00220345820610100901 (1982).

33 Takano, T. *et al.* Intra- and inter-investigator reliabilities of oral moisture measured using an oral moisture-checking device. *J Oral Rehabil* **47**, 480-484, doi:10.1111/joor.12919 (2020).

34 Fukushima, Y. *et al.* Evaluation of oral wetness using an improved moisture-checking device for the diagnosis of dry mouth. *Oral Science International* **14**, 33-36, doi:10.1016/s1348-8643(17)30017-4 (2017).

35 Afzelius, P., Nielsen, M. Y., Ewertsen, C. & Bloch, K. P. Imaging of the major salivary glands. *Clin Physiol Funct Imaging* **36**, 1-10, doi:10.1111/cpf.12199 (2016).

36 Nömayr, A., Lell, M., Sweeney, R., Bautz, W. & Lukas, P. MRI appearance of radiation-induced changes of normal cervical tissues. *Eur Radiol* **11**, 1807-1817, doi:10.1007/s003300000728 (2001).

37 Chen, Y. C., Chen, H. Y. & Hsu, C. H. Recent Advances in Salivary Scintigraphic Evaluation of Salivary Gland Function. *Diagnostics (Basel)* **11**, doi:10.3390/diagnostics11071173 (2021).

38 Wu, V. W. C. & Leung, K. Y. A Review on the Assessment of Radiation Induced Salivary Gland Damage After Radiotherapy. *Front Oncol* **9**, 1090, doi:10.3389/fonc.2019.01090 (2019).

39 Ou, D. *et al.* Magnetic resonance sialography for investigating major salivary gland duct system after intensity-modulated radiotherapy of nasopharyngeal carcinoma. *Int J Clin Oncol* **18**, 801-807, doi:10.1007/s10147-012-0464-y (2013).

40 Mattingly, A., Finley, J. K. & Knox, S. M. Salivary gland development and disease. *Wiley Interdiscip Rev Dev Biol* **4**, 573-590, doi:10.1002/wdev.194 (2015).

41 Jaskoll, T. & Melnick, M. in *Branching Morphogenesis Molecular Biology Intelligence Unit* Ch. Chapter 9, 160-175 (2005).

42 Jimenez-Rojo, L., Granchi, Z., Graf, D. & Mitsiadis, T. A. Stem Cell Fate Determination during Development and Regeneration of Ectodermal Organs. *Front Physiol* **3**, 107, doi:10.3389/fphys.2012.00107 (2012).

43 Borghese, E. The development in vitro of the submandibular and sublingual glands of Mus musculus. *J Anat* **84**, 287-302 (1950).

44 Sakai, T., Onodera, T. & Yamada, K. M. in *Interface Oral Health Science 2009* Ch. Chapter 2, 13-19 (2010).

45 Patel, V. N., Rebustini, I. T. & Hoffman, M. P. Salivary gland branching morphogenesis. *Differentiation* **74**, 349-364, doi:10.1111/j.1432-0436.2006.00088.x (2006).

46 Dr. Sangeetha Priya.P, D. N. A., Dr.E.Rajesh, Dr.K.M.K.Masthan. Embryology and development of salivary gland. *European Journal of Molecular & Clinical Medicine* **07** (2020).

47 Holmberg, K. V. & Hoffman, M. P. Anatomy, biogenesis and regeneration of salivary glands. *Monogr Oral Sci* **24**, 1-13, doi:10.1159/000358776 (2014).

48 Iorgulescu, G. Saliva between normal and pathological. Important factors in determining systemic and oral health. *J Med Life* **2**, 303-307 (2009).

49 Lazaridou, M. *et al.* Salivary gland trauma: a review of diagnosis and treatment. *Craniomaxillofac Trauma Reconstr* **5**, 189-196, doi:10.1055/s-0032-1313356 (2012).

50 Harrison, J. D. in *Surgery of the Salivary Glands* 37-42 (2021).

51 Gupta, S. & Ahuja, N. in *Histology* Ch. Chapter 4, (2019).

52 Chibly, A. M., Aure, M. H., Patel, V. N. & Hoffman, M. P. Salivary gland function, development, and regeneration. *Physiol Rev* **102**, 1495-1552, doi:10.1152/physrev.00015.2021 (2022).

53 Weinreb, I. *et al.* Ductal adenomas of salivary gland showing features of striated duct differentiation ('striated duct adenoma'): a report of six cases. *Histopathology* **57**, 707-715, doi:10.1111/j.1365-2559.2010.03682.x (2010).

54 Porcheri, C. & Mitsiadis, T. A. Physiology, Pathology and Regeneration of Salivary Glands. *Cells* **8**, doi:10.3390/cells8090976 (2019).

55 Shah, A. A., Mulla, A. F. & Mayank, M. Pathophysiology of myoepithelial cells in salivary glands. *J Oral Maxillofac Pathol* **20**, 480-490, doi:10.4103/0973-029x.190952 (2016).

56 San Martin, R. *et al.* Recruitment of CD34(+) fibroblasts in tumor-associated reactive stroma: the reactive microvasculature hypothesis. *Am J Pathol* **184**, 1860-1870, doi:10.1016/j.ajpath.2014.02.021 (2014).

57 Krishnamurthy, S. Salivary gland disorders: A comprehensive review. *World Journal of Stomatology* **4**, doi:10.5321/wjs.v4.i2.56 (2015).

58 Rocchi, C. & Emmerson, E. Mouth-Watering Results: Clinical Need, Current Approaches, and Future Directions for Salivary Gland Regeneration. *Trends Mol Med* **26**, 649-669, doi:10.1016/j.molmed.2020.03.009 (2020).

59 Bernier, J. & Horiot, J. C. Altered-fractionated radiotherapy in locally advanced head and neck cancer. *Curr Opin Oncol* **24**, 223-228, doi:10.1097/CCO.0b013e32834ea6fe (2012).

60 Henson, B. S., Eisbruch, A., D'Hondt, E. & Ship, J. A. Two-year longitudinal study of parotid salivary flow rates in head and neck cancer patients receiving unilateral neck parotid-sparing radiotherapy treatment. *Oral Oncol* **35**, 234-241, doi:10.1016/s1368-8375(98)00104-3 (1999).

61 Avila, J. L., Grundmann, O., Burd, R. & Limesand, K. H. Radiation-induced salivary gland dysfunction results from p53-dependent apoptosis. *Int J Radiat Oncol Biol Phys* **73**, 523-529, doi:10.1016/j.ijrobp.2008.09.036 (2009).

62 Limesand, K. H., Said, S. & Anderson, S. M. Suppression of radiation-induced salivary gland dysfunction by IGF-1. *PLoS One* **4**, e4663, doi:10.1371/journal.pone.0004663 (2009).

63 Konings, A. W. T., Coppes, R. P. & Vissink, A. On the mechanism of salivary gland radiosensitivity. *International Journal of Radiation Oncology*Biology*Physics* **62**, 1187-1194, doi:https://doi.org/10.1016/j.ijrobp.2004.12.051 (2005).

64 Coppes, R. P., Roffel, A. F., Zeilstra, L. J. W., Vissink, A. & Konings, A. W. T. Early Radiation Effects on Muscarinic Receptor-Induced Secretory Responsiveness of the Parotid Gland in the Freely Moving Rat. *Radiation Research* **153**, 339-346, doi:10.1667/0033-7587(2000)153[0339:Ereomr]2.0.Co;2 (2000).

65 Lombaert, I. M. *et al.* Cytokine treatment improves parenchymal and vascular damage of salivary glands after irradiation. *Clin Cancer Res* **14**, 7741-7750, doi:10.1158/1078-0432.Ccr-08-1449 (2008).

66 Abdel Razek, A. A. K. & Mukherji, S. Imaging of sialadenitis. *Neuroradiol J* **30**, 205-215, doi:10.1177/1971400916682752 (2017).

67 Hou, J. *et al.* Distinct shifts in the oral microbiota are associated with the progression and aggravation of mucositis during radiotherapy. *Radiother Oncol* **129**, 44-51, doi:10.1016/j.radonc.2018.04.023 (2018).

68 Limesand, K. H. *et al.* Insulin-like growth factor-1 preserves salivary gland function after fractionated radiation. *Int J Radiat Oncol Biol Phys* **78**, 579-586, doi:10.1016/j.ijrobp.2010.03.035 (2010).

69 Knox, S. M. *et al.* Parasympathetic stimulation improves epithelial organ regeneration. *Nat Commun* **4**, 1494, doi:10.1038/ncomms2493 (2013).

70 Mizrachi, A. *et al.* Radiation-Induced Microvascular Injury as a Mechanism of Salivary Gland Hypofunction and Potential Target for Radioprotectors. *Radiat Res* **186**, 189-195, doi:10.1667/RR14431.1 (2016).

71 Fox, R. I. Sjögren's syndrome. *Lancet* **366**, 321-331, doi:10.1016/s0140-6736(05)66990-5 (2005).

72 Choudhry, H. S. *et al.* Updates in diagnostics, treatments, and correlations between oral and ocular manifestations of Sjogren's syndrome. *Ocul Surf* **26**, 75-87, doi:10.1016/j.jtos.2022.08.001 (2022).

73 Shiboski, C. H. *et al.* 2016 American College of Rheumatology/European League Against Rheumatism Classification Criteria for Primary Sjogren's Syndrome: A Consensus and Data-Driven Methodology Involving Three International Patient Cohorts. *Arthritis Rheumatol* **69**, 35-45, doi:10.1002/art.39859 (2017).

74 Seror, R. *et al.* EULAR Sjogren's Syndrome Patient Reported Index (ESSPRI): development of a consensus patient index for primary Sjogren's syndrome. *Ann Rheum Dis* **70**, 968-972, doi:10.1136/ard.2010.143743 (2011).

75 Scardina, G. A. *et al.* Diagnostic evaluation of serial sections of labial salivary gland biopsies in Sjögren's syndrome. *Med Oral Patol Oral Cir Bucal* **12**, E565-568 (2007).

76 Nocturne, G. & Mariette, X. B cells in the pathogenesis of primary Sjogren syndrome. *Nat Rev Rheumatol* **14**, 133-145, doi:10.1038/nrrheum.2018.1 (2018).

77 Kaneko, N. *et al.* Cytotoxic CD8⁺ T cells may be drivers of tissue destruction in Sjogren's syndrome. *Sci Rep* **12**, 15427, doi:10.1038/s41598-022-19397-w (2022).

78 Tapinos, N. I., Polihronis, M., Tzioufas, A. G. & Moutsopoulos, H. M. Sjögren's syndrome. Autoimmune epithelitis. *Adv Exp Med Biol* **455**, 127-134 (1999).

79 Robinson, C. P., Yamamoto, H., Peck, A. B. & Humphreys-Beher, M. G. Genetically programmed development of salivary gland abnormalities in the NOD (nonobese diabetic)-scid mouse in the absence of detectable lymphocytic infiltration: a potential trigger for sialoadenitis of NOD mice. *Clin Immunol Immunopathol* **79**, 50-59, doi:10.1006/clin.1996.0050 (1996).

80 Salomonsson, S. *et al.* Expression of the B cell-attracting chemokine CXCL13 in the target organ and autoantibody production in ectopic lymphoid tissue in the chronic inflammatory disease Sjogren's syndrome. *Scand J Immunol* **55**, 336-342, doi:10.1046/j.1365-3083.2002.01058.x (2002).

81 Xanthou, G. *et al.* "Lymphoid" chemokine messenger RNA expression by epithelial cells in the chronic inflammatory lesion of the salivary glands of Sjögren's syndrome patients: possible participation in lymphoid structure formation. *Arthritis Rheum* **44**, 408-418, doi:10.1002/1529-0131(200102)44:2<408::Aid-anr60>3.0.Co;2-0 (2001).

82 Ma-Krupa, W. *et al.* Activation of arterial wall dendritic cells and breakdown of self-tolerance in giant cell arteritis. *J Exp Med* **199**, 173-183, doi:10.1084/jem.20030850 (2004).

83 Gao, Y., Chen, Y., Zhang, Z., Yu, X. & Zheng, J. Recent Advances in Mouse Models of Sjogren's Syndrome. *Front Immunol* **11**, 1158, doi:10.3389/fimmu.2020.01158 (2020).

84 Senthilkumar, B. & Mahabob, M. N. Mucocele: An unusual presentation of the minor salivary gland lesion. *J Pharm Bioallied Sci* **4**, S180-182, doi:10.4103/0975-7406.100265 (2012).

85 Sung, H. *et al.* Global Cancer Statistics 2020: GLOBOCAN Estimates of Incidence and Mortality Worldwide for 36 Cancers in 185 Countries. *CA Cancer J Clin* **71**, 209-249, doi:10.3322/caac.21660 (2021).

86 Jegadeesh, N. *et al.* Outcomes and prognostic factors in modern era management of major salivary gland cancer. *Oral Oncol* **51**, 770-777, doi:10.1016/j.oraloncology.2015.05.005 (2015).

87 Skálová, A., Hyrcza, M. D. & Leivo, I. Update from the 5th Edition of the World Health Organization Classification of Head and Neck Tumors: Salivary Glands. *Head Neck Pathol* **16**, 40-53, doi:10.1007/s12105-022-01420-1 (2022).

88 Hellquist, H. *et al.* Analysis of the Clinical Relevance of Histological Classification of Benign Epithelial Salivary Gland Tumours. *Adv Ther* **36**, 1950-1974, doi:10.1007/s12325-019-01007-3 (2019).

89 Ferrarotto, R. *et al.* Proteogenomic Analysis of Salivary Adenoid Cystic Carcinomas Defines Molecular Subtypes and Identifies Therapeutic Targets. *Clin Cancer Res* **27**, 852-864, doi:10.1158/1078-0432.Ccr-20-1192 (2021).

90 Zhao, M. *et al.* Clinicopathologic and molecular genetic analysis of secretory carcinoma of salivary gland. *Zhonghua Kou Qiang Yi Xue Za Zhi* **53**, 533-538, doi:10.3760/cma.j.issn.1002-0098.2018.08.007 (2018).

91 Manvikar, V., Ramulu, S., Ravishanker, S. T. & Chakravarthy, C. Squamous cell carcinoma of submandibular salivary gland: A rare case report. *J Oral Maxillofac Pathol* **18**, 299-302, doi:10.4103/0973-029x.140909 (2014).

92 Yan, K., Yesensky, J., Hasina, R. & Agrawal, N. Genomics of mucoepidermoid and adenoid cystic carcinomas. *Laryngoscope Investig Otolaryngol* **3**, 56-61, doi:10.1002/lio2.139 (2018).

93 Emmerson, E. & Knox, S. M. Salivary gland stem cells: A review of development, regeneration and cancer. *Genesis* **56**, e23211, doi:10.1002/dvg.23211 (2018).

94 Mimica, X. *et al.* Polymorphous adenocarcinoma of salivary glands. *Oral Oncol* **95**, 52-58, doi:10.1016/j.oraloncology.2019.06.002 (2019).

95 Gaidano, G., Pastore, C. & Volpe, G. Molecular pathogenesis of non-Hodgkin lymphoma: a clinical perspective. *Haematologica* **80**, 454-472 (1995).

96 Mendenhall, W. M., Mendenhall, C. M., Werning, J. W., Malyapa, R. S. & Mendenhall, N. P. Salivary gland pleomorphic adenoma. *Am J Clin Oncol* **31**, 95-99, doi:10.1097/COC.0b013e3181595ae0 (2008).

97 Kim, J. Y., An, C. H., Kim, J. Y. & Jung, J. K. Experimental Animal Model Systems for Understanding Salivary Secretory Disorders. *Int Journal Mol Sci* **21**, doi:10.3390/ijms21228423 (2020).

98 Cheng, S. C. H., Wu, V. W. C., Kwong, D. L. W. & Ying, M. T. C. Assessment of post-radiotherapy salivary glands. *The British Journal of Radiology* **84**, 393-402, doi:10.1259/bjr/66754762 (2011).

99 Torun, N., Muratli, A., Serim, B. D., Ergulen, A. & Altun, G. D. Radioprotective Effects of Amifostine, L-Carnitine and Vitamin E in Preventing Early Salivary Gland Injury due to Radioactive Iodine Treatment. *Curr Med Imaging Rev* **15**, 395-404, doi:10.2174/1573405614666180314150808 (2019).

100 Correia, P. N., Carpenter, G. H., Osailan, S. M., Paterson, K. L. & Proctor, G. B. Acute salivary gland hypofunction in the duct ligation model in the absence of inflammation. *Oral Dis* **14**, 520-528, doi:10.1111/j.1601-0825.2007.01413.x (2008).

101 Lavoie, T. N., Lee, B. H. & Nguyen, C. Q. Current concepts: mouse models of Sjögren's syndrome. *J Biomed Biotechnol* **2011**, 549107, doi:10.1155/2011/549107 (2011).

102 Nam, K. *et al.* Laminin-111-derived peptide conjugated fibrin hydrogel restores salivary gland function. *PLoS One* **12**, e0187069, doi:10.1371/journal.pone.0187069 (2017).

103 Romero, A. C., Bergamaschi, C. T., de Souza, D. N. & Nogueira, F. N. Salivary Alterations in Rats with Experimental Chronic Kidney Disease. *PLoS One* **11**, e0148742, doi:10.1371/journal.pone.0148742 (2016).

104 Kim, J. H. *et al.* Alpha-Lipoic Acid Ameliorates Radiation-Induced Salivary Gland Injury by Preserving Parasympathetic Innervation in Rats. *Int J Mol Sci* **21**, doi:10.3390/ijms21072260 (2020).

105 Cheng, Y. *et al.* Principles of regulatory information conservation between mouse and human. *Nature* **515**, 371-375, doi:10.1038/nature13985 (2014).

106 Lin, S. *et al.* Comparison of the transcriptional landscapes between human and mouse tissues. *Proc Natl Acad Sci U S A* **111**, 17224-17229, doi:10.1073/pnas.1413624111 (2014).

107 Amano, O., Mizobe, K., Bando, Y. & Sakiyama, K. Anatomy and histology of rodent and human major salivary glands: -overview of the Japan salivary gland society-sponsored workshop. *Acta Histochem Cytochem* **45**, 241-250, doi:10.1267/ahc.12013 (2012).

108 Maruyama, C. L., Monroe, M. M., Hunt, J. P., Buchmann, L. & Baker, O. J. Comparing human and mouse salivary glands: A practice guide for salivary researchers. *Oral Dis* **25**, 403-415, doi:10.1111/odi.12840 (2019).

109 Kurabuchi, S. Morphologic changes in the granular convoluted tubule cells of the mouse submandibular gland following hypophysectomy and hormonal replacement. *Odontology* **90**, 27-34, doi:10.1007/s102660200004 (2002).

110 Pinkstaff, C. A. Salivary gland sexual dimorphism: a brief review. *Eur J Morphol* **36 Suppl**, 31-34 (1998).

111 Nguyen, V. T., Dawson, P., Zhang, Q., Harris, Z. & Limesand, K. H. Administration of growth factors promotes salisphere formation from irradiated parotid salivary glands. *PLoS One* **13**, e0193942, doi:10.1371/journal.pone.0193942 (2018).

112 Grundmann, O., Fillinger, J. L., Victory, K. R., Burd, R. & Limesand, K. H. Restoration of radiation therapy-induced salivary gland dysfunction in mice by post therapy IGF-1 administration. *BMC Cancer* **10**, 417, doi:10.1186/1471-2407-10-417 (2010).

113 Marmary, Y. *et al.* Radiation-Induced Loss of Salivary Gland Function Is Driven by Cellular Senescence and Prevented by IL6 Modulation. *Cancer Res* **76**, 1170-1180, doi:10.1158/0008-5472.CAN-15-1671 (2016).

114 Liu, X. *et al.* Loss of TRPM2 function protects against irradiation-induced salivary gland dysfunction. *Nat Commun* **4**, 1515, doi:10.1038/ncomms2526 (2013).

115 Kim, J. H. *et al.* Protective effects of alpha lipoic acid on radiation-induced salivary gland injury in rats. *Oncotarget* **7**, 29143-29153, doi:10.18632/oncotarget.8661 (2016).

116 Radfar, L. & Sirois, D. A. Structural and functional injury in minipig salivary glands following fractionated exposure to 70 Gy of ionizing radiation: an animal model for human radiation-induced salivary gland injury. *Oral Surgery, Oral Medicine, Oral Pathology, Oral Radiology and Endodontics* **96**, 267-274, doi:10.1016/S1079-2104(03)00369-X (2003).

117 Price, R. E., Ang, K. K., Stephens, L. C. & Peters, L. J. Effects of continuous hyperfractionated accelerated and conventionally fractionated radiotherapy on the parotid and submandibular salivary glands of rhesus monkeys. *Radiother Oncol* **34**, 39-46, doi:10.1016/0167-8140(94)01491-k (1995).

118 Kujan, O., Othman, R., Alshehri, M., Iqbal, F. & Kochaji, N. Proliferative Activity of Myoepithelial Cells in Irradiated Rabbit Parotid and Submandibular Salivary Glands. *J Int Oral Health* **7**, 1-5 (2015).

119 Sławińska, N. & Krupa, R. Molecular Aspects of Senescence and Organismal Ageing-DNA Damage Response, Telomeres, Inflammation and Chromatin. *Int J Mol Sci* **22**, doi:10.3390/ijms22020590 (2021).

120 McHugh, D. & Gil, J. Senescence and aging: Causes, consequences, and therapeutic avenues. *J Cell Biol* **217**, 65-77, doi:10.1083/jcb.201708092 (2018).

121 Herranz, N. & Gil, J. Mechanisms and functions of cellular senescence. *J Clin Invest* **128**, 1238-1246, doi:10.1172/jci95148 (2018).

122 Kim, K. S. *et al.* Induction of cellular senescence by insulin-like growth factor binding protein-5 through a p53-dependent mechanism. *Mol Biol Cell* **18**, 4543-4552, doi:10.1091/mbc.e07-03-0280 (2007).

123 Mitchell, G. C. *et al.* IGF1 activates cell cycle arrest following irradiation by reducing binding of ΔNp63 to the p21 promoter. *Cell Death Dis* **1**, e50, doi:10.1038/cddis.2010.28 (2010).

124 Debacq-Chainiaux, F., Erusalimsky, J. D., Campisi, J. & Toussaint, O. Protocols to detect senescence-associated beta-galactosidase (SA-betagal) activity, a biomarker of senescent cells in culture and in vivo. *Nat Protoc* **4**, 1798-1806, doi:10.1038/nprot.2009.191 (2009).

125 Peng, X. *et al.* Cellular senescence contributes to radiation-induced hyposalivation by affecting the stem/progenitor cell niche. *Cell Death & Disease* **11**, 854, doi:10.1038/s41419-020-03074-9 (2020).

126 Xu, L. *et al.* Radiation-Induced Osteocyte Senescence Alters Bone Marrow Mesenchymal Stem Cell Differentiation Potential via Paracrine Signaling. *Int J Mol Sci* **22**, doi:10.3390/ijms22179323 (2021).

127 Salum, F. G., Medella-Junior, F. A. C., Figueiredo, M. A. Z. & Cherubini, K. Salivary hypofunction: An update on therapeutic strategies. *Gerodontology* **35**, 305-316, doi:10.1111/ger.12353 (2018).

128 Vissink, A. *et al.* Clinical management of salivary gland hypofunction and xerostomia in head-and-neck cancer patients: successes and barriers. *Int J Radiat Oncol Biol Phys* **78**, 983-991, doi:10.1016/j.ijrobp.2010.06.052 (2010).

129 Łysik, D., Niemirowicz-Laskowska, K., Bucki, R., Tokajuk, G. & Mystkowska, J. Artificial Saliva: Challenges and Future Perspectives for the Treatment of Xerostomia. *Int J Mol Sci* **20**, doi:10.3390/ijms20133199 (2019).

130 Kho, H. S. Understanding of xerostomia and strategies for the development of artificial saliva. *Chin J Dent Res* **17**, 75-83 (2014).

131 Pathak, J. L., Yan, Y., Zhang, Q., Wang, L. & Ge, L. The role of oral microbiome in respiratory health and diseases. *Respir Med* **185**, 106475, doi:10.1016/j.rmed.2021.106475 (2021).

132 J, J. P.-P., Jakubik, A., Przeklasa-Bierowiec, A. & Muszynska, B. Artificial saliva and its use in biological experiments. *J Physiol Pharmacol* **68**, 807-813 (2017).

133 Faruque, M., Wanschers, M., Ligtenberg, A. J., Laine, M. L. & Bikker, F. J. A review on the role of salivary MUC5B in oral health. *J Oral Biosci* **64**, 392-399, doi:10.1016/j.job.2022.09.005 (2022).

134 Glantz, P.-O. Interfacial phenomena in the oral cavity. *Colloids and Surfaces A: Physicochemical and Engineering Aspects* **123-124**, 657-670, doi:https://doi.org/10.1016/S0927-7757(96)03817-4 (1997).

135 Chaudhury, N. M., Shirlaw, P., Pramanik, R., Carpenter, G. H. & Proctor, G. B. Changes in Saliva Rheological Properties and Mucin Glycosylation in Dry Mouth. *J Dent Res* **94**, 1660-1667, doi:10.1177/0022034515609070 (2015).

136 Hinic, S. *et al.* Viscosity and mixing properties of artificial saliva and four different mouthwashes. *Biorheology* **57**, 87-100, doi:10.3233/bir-201008 (2020).

137 Jha, N. *et al.* Prevention of radiation induced xerostomia by surgical transfer of submandibular salivary gland into the submental space. *Radiother Oncol* **66**, 283-289, doi:10.1016/s0167-8140(03)00023-9 (2003).

138 Seikaly, H. *et al.* Submandibular gland transfer: a new method of preventing radiation-induced xerostomia. *Laryngoscope* **111**, 347-352, doi:10.1097/00005537-200102000-00028 (2001).

139 Liu, R., Seikaly, H. & Jha, N. Anatomic study of submandibular gland transfer in an attempt to prevent postradiation xerostomia. *J Otolaryngol* **31**, 76-79, doi:10.2310/7070.2002.19035 (2002).

140 Sood, A. J. *et al.* Salivary gland transfer to prevent radiation-induced xerostomia: A systematic review and meta-analysis. *Oral Oncology* **50**, 77-83, doi:10.1016/j.oraloncology.2013.10.010 (2014).

141 Scrimger, R. A. *et al.* Combination of submandibular salivary gland transfer and intensity-modulated radiotherapy to reduce dryness of mouth (xerostomia) in patients with head and neck cancer. *Head Neck* **40**, 2353-2361, doi:10.1002/hed.25339 (2018).

142 Jha, N. *et al.* A phase II study of submandibular gland transfer prior to radiation for prevention of radiation-induced xerostomia in head-and-neck cancer (RTOG 0244). *Int J Radiat Oncol Biol Phys* **84**, 437-442, doi:10.1016/j.ijrobp.2012.02.034 (2012).

143 Rieger, J. *et al.* Submandibular Gland Transfer for Prevention of Xerostomia After Radiation Therapy: Swallowing Outcomes. *Archives of Otolaryngology–Head & Neck Surgery* **131**, 140-145, doi:10.1001/archotol.131.2.140 (2005).

144 Brizel, D. M. *et al.* Phase III randomized trial of amifostine as a radioprotector in head and neck cancer. *J Clin Oncol* **18**, 3339-3345, doi:10.1200/jco.2000.18.19.3339 (2000).

145 Gu, J. *et al.* Effect of amifostine in head and neck cancer patients treated with radiotherapy: a systematic review and meta-analysis based on randomized controlled trials. *PLoS One* **9**, e95968, doi:10.1371/journal.pone.0095968 (2014).

146 Kamran, M. Z., Ranjan, A., Kaur, N., Sur, S. & Tandon, V. Radioprotective Agents: Strategies and Translational Advances. *Med Res Rev* **36**, 461-493, doi:10.1002/med.21386 (2016).

147 Yang, W.-f. *et al.* Is Pilocarpine Effective in Preventing Radiation-Induced Xerostomia? A Systematic Review and Meta-analysis. *International Journal of Radiation Oncology*Biology*Physics* **94**, 503-511, doi:https://doi.org/10.1016/j.ijrobp.2015.11.012 (2016).

148 Jaguar, G. C. *et al.* Double blind randomized prospective trial of bethanechol in the prevention of radiation-induced salivary gland dysfunction in head and neck cancer patients. *Radiother Oncol* **115**, 253-256, doi:10.1016/j.radonc.2015.03.017 (2015).

149 Chung, M. K. *et al.* Randomized Trial of Vitamin C/E Complex for Prevention of Radiation-Induced Xerostomia in Patients with Head and Neck Cancer. *Otolaryngol Head Neck Surg* **155**, 423-430, doi:10.1177/0194599816642418 (2016).

150 Fox, N. F. *et al.* Hyperbaric oxygen therapy for the treatment of radiation-induced xerostomia: a systematic review. *Oral Surg Oral Med Oral Pathol Oral Radiol* **120**, 22-28, doi:10.1016/j.oooo.2015.03.007 (2015).

151 Jensen, S. B. *et al.* A systematic review of salivary gland hypofunction and xerostomia induced by cancer therapies: management strategies and economic impact. *Support Care Cancer* **18**, 1061-1079, doi:10.1007/s00520-010-0837-6 (2010).

152 Nutting, C. M. *et al.* Parotid-sparing intensity modulated versus conventional radiotherapy in head and neck cancer (PARSPORT): a phase 3 multicentre randomised controlled trial. *Lancet Oncol* **12**, 127-136, doi:10.1016/s1470-2045(10)70290-4 (2011).

153 van Luijk, P. *et al.* Sparing the region of the salivary gland containing stem cells preserves saliva production after radiotherapy for head and neck cancer. *Sci Transl Med* **7**, 305ra147, doi:10.1126/scitranslmed.aac4441 (2015).

154 Baum, B. J. *et al.* Early responses to adenoviral-mediated transfer of the aquaporin-1 cDNA for radiation-induced salivary hypofunction. *Proc Natl Acad Sci U S A* **109**, 19403-19407, doi:10.1073/pnas.1210662109 (2012).

155 Lai, Z. *et al.* Aquaporin gene therapy corrects Sjogren's syndrome phenotype in mice. *Proc Natl Acad Sci U S A* **113**, 5694-5699, doi:10.1073/pnas.1601992113 (2016).

156 Corden, A. *et al.* Neutralizing antibodies against adeno-associated viruses in Sjogren's patients: implications for gene therapy. *Gene Ther* **24**, 241-244, doi:10.1038/gt.2017.1 (2017).

157 Alevizos, I. *et al.* Late responses to adenoviral-mediated transfer of the aquaporin-1 gene for radiation-induced salivary hypofunction. *Gene Ther* **24**, 176-186, doi:10.1038/gt.2016.87 (2017).

158 Holmberg, K. V. & Hoffman, M. P. in *Monographs in Oral Science* 1-13 (S. Karger AG, 2014).

159 Martin, K. L. *et al.* Prevention of radiation-induced salivary gland dysfunction utilizing a CDK inhibitor in a mouse model. *PLoS One* **7**, e51363, doi:10.1371/journal.pone.0051363 (2012).

160 Pringle, S., Van Os, R. & Coppes, R. P. Concise review: Adult salivary gland stem cells and a potential therapy for xerostomia. *Stem Cells* **31**, 613-619, doi:10.1002/stem.1327 (2013).

161 Chansaenroj, A., Yodmuang, S. & Ferreira, J. N. Trends in Salivary Gland Tissue Engineering: From Stem Cells to Secretome and Organoid Bioprinting. *Tissue Eng Part B Rev* **27**, 155-165, doi:10.1089/ten.TEB.2020.0149 (2021).

162 Jensen, D. H. *et al.* Mesenchymal stem cell therapy for salivary gland dysfunction and xerostomia: a systematic review of preclinical studies. *Oral Surg Oral Med Oral Pathol Oral Radiol* **117**, 335-342 e331, doi:10.1016/j.oooo.2013.11.496 (2014).

163 Kichenbrand, C., Velot, E., Menu, P. & Moby, V. Dental Pulp Stem Cell-Derived Conditioned Medium: An Attractive Alternative for Regenerative Therapy. *Tissue Eng Part B Rev* **25**, 78-88, doi:10.1089/ten.TEB.2018.0168 (2019).

164 Mulyani, S. W. M., Astuti, E. R., Wahyuni, O. R., Ernawati, D. S. & Ramadhani, N. F. Xerostomia Therapy Due to Ionized Radiation Using Preconditioned Bone Marrow-Derived Mesenchymal Stem Cells. *Eur J Dent* **13**, 238-242, doi:10.1055/s-0039-1694697 (2019).

165 Grønhøj, C. *et al.* Safety and Efficacy of Mesenchymal Stem Cells for Radiation-Induced Xerostomia: A Randomized, Placebo-Controlled Phase 1/2 Trial (MESRIX). *Int J Radiat Oncol Biol Phys* **101**, 581-592, doi:10.1016/j.ijrobp.2018.02.034 (2018).

166 Liu, Q. W. *et al.* Characteristics and Therapeutic Potential of Human Amnion-Derived Stem Cells. *Int J Mol Sci* **22**, doi:10.3390/ijms22020970 (2021).

167 Bento, G. *et al.* Urine-Derived Stem Cells: Applications in Regenerative and Predictive Medicine. *Cells* **9**, doi:10.3390/cells9030573 (2020).

168 Zakrzewski, W., Dobrzynski, M., Szymonowicz, M. & Rybak, Z. Stem cells: past, present, and future. *Stem Cell Res Ther* **10**, 68, doi:10.1186/s13287-019-1165-5 (2019).

169 Alaa El-Din, Y., Sabry, D., Abdelrahman, A. H. & Fathy, S. Potential therapeutic effects of induced pluripotent stem cells on induced salivary gland cancer in experimental rats. *Biotech Histochem* **94**, 92-99, doi:10.1080/10520295.2018.1508747 (2019).

170 I, T. *et al.* Anti-inflammatory and vasculogenic conditioning of peripheral blood mononuclear cells reinforces their therapeutic potential for radiation-injured salivary glands. *Stem Cell Res Ther* **10**, 304, doi:10.1186/s13287-019-1414-7 (2019).

171 S, E. L. A., Mager, I., Breakefield, X. O. & Wood, M. J. Extracellular vesicles: biology and emerging therapeutic opportunities. *Nat Rev Drug Discov* **12**, 347-357, doi:10.1038/nrd3978 (2013).

172 Yu, C. & Abbott, P. V. An overview of the dental pulp: its functions and responses to injury. *Aust Dent J* **52**, S4-16, doi:10.1111/j.1834-7819.2007.tb00525.x (2007).

173 Al Madhoun, A. *et al.* Dental Pulp Stem Cells Derived From Adult Human Third Molar Tooth: A Brief Review. *Front Cell Dev Biol* **9**, 717624, doi:10.3389/fcell.2021.717624 (2021).

174 Yuan, S. M., Yang, X. T., Zhang, S. Y., Tian, W. D. & Yang, B. Therapeutic potential of dental pulp stem cells and their derivatives: Insights from basic research toward clinical applications. *World J Stem Cells* **14**, 435-452, doi:10.4252/wjsc.v14.i7.435 (2022).

175 Tamaoki, N. *et al.* Dental pulp cells for induced pluripotent stem cell banking. *J Dent Res* **89**, 773-778, doi:10.1177/0022034510366846 (2010).

176 Lei, T. *et al.* Calreticulin as a special marker to distinguish dental pulp stem cells from gingival mesenchymal stem cells. *Int J Biol Macromol* **178**, 229-239, doi:10.1016/j.ijbiomac.2021.02.126 (2021).

177 Lee, S. Y. *et al.* Effects of cryopreservation of intact teeth on the isolated dental pulp stem cells. *J Endod* **36**, 1336-1340, doi:10.1016/j.joen.2010.04.015 (2010).

178 Takebe, Y. *et al.* Cryopreservation Method for the Effective Collection of Dental Pulp Stem Cells. *Tissue Eng Part C Methods* **23**, 251-261, doi:10.1089/ten.TEC.2016.0519 (2017).

179 Yoo, C. *et al.* Adult stem cells and tissue engineering strategies for salivary gland regeneration: a review. *Biomater Res* **18**, 9, doi:10.1186/2055-7124-18-9 (2014).

180 Weng, P. L., Aure, M. H. & Ovitt, C. E. Concise Review: A Critical Evaluation of Criteria Used to Define Salivary Gland Stem Cells. *Stem Cells* **37**, 1144-1150, doi:10.1002/stem.3046 (2019).

181 Rocchi, C., Barazzuol, L. & Coppes, R. P. The evolving definition of salivary gland stem cells. *NPJ Regen Med* **6**, 4, doi:10.1038/s41536-020-00115-x (2021).

182 Chibly, A. M., Querin, L., Harris, Z. & Limesand, K. H. Label-retaining cells in the adult murine salivary glands possess characteristics of adult progenitor cells. *PLoS One* **9**, e107893, doi:10.1371/journal.pone.0107893 (2014).

183 Nanduri, L. S. *et al.* Salisphere derived c-Kit+ cell transplantation restores tissue homeostasis in irradiated salivary gland. *Radiother Oncol* **108**, 458-463, doi:10.1016/j.radonc.2013.05.020 (2013).

184 Emmerson, E. *et al.* SOX2 regulates acinar cell development in the salivary gland. *Elife* **6**, doi:10.7554/eLife.26620 (2017).

185 Chatzeli, L., Gaete, M. & Tucker, A. S. Fgf10 and Sox9 are essential for the establishment of distal progenitor cells during mouse salivary gland development. *Development* **144**, 2294-2305, doi:10.1242/dev.146019 (2017).

186 Knox, S. M. *et al.* Parasympathetic innervation maintains epithelial progenitor cells during salivary organogenesis. *Science* **329**, 1645-1647, doi:10.1126/science.1192046 (2010).

187 Nanduri, L. S. *et al.* Purification and ex vivo expansion of fully functional salivary gland stem cells. *Stem Cell Reports* **3**, 957-964, doi:10.1016/j.stemcr.2014.09.015 (2014).

188 Togarrati, P. P., Dinglasan, N., Desai, S., Ryan, W. R. & Muench, M. O. CD29 is highly expressed on epithelial, myoepithelial, and mesenchymal stromal cells of human salivary glands. *Oral Dis* **24**, 561-572, doi:10.1111/odi.12812 (2018).

189 Hisatomi, Y. *et al.* Flow cytometric isolation of endodermal progenitors from mouse salivary gland differentiate into hepatic and pancreatic lineages. *Hepatology* **39**, 667-675, doi:10.1002/hep.20063 (2004).

190 Pringle, S. *et al.* Human Salivary Gland Stem Cells Functionally Restore Radiation Damaged Salivary Glands. *Stem Cells* **34**, 640-652, doi:10.1002/stem.2278 (2016).

191 Lombaert, I. M. *et al.* Rescue of salivary gland function after stem cell transplantation in irradiated glands. *PLoS One* **3**, e2063, doi:10.1371/journal.pone.0002063 (2008).

192 Arnold, K. *et al.* Sox2+ Adult Stem and Progenitor Cells Are Important for Tissue Regeneration and Survival of Mice. *Cell Stem Cell* **9**, 317-329, doi:https://doi.org/10.1016/j.stem.2011.09.001 (2011).

193 Yoshida, S. *et al.* Sgn1, a Basic Helix-Loop-Helix Transcription Factor Delineates the Salivary Gland Duct Cell Lineage in Mice. *Developmental Biology* **240**, 517-530, doi:https://doi.org/10.1006/dbio.2001.0473 (2001).

194 Iso, Y. *et al.* Multipotent human stromal cells improve cardiac function after myocardial infarction in mice without long-term engraftment. *Biochem Biophys Res Commun* **354**, 700-706, doi:10.1016/j.bbrc.2007.01.045 (2007).

195 Jin, Y. *et al.* Extracellular signals regulate the biogenesis of extracellular vesicles. *Biol Res* **55**, 35, doi:10.1186/s40659-022-00405-2 (2022).

196 Gurunathan, S., Kang, M. H., Jeyaraj, M., Qasim, M. & Kim, J. H. Review of the Isolation, Characterization, Biological Function, and Multifarious Therapeutic Approaches of Exosomes. *Cells* **8**, doi:10.3390/cells8040307 (2019).

197 Nie, H. *et al.* Use of lung-specific exosomes for miRNA-126 delivery in non-small cell lung cancer. *Nanoscale* **12**, 877-887, doi:10.1039/c9nr09011h (2020).

198 Kim, H. *et al.* Exosomes: Cell-Derived Nanoplatforms for the Delivery of Cancer Therapeutics. *Int J Mol Sci* **22**, doi:10.3390/ijms22010014 (2020).

199 Matejovic, A., Wakao, S., Kitada, M., Kushida, Y. & Dezawa, M. Comparison of separation methods for tissue-derived extracellular vesicles in the liver, heart, and skeletal muscle. *FEBS Open Bio* **11**, 482-493, doi:10.1002/2211-5463.13075 (2021).

200 Phan, J. *et al.* Engineering mesenchymal stem cells to improve their exosome efficacy and yield for cell-free therapy. *J Extracell Vesicles* **7**, 1522236, doi:10.1080/20013078.2018.1522236 (2018).

201 Patil, S. M., Sawant, S. S. & Kunda, N. K. Exosomes as drug delivery systems: A brief overview and progress update. *Eur J Pharm Biopharm* **154**, 259-269, doi:10.1016/j.ejpb.2020.07.026 (2020).

202 Li, P., Kaslan, M., Lee, S. H., Yao, J. & Gao, Z. Progress in Exosome Isolation Techniques. *Theranostics* **7**, 789-804, doi:10.7150/thno.18133 (2017).

203 Chen, J. *et al.* Review on Strategies and Technologies for Exosome Isolation and Purification. *Front Bioeng Biotechnol* **9**, 811971, doi:10.3389/fbioe.2021.811971 (2021).

204 Langer, R. & Vacanti, J. P. Tissue engineering. *Science* **260**, 920-926, doi:10.1126/science.8493529 (1993).

205 Salgado, A. J. *et al.* Tissue engineering and regenerative medicine: past, present, and future. *Int Rev Neurobiol* **108**, 1-33, doi:10.1016/B978-0-12-410499-0.00001-0 (2013).

206 Chaicharoenaudomrung, N., Kunhorm, P. & Noisa, P. Three-dimensional cell culture systems as an in vitro platform for cancer and stem cell modeling. *World J Stem Cells* **11**, 1065-1083, doi:10.4252/wjsc.v11.i12.1065 (2019).

207 Bialkowska, K., Komorowski, P., Bryszewska, M. & Milowska, K. Spheroids as a Type of Three-Dimensional Cell Cultures-Examples of Methods of Preparation and the Most Important Application. *Int J Mol Sci* **21**, doi:10.3390/ijms21176225 (2020).

208 Fernandes, H., Moroni, L., van Blitterswijk, C. & de Boer, J. Extracellular matrix and tissue engineering applications. *Journal of Materials Chemistry* **19**, doi:10.1039/b822177d (2009).

209 O'Brien, F. J. Biomaterials & scaffolds for tissue engineering. *Materials Today* **14**, 88-95, doi:10.1016/s1369-7021(11)70058-x (2011).

210 Kim, S. *et al.* Tissue extracellular matrix hydrogels as alternatives to Matrigel for culturing gastrointestinal organoids. *Nat Commun* **13**, 1692, doi:10.1038/s41467-022-29279-4 (2022).

211 Chan, B. P. & Leong, K. W. Scaffolding in tissue engineering: general approaches and tissue-specific considerations. *Eur Spine J* **17 Suppl 4**, 467-479, doi:10.1007/s00586-008-0745-3 (2008).

212 Tonti, O. R. *et al.* Tissue-specific parameters for the design of ECM-mimetic biomaterials. *Acta Biomater* **132**, 83-102, doi:10.1016/j.actbio.2021.04.017 (2021).

213 Parrish, A. R., Gandolfi, A. J. & Brendel, K. Precision-cut tissue slices: applications in pharmacology and toxicology. *Life Sci* **57**, 1887-1901, doi:10.1016/0024-3205(95)02176-j (1995).

214 Graaf IA, G. G., Olinga P. Precision-cut tissue slices as a tool to predict metabolism of novel drugs. *Expert Opinion Drug Metabolism Toxicology* **6**, 879-898, doi:10.1517/17425255.3.6.879. (2007).

215 Bigaeva, E. *et al.* Transcriptomic characterization of culture-associated changes in murine and human precision-cut tissue slices. *Arch Toxicol* **93**, 3549-3583, doi:10.1007/s00204-019-02611-6 (2019).

216 Giuliani, M. E. *et al.* Precision-Cut Tissue Slices (PCTS) from the digestive gland of the Mediterranean mussel Mytilus galloprovincialis: An ex vivo approach for molecular and cellular responses in marine invertebrates. *Toxicol In Vitro* **61**, 104603, doi:10.1016/j.tiv.2019.104603 (2019).

217 Majorova, D. *et al.* Use of Precision-Cut Tissue Slices as a Translational Model to Study Host-Pathogen Interaction. *Front Vet Sci* **8**, 686088, doi:10.3389/fvets.2021.686088 (2021).

218 Warner, J. D. *et al.* Visualizing form and function in organotypic slices of the adult mouse parotid gland. *Am J Physiol Gastrointest Liver Physiol* **295**, G629-640, doi:10.1152/ajpgi.90217.2008 (2008).

219 Su, X. *et al.* Three-dimensional organotypic culture of human salivary glands: the slice culture model. *Oral Dis* **22**, 639-648, doi:10.1111/odi.12508 (2016).

220 Chen, Y., Warner, J. D., Yule, D. I. & Giovannucci, D. R. Spatiotemporal analysis of exocytosis in mouse parotid acinar cells. *Am J Physiol Cell Physiol* **289**, C1209-1219, doi:10.1152/ajpcell.00159.2005 (2005).

221 Meyer, R., Wong, W. Y., Guzman, R., Burd, R. & Limesand, K. Radiation Treatment of Organotypic Cultures from Submandibular and Parotid Salivary Glands Models Key In Vivo Characteristics. *J Vis Exp*, doi:10.3791/59484 (2019).

222 Khajavi, B. *et al.* Multimodal high-resolution embryonic imaging with light sheet fluorescence microscopy and optical coherence tomography. *Opt Lett* **46**, 4180-4183, doi:10.1364/ol.430202 (2021).

223 Greger, K., Swoger, J. & Stelzer, E. H. Basic building units and properties of a fluorescence single plane illumination microscope. *Rev Sci Instrum* **78**, 023705, doi:10.1063/1.2428277 (2007).

224 Santi, P. A. Light sheet fluorescence microscopy: a review. *J Histochem Cytochem* **59**, 129-138, doi:10.1369/0022155410394857 (2011).

225 Wu, Y. *et al.* Spatially isotropic four-dimensional imaging with dual-view plane illumination microscopy. *Nat Biotechnol* **31**, 1032-1038, doi:10.1038/nbt.2713 (2013).

226 Icha, J. *et al.* Using Light Sheet Fluorescence Microscopy to Image Zebrafish Eye Development. *J Vis Exp*, e53966, doi:10.3791/53966 (2016).

227 Migliori, B. *et al.* Light sheet theta microscopy for rapid high-resolution imaging of large biological samples. *BMC Biol* **16**, 57, doi:10.1186/s12915-018-0521-8 (2018).

228 Glaser, A. K. *et al.* Light-sheet microscopy for slide-free non-destructive pathology of large clinical specimens. *Nat Biomed Eng* **1**, doi:10.1038/s41551-017-0084 (2017).

229 Bhattacharya, S. K. *Contribution of Purinergic Receptors to Calcium Signaling in Salivary Gland.* the Doctor of Philosophy Degree thesis, the University of Toledo, (2012).

230 Fox, H. Is H&E morphology coming to an end? *J Clin Pathol* **53**, 38-40, doi:10.1136/jcp.53.1.38 (2000).

231 Weinstein, R. S. *et al.* Overview of telepathology, virtual microscopy, and whole slide imaging: prospects for the future. *Hum Pathol* **40**, 1057-1069, doi:10.1016/j.humpath.2009.04.006 (2009).

232 Hussein, I. H. & Raad, M. Once Upon a Microscopic Slide: The Story of Histology. *Journal of Cytology & Histology* **06**, doi:10.4172/2157-7099.1000377 (2015).

233 de Aquino, T., Zenkner, F. F., Ellwanger, J. H., Prá, D. & Rieger, A. DNA damage and cytotoxicity in pathology laboratory technicians exposed to organic solvents. *An Acad Bras Cienc* **88**, 227-236, doi:10.1590/0001-3765201620150194 (2016).

234 Falkeholm, L., Grant, C. A., Magnusson, A. & Möller, E. Xylene-free method for histological preparation: a multicentre evaluation. *Lab Invest* **81**, 1213-1221, doi:10.1038/labinvest.3780335 (2001).

235 Alwahaibi, N., Aljaradi, S. & Alazri, H. Alternative to xylene as a clearing agent in histopathology. *J Lab Physicians* **10**, 189-193, doi:10.4103/jlp.Jlp_111_17 (2018).236

236 Treuting, P. M. & Boyd, K. L. Histopathological Scoring. *Veterinary Pathology* **56**, 17-18, doi:10.1177/0300985818785699 (2019).

237 Klopfleisch, R. Multiparametric and semiquantitative scoring systems for the evaluation of mouse model histopathology - a systematic review. *BMC Veterinary Research* **9**, 123, doi:10.1186/1746-6148-9-123 (2013).

238 Gibson-Corley, K. N., Olivier, A. K. & Meyerholz, D. K. Principles for valid histopathologic scoring in research. *Vet Pathol* **50**, 1007-1015, doi:10.1177/0300985813485099 (2013).

239 Watanabe, J. *et al.* Extracellular Vesicles of Stem Cells to Prevent BRONJ. *Journal of Dental Research* **99**, 552-560, doi:10.1177/0022034520906793 (2020).

240 Kurosawa, M. *et al.* Chemokines Up-Regulated in Epithelial Cells Control Senescence-Associated T Cell Accumulation in Salivary Glands of Aged and Sjögren's Syndrome Model Mice. *International Journal of Molecular Sciences* **22** (2021).

241 Beucler, M. J. & Miller, W. E. Isolation of Salivary Epithelial Cells from Human Salivary Glands for In Vitro Growth as Salispheres or Monolayers. LID - 10.3791/59868 [doi].

242 Alsafadi, H. N. *et al.* An ex vivo model to induce early fibrosis-like changes in human precision-cut lung slices. *Am J Physiol Lung Cell Mol Physiol* **312**, L896-L902, doi:10.1152/ajplung.00084.2017 (2017).

243 Ohara, Y. *et al.* Connective tissue growth factor produced by cancer-associated fibroblasts correlates with poor prognosis in epithelioid malignant pleural mesothelioma. *Oncol Rep* **44**, 838-848, doi:10.3892/or.2020.7669 (2020).

244 Silva, I. A. N. *et al.* A Semi-quantitative Scoring System for Green Histopathological Evaluation of Large Animal Models of Acute Lung Injury. *Bio Protoc* **12**, doi:10.21769/BioProtoc.4493 (2022).

245 Otali, D. et al. Combined effects of formalin fixation and tissue processing on immunorecognition. *Biotech Histochem* **84**, 223-247, doi:10.3109/-10520290903039094 (2009).

246 Stegmayr, J. *et al.* Isolation of high-yield and -quality RNA from human precision-cut lung slices for RNA-sequencing and computational integration with larger patient cohorts. *Am J Physiol Lung Cell Mol Physiol* **320**, L232-L240, doi:10.1152/ajplung.00401.2020 (2021).

247 Renier, N. *et al.* iDISCO: A Simple, Rapid Method to Immunolabel Large Tissue Samples for Volume Imaging. *Cell* **159**, 896-910, doi:10.1016/j.cell.2014.10.010 (2014).

248 Masselink, W. *et al.* Broad applicability of a streamlined ethyl cinnamate-based clearing procedure. *Development* **146**, doi:10.1242/dev.166884 (2019).

249 Kimiz-Gebologlu, I. & Oncel, S. S. Exosomes: Large-scale production, isolation, drug loading efficiency, and biodistribution and uptake. *J Control Release* **347**, 533-543, doi:10.1016/j.jconrel.2022.05.027 (2022).

250 Lässer, C. *et al.* The International Society for Extracellular Vesicles launches the first massive open online course on extracellular vesicles. *J Extracell Vesicles* **5**, 34299, doi:10.3402/jev.v5.34299 (2016).

251 Yuan, J., Adamski, R. & Chen, J. Focus on histone variant H2AX: to be or not to be. *FEBS Lett* **584**, 3717-3724, doi:10.1016/j.febslet.2010.05.021 (2010).

252 Yun, M. H. Cellular senescence in tissue repair: every cloud has a silver lining. *Int J Dev Biol* **62**, 591-604, doi:10.1387/ijdb.180081my (2018).

253 Hargitai, R. *et al.* Oxidative Stress and Gene Expression Modifications Mediated by Extracellular Vesicles: An In Vivo Study of the Radiation-Induced Bystander Effect. *Antioxidants (Basel)* **10**, doi:10.3390/antiox10020156 (2021).

254 Mas-Bargues, C. *et al.* Extracellular Vesicles from Healthy Cells Improves Cell Function and Stemness in Premature Senescent Stem Cells by miR-302b and HIF-1alpha Activation. *Biomolecules* **10**, doi:10.3390/biom10060957 (2020).

255 Mothersill, C., Cusack, A., Seymour, C. B. & Hennessy, T. P. Optimisation of media for the culture of normal human epithelial cells from oesophageal mucosa. *Cell Biol Int Rep* **13**, 625-633, doi:10.1016/0309-1651(89)90113-6 (1989).

256 Berdel, H. O. *et al.* Targeting serum glucocorticoid-regulated kinase-1 in squamous cell carcinoma of the head and neck: a novel modality of local control. *PLoS One* **9**, e113795, doi:10.1371/journal.pone.0113795 (2014).

257 DeBono, R., Rao, G. S. & Berry, R. B. The survival of human skin stored by refrigeration at 4 degrees C in McCoy's 5A medium: does oxygenation of the medium improve storage time? *Plast Reconstr Surg* **102**, 78-83, doi:10.1097/00006534-199807000-00012 (1998).

258 Woods, T. L., Smith, C. W., Zeece, M. G. & Jones, S. J. Conditions for the culture of bovine embryonic myogenic cells. *Tissue Cell* **29**, 207-215, doi:10.1016/s0040-8166(97)80020-1 (1997).

259 Yu, X. & Petersen, F. A methodological review of induced animal models of autoimmune diseases. *Autoimmun Rev* **17**, 473-479, doi:10.1016/j.autrev.2018.03.001 (2018).

260 Petersen, F., Yue, X., Riemekasten, G. & Yu, X. Dysregulated homeostasis of target tissues or autoantigens - A novel principle in autoimmunity. *Autoimmun Rev* **16**, 602-611, doi:10.1016/j.autrev.2017.04.006 (2017).

261 Delaleu, N., Nguyen, C. Q., Peck, A. B. & Jonsson, R. Sjogren's syndrome: studying the disease in mice. *Arthritis Res Ther* **13**, 217, doi:10.1186/ar3313 (2011).

262 Mestas, J. & Hughes, C. C. Of mice and not men: differences between mouse and human immunology. *J Immunol* **172**, 2731-2738, doi:10.4049/jimmunol.172.5.2731 (2004).

263 Hu, Y., Nakagawa, Y., Purushotham, K. R. & Humphreys-Beher, M. G. Functional changes in salivary glands of autoimmune disease-prone NOD mice. *Am J Physiol* **263**, E607-614, doi:10.1152/ajpendo.1992.263.4.E607 (1992).

264 Humphreys-Beher, M. G. *et al.* Characterization of Antinuclear Autoantibodies Present in the Serum from Nonobese Diabetic (NOD) Mice. *Clinical Immunology and Immunopathology* **68**, 350-356, doi:https://doi.org/10.1006/clin.1993.1137 (1993).

265 Skarstein, K., Wahren, M., Zaura, E., Hattori, M. & Jonsson, R. Characterization of T cell receptor repertoire and anti-Ro/SSA autoantibodies in relation to sialadenitis of NOD mice. *Autoimmunity* **22**, 9-16, doi:10.3109/08916939508995294 (1995).

266 Kern, J., Drutel, R., Leanhart, S., Bogacz, M. & Pacholczyk, R. Reduction of T cell receptor diversity in NOD mice prevents development of type 1 diabetes but not Sjögren's syndrome. *PLoS One* **9**, e112467, doi:10.1371/journal.pone.0112467 (2014).

267 Brayer, J. *et al.* Alleles from chromosomes 1 and 3 of NOD mice combine to influence Sjögren's syndrome-like autoimmune exocrinopathy. *J Rheumatol* **27**, 1896-1904 (2000).

268 Wieczorek, G. *et al.* Blockade of CD40-CD154 pathway interactions suppresses ectopic lymphoid structures and inhibits pathology in the NOD/ShiLtJ mouse model of Sjögren's syndrome. *Ann Rheum Dis* **78**, 974-978, doi:10.1136/annrheumdis-2018-213929 (2019).

269 Verweij, F. J. *et al.* Live Tracking of Inter-organ Communication by Endogenous Exosomes In Vivo. *Dev Cell* **48**, 573-589 e574, doi:10.1016/j.devcel.2019.01.004 (2019).

270 Betzer, O. *et al.* In Vivo Neuroimaging of Exosomes Using Gold Nanoparticles. *ACS Nano* **11**, 10883-10893, doi:10.1021/acsnano.7b04495 (2017).

271 James, M. L. & Gambhir, S. S. A molecular imaging primer: modalities, imaging agents, and applications. *Physiol Rev* **92**, 897-965, doi:10.1152/physrev.00049.2010 (2012).

272 Dimri, G. P. *et al.* A biomarker that identifies senescent human cells in culture and in aging skin in vivo. *Proc Natl Acad Sci U S A* **92**, 9363-9367, doi:10.1073/pnas.92.20.9363 (1995).

273 Shay, J. W. & Roninson, I. B. Hallmarks of senescence in carcinogenesis and cancer therapy. *Oncogene* **23**, 2919-2933, doi:10.1038/sj.onc.1207518 (2004).

274 Brunk, U. T. & Terman, A. Lipofuscin: mechanisms of age-related accumulation and influence on cell function. *Free Radic Biol Med* **33**, 611-619, doi:10.1016/s0891-5849(02)00959-0 (2002).

275 Jung, T., Bader, N. & Grune, T. Lipofuscin: formation, distribution, and metabolic consequences. *Ann N Y Acad Sci* **1119**, 97-111, doi:10.1196/annals.1404.008 (2007).

276 Glees, P. & Hasan, M. Lipofuscin in neuronal aging and diseases. *Norm Pathol Anat (Stuttg)* **32**, 1-68 (1976).

277 Robles, L. J. Accumulation and identification of lipofuscin-like pigment in the neurons of Bulla gouldiana (Gastropoda: Opisthobranchia). *Mech Ageing Dev* **7**, 53-64, doi:10.1016/0047-6374(78)90052-0 (1978).

278 Gronthos, S., Mankani, M., Brahim, J., Robey, P. G. & Shi, S. Postnatal human dental pulp stem cells (DPSCs) in vitro and in vivo. *Proc Natl Acad Sci U S A* **97**, 13625-13630, doi:10.1073/pnas.240309797 (2000).

279 Mulcahy, L. A., Pink, R. C. & Carter, D. R. F. Routes and mechanisms of extracellular vesicle uptake. *Journal of Extracellular Vesicles* **3**, 24641, doi:10.3402/jev.v3.24641 (2014).

280 Smyth, T. *et al.* Biodistribution and delivery efficiency of unmodified tumor-derived exosomes. *Journal of Controlled Release* **199**, 145-155 (2015).

281 Charoenviriyakul, C. *et al.* Cell type-specific and common characteristics of exosomes derived from mouse cell lines: Yield, physicochemical properties, and pharmacokinetics. *European Journal of Pharmaceutical Sciences* **96**, 316-322 (2017).

282 Liu, B. *et al.* Cardiac recovery via extended cell-free delivery of extracellular vesicles secreted by cardiomyocytes derived from induced pluripotent stem cells. *Nature biomedical engineering* **2**, 293-303 (2018).

283 Dutra Silva, J. *et al.* Mesenchymal stromal cell extracellular vesicles rescue mitochondrial dysfunction and improve barrier integrity in clinically relevant models of ARDS. *Eur Respir J* **58**, doi:10.1183/13993003.02978-2020 (2021).

284 Liu, X., Subedi, K. P., Zheng, C. & Ambudkar, I. Mitochondria-targeted antioxidant protects against irradiation-induced salivary gland hypofunction. *Sci Rep* **11**, 7690, doi:10.1038/s41598-021-86927-3 (2021).

285 Grundmann, O., Mitchell, G. C. & Limesand, K. H. Sensitivity of salivary glands to radiation: from animal models to therapies. *J Dent Res* **88**, 894-903, doi:10.1177/0022034509343143 (2009).

286 Peter, B., Van Waarde, M. A., Vissink, A., s-Gravenmade, E. J. & Konings, A. W. Radiation-induced cell proliferation in the parotid and submandibular glands of the rat. *Radiat Res* **140**, 257-265 (1994).

287 Jansson, P. M. et al. Mesenchymal stromal/stem cell therapy for radiation-induced salivary gland hypofunction in animal models: a protocol for a systematic review and meta-analysis. *Systematic Reviews* **11**, 72, doi:10.1186/s13643-022-01943-2 (2022).

288 Han, J., Fujisawa, T., Husain, S. R. & Puri, R. K. Identification and characterization of cancer stem cells in human head and neck squamous cell carcinoma. *BMC Cancer* **14**, 173, doi:10.1186/1471-2407-14-173 (2014).

289 Stoppini, L., Buchs, P. A. & Muller, D. A simple method for organotypic cultures of nervous tissue. *J Neurosci Methods* **37**, 173-182, doi:10.1016/0165-0270(91)90128-m (1991).

290 Hughes, J. R. & Parsons, J. L. FLASH Radiotherapy: Current Knowledge and Future Insights Using Proton-Beam Therapy. *Int J Mol Sci* **21**, doi:10.3390/ijms21186492 (2020).

291 Esplen, N., Mendonca, M. S. & Bazalova-Carter, M. Physics and biology of ultrahigh dose-rate (FLASH) radiotherapy: a topical review. *Phys Med Biol* **65**, 23tr03, doi:10.1088/1361-6560/abaa28 (2020).

292 Gao, Y. *et al.* A potential revolution in cancer treatment: A topical review of FLASH radiotherapy. *J Appl Clin Med Phys* **23**, e13790, doi:10.1002/acm2.13790 (2022).

293 Matuszak, N. *et al.* FLASH radiotherapy: an emerging approach in radiation therapy. *Rep Pract Oncol Radiother* **27**, 344-351, doi:10.5603/RPOR.a2022.0038 (2022).

294 Chapman, J. A., Lee, L. M. J. & Swailes, N. T. From Scope to Screen: The Evolution of Histology Education. *Adv Exp Med Biol* **1260**, 75-107, doi:10.1007/978-3-030-47483-6_5 (2020).

295 Madabhushi, A. & Lee, G. Image analysis and machine learning in digital pathology: Challenges and opportunities. *Med Image Anal* **33**, 170-175, doi:10.1016/j.media.2016.06.037 (2016).

296 Komura, D. & Ishikawa, S. Machine Learning Methods for Histopathological Image Analysis. *Computational and Structural Biotechnology Journal* **16**, 34-42, doi:https://doi.org/10.1016/j.csbj.2018.01.001 (2018).

297 Acs, B., Rantalainen, M. & Hartman, J. Artificial intelligence as the next step towards precision pathology. *J Intern Med* **288**, 62-81, doi:10.1111/joim.13030 (2020).

About the author

Jiao DONG is a clinician in China, but she is passionate about new regenerative therapies. She was admitted to Nagoya University as a Ph.D student in April 2019, majoring in stomatology and studying regenerative medicine as an clinical application 'exit' for salivary gland disorders. During the 15 months since June 2021, she has been part of a Joint-Degree Program between Nagoya University (Japan) and Lund University (Sweden) that allowed she to join Lung bioengineering and regeneration (LBR) lab leaded by Dr. Darcy Wagner, to work on a project about bioengineering therapy for salivary gland regeneration. Xerostomia (dry mouth) is an incurable condition caused by radiation, chemicals, or aberrant inflammation in the salivary glands. Besides causing rampant teeth and dysphagia, dry mouth also affects a patient's quality of life and overall health. It's so important to find a better treatment for salivary gland dysfunction. A key objective of her PhD research was to determine if cell-derived strategies (such as extracellular vesicles, EVs) could be used to ameliorate salivary gland injuries and restore function following radiotherapy or autoimmune diseases. In addition, she explored the possibility of promoting a precision cut salivary gland slice ex vivo model for analyzing salivary gland disease mechanisms or potential therapy applications. In particular, she worked to develop new imaging techniques for both 2D and 3D analysis of larger samples, enabling the quantification of disease-related and regenerative characteristics. It is her hope that more options can be provided for regaining salivary gland function and repairing the diverse tissue disorders surrounding it.

Printed by Media-Tryck, Lund 2023 NORDIC SWAN ECOLABEL 3041 0903

LUND UNIVERSITY

FACULTY OF MEDICINE

Department of Experimental Medical Science
Lund University, Faculty of Medicine
Doctoral Dissertation Series 2023:15
ISBN 978-91-8021-354-7
ISSN 1652-8220